Smart Microgrid Management using Multi Agent System

Ph.D. Thesis

SUJIL A

ID No. 2014REE9531

DEPARTMENT OF ELECTRICAL ENGINEERING

MALAVIYA NATIONAL INSTITUTE OF TECHNOLOGY JAIPUR

April 2019

Smart Microgrid Management using Multi Agent System

Submitted in

fulfillment of the requirements for the degree of

Doctor of Philosophy

by

Sujil A

ID: 2014REE9531

Under the Supervision of

Prof. Rajesh Kumar

DEPARTMENT OF ELECTRICAL ENGINEERING

MALAVIYA NATIONAL INSTITUTE OF TECHNOLOGY JAIPUR

April 2019

DECLARATION

I, **Sujil A**, declare that this thesis titled, "**Smart Microgrid Management using Multi Agent System**" and the work presented in it are my own. I confirm that:

- This work was done wholly or mainly while in candidature for a research degree at this university.
- Where any part of this thesis has previously been submitted for a degree or any other qualification at this university or any other institution, this has been clearly stated.
- Where I have consulted the published work of others, this is always clearly attributed.
- Where I have quoted from the work of others, the source is always given. With the exception of such quotations, this thesis is entirely my own work.
- I have acknowledged all main sources of help.
- Where the thesis is based on work done by myself, jointly with others, I have made clear exactly what was done by others and what I have contributed myself.

Date:

SUJIL A
(2014REE9531)

CERTIFICATE

This is to certify that the thesis entitled "**Smart Microgrid Management using Multi Agent System**" being submitted by **Sujil A (2014REE9531)** is a bonafide research work carried out under my supervision and guidance in fulfillment of the requirement for the award of the degree of **Doctor of Philosophy** in the Department of Electrical Engineering, Malaviya National Institute of Technology, Jaipur, India. The matter embodied in this thesis is original and has not been submitted to any other University or Institute for the award of any other degree.

Dr. Rajesh Kumar
Professor
Dept. of Electrical Engineering
MNIT Jaipur

Place: Jaipur
Date:

ACKNOWLEDGMENTS

It gives me immense pleasure to express gratitude and regards to all those people who supported me during the course of this doctoral research work at MNIT Jaipur. I acknowledge the involvement and contribution of each one of them.

I deeply owe a debt of gratitude to my supervisor Prof. Rajesh Kumar, Head of the Department of Electrical Engineering at our institute for all the support and motivation that he showered upon me throughout the doctoral program. He kept the faith in me and always backed my research proposal and ideas. I attribute the successful realization of this research work to his sincere and consistent guidance, versatile and unconventional thinking and his penchant for trying something new and taking risks.

I express my sincere gratitude and respect to Prof. Harpal Tiwari, (DPGC Convenor, Department of Electrical Engineering, Malaviya National Institute of Technology, Jaipur) for engaging in rounds of beneficial discussion and letting me avail all the facilities to pursue this work. I am also grateful to the members of my DREC: Prof. Vikas Gupta, Professor, Department of Electrical Engineering at our institute, Prof. Rajive Tiwari, Professor, Department of Electrical Engineering and Dr. Kusum Verma, Associate Professor, Department of Electrical Engineering for their constant support and encouragement. I also would like to thank all the faculty members in the Electrical Engineering Department, MNIT, Jaipur for their support and motivation.

This thesis work was carried under the Visvesvaraya Ph.D. Scheme for Electronics and IT. I acknowledge the financial support provided by the Ministry of Electronics & Information Technology (MeitY) Government of India, under this flagship scheme.

I also wish to record my gratitude to the team of the office staff at the EED for being always willing to provide logistics-related help.

This thesis work involved interactions and deliberations over various aspects to assess the relevance of the research problem and practical applicability of the proposed solution. Therefore, I wish to acknowledge the help provided and support extended by Prof. Ramesh C Bansal, Department of Electrical, Electronic and Computer Engineering, University of Pretoria, Pretoria, South Africa.

Special regards to colleagues and friends at RAMAN Lab family, MNIT namely Chandra Prakash, Shashank Vyas, Venu, Akanksha, Om Ji, Shalini, Vishu, Rahul

Singhal, Srikanth, Lokesh, Harish, Dr. Vaiju, Mrs. Shivali and Aarohi for their constant support, warmth and affection. Thanks to all members of the robotics group ZINE for being a source of inspiration. Special thanks to Pradeep, Abhilash, Ajeet K Singh, B P Soni, Pranda, J P, Prerak, Vijay, Sonam, Pankaj, Sreenu, Jatin Verma for always being there.

As regards to my family, I express my deepest gratitude (inexpressible through mere words) to my father, Mr. Vijayan A, mother, Mrs. Sudha Vijayan, sister, Ms. Anusha A for having encouraged me. Special thanks to my wife Dayana Sujil and my daughter Jiya Malavika for being an important and indispensable source of motivation and inspiration.

Special regards to Mr.Surendran, Mr. A N Sathyan for their help and support. Last but not the least, my sincere regards to Mr. Sathyan V M who is no longer with us for his love, support and care.

Abstract

The integration of highly intermittent and unpredictable distributed energy resources increases the complexities in energy management system (EMS). Therefore, the conventional control used in microgrid (MG) EMS is no more effective and requires alternative control strategies that can cope up with the new dynamics in the system. Adopted from computer science, a new distributed artificial intelligence technique called multi agent system (MAS) can serve this purpose well due to its inherent autonomous nature, scalability, flexibility, and adaptability. The EMS in an MG is responsible for providing dispatch strategies for the generation units requiring both the renewable and load forecast. Consequently, this thesis preliminarily proposes a new three-layer multi agent architecture namely forecasting and estimation layer, control and action layer and real time monitoring layer for MG energy management. The forecasting and estimation layer in the proposed system constitutes of different forecasting agents (PV, wind, and load), state of charge estimation agent and the unit commitment agent. The real time monitoring layer in the proposed system is deployed with a correction agent which provides the real time correction information to the control and action layer where battery agent and diesel generator agents are deployed. After receiving all the informations from the different agents deployed in the proposed system the control and action layer takes decision accordingly for the optimum utilization of each component in the MG while satisfying the load requirements. The PV and wind forecasting agents in the proposed system are developed by an adaptive neuro-fuzzy inference system (ANFIS) based forecasting model. The load forecasting agent in the proposed architecture is developed by the proposed Bayesian Multivariate Linear Spline (BMLS) model. The performance of proposed MAS based MG EMS modeled in a new platform called Stateflow has been evaluated by developing different scenarios considering resource fluctuations and load variations. The simulation results demonstrate the effectiveness of the proposed architecture in optimum utilization of each component of the MG. Later, this work is further extended and developed a MAS based EMS with self-healing capabilities by employing a four-layer multi agent concept. The first three layers in the system are same as in the preliminarily developed model, and the fourth layer is fault detection and action layer that facilitates the self-healing capability in the proposed MG. The performance and the applicability of the proposed architecture are tested by simulating the faults at different locations in the system.

Contents

List of Figures

List of Tables

List of Abbreviations

AI	Artificial Intelligence
AIS	Adaptive Intelligent System
ANFIS	Adaptive Neural Fuzzy Inference System
ANN	Artificial Neural Network
BA	Battery Agent
CA	Correction Agent
CAL	Control And Action Layer
CB	Circuit Breaker
CDPS	Cooperative Distributed Problem Solving System
CI	Computational Intelligence
DAI	Distributed Artificial Intelligence
DER	Distributed Energy Resources
DES	Distributed Energy Storage
DG	Diesel Generator
DGA	Diesel Generator Agent
DN	Distribution Network
EA	Evolutionary Algorithm
EMS	Energy Management System
EP	Evolutionary Programming
EV	Electric Vehicle
FCM	Fuzzy C Means Clustering
FDAL	Fault Detection And Action Layer
FDIRA	Fault Detection And Isolation And Restoration Agent
FEL	Forecasting And Estimation Layer
FIM	First Inter Monsoon
FIS	Fuzzy Inference System
GA	Genetic Algorithm
GP	Grid Partitioning
HES	Hybrid Energy Systems

ICU	Intensive Care Unit
IFS	Iterative Function System
LF	Load Forecasting
LFA	Load Forecasting Agent
LP	Linear Programming
LTS	Linear Time Series
MAE	Mean Absolute Error
MAPE	Mean Absolute Percentage Error
MAS	Multi Agent System
MAX E	Maximum Error
MCMC	Multivariate Linear Spline Model
MF	Membership Function
MG	Microgrid
MRE	Mean Relative Error
MSE	Mean Square Error
NEM	Northeast Monsoon
OCR	Over Current Relay
PSO	Particle Swarm Optimization
PVA	PV Agent
RES	Renewable Energy Source
RMSE	Root Mean Square Error
RTML	Real Time Monitoring Layer
SC	Subtractive Clustering
SFCL	Super Conducting Fault Current Limiter
SIM	Second Inter Monsoon
SOC	State Of Charge
SOCA	Soc Agent
STLF	Short Term Load Forecasting
SVM	Support Vector Machine
SVR	Support Vector Regression
SWM	Southwest Monsoon
UC	Unit Commitment
UCA	Unit Commitment Agent
V2G	Vehicle To Grid
WA	Wind Agent
WAM	Wide Area Measurement
WT	Wavelet Transform

Chapter 1

Introduction

1.1 Motivation for the Present Work

A microgrid (MG) consists of a cluster of loads and DGs operating as a single controllable entity that can be operated independently or in conjunction with the main grid to supply power to its local area and act as a small building block of a smart grid [1]. The grid-connected mode of operation of an MG can help to enhance the reliability, efficiency and reduce emissions in the power system. On the other hand, the islanded microgrid is an alternative way to electrify remote areas by the utilization of distributed renewable energy resources and avoiding the erection of new power lines[2, 3]. The addition of new renewable energy resources increases the complexity and changes the dynamics of the system due to highly intermittent and unpredictable nature of DERs. Accordingly, the control strategies for energy management that have been used in past decades need to be replaced with modern control paradigms and control techniques for smooth operation of the system [4, 5]. The energy management system (EMS) in a microgrid is responsible for maintaining the demand-supply balance and also for ensuring the flexibility, reliability and power quality of the system.

Initially, most of the researchers in the field of microgrid energy management system are concentrated on conventional EMS, i.e., centralized control schemes. In the centralized scheme, a microgrid central controller is used to optimize the economic power dispatch for DERs and storage system [6, 7]. As the number of components in the microgrid increases, the central controller faces certain issues like requirement of large measurements and it also increases the complexities in solving the optimization problem. Another major concern with the centralized

scheme is the chance of single point failure in the system that can lead to a complete system failure which questions the reliability of the system [6]. Although the design of a practical centralized MG controller can be achieved with expert systems and heuristic algorithms, it does not guarantee the flexibility and scalability of the system [8, 9].

When compared to centralized management, the distributed control for microgrid energy management system is less complicated and more vigorous [10, 11]. The components of distributed management are treated as a module having enough intelligence to provide the control calculations and actions. Also, the control modules in the distributed management help to fulfill the requirements of other modules as well as reduce the communication and computation burden [12]. A Distributed Artificial Intelligence (DAI) technique called Multi Agent System (MAS) has the aforementioned capability to solve an extremely difficult problem by breaking it into simple subproblems and solving them in a distributed way. These inherent properties of a MAS enable the researchers to think of control of microgrid in coordination with MAS to meet dynamic load variations in the presence of intermittent and unpredictable DERs.

1.2 Research Background

As evident from the survey of recent literature, researchers in the domain of power systems are shifting towards the implementation of multi agent systems for MG energy management. A detailed review of MAS applications in the electrical power systems can be found in [13, 14]. Reference [15] demonstrated a system constituting a DER agent, energy storage system agents and load agents and presented MG real-time operation with MAS in grid-connected and islanded mode for managing the DER and loads. During islanded mode of operation, a MAS that can minimize the operational cost and amplify the local DG power generation of MG subjected to system and unit constraints was developed in [16]. In [17], the authors introduced an intelligent interconnection agent that can purposefully disconnect and reconnect main grid in accordance with the grid status to resolve the issue of undesirable overcurrent transients because of the connection and disconnection of MG during grid failure in the presence of high penetration of DER. The authors also demonstrated the simulated and experimental results. In [18], the authors have presented management and control strategies for an integrated hybrid energy system with a multi agent system. A multi agent approach to solve

the energy imbalance problem, and also to promote the resource sharing between different MGs have been reported in [19]. A distributed management of MG with MAS can be found in [20], in which the authors have represented each component in the system as an agent with particular functions that can either maximize DG output or surplus load or both. A multi agent based grid control for maintaining the adequate power balance in dynamic system conditions can be found in [21]. The real-time operation of the MG that focuses on generation scheduling and DSM with a MAS was presented in [22]. In [22], the authors developed a scheduler coordinator agent having the task of real-time and day ahead scheduling and DSM agent having the task of load shifting and curtailment whenever possible and required. By developing multiple levels of agent architecture namely bottom level, intermediate level control agents and top-level energy management agent, a MAS based hybrid control scheme for improving the environmental and economic benefits and ensuring secure voltage can be found in [23]. A two-level hierarchical distributed control scheme based on MAS for enhancing the security and stability of MG can be found in [24]. The authors of the cited work developed upper and lower level agents having the goal to develop the switching control strategies for enhancing the MG security and decentralized continuous control for guaranteeing stability respectively.

In [25], an agent based control strategy was developed for an islanded MG, and it was shown that the load requirement can be satisfied with the output power produced by DGs. A MAS based pinning based control strategies for autonomous MG were introduced in [26]. In [26], only a fraction of the pinned agents was controlled directly by feedback controllers and the distributed communication coupling among the pinned agents enables the MAS synchronization with all other DG agents. A fully distributed control that avoids the requirement of the central controller and complicated communication topology and also enabled the plug and play capabilities are highlights of the work. A dynamic energy level balancing strategy between storage devices for improving the frequency and reliability in a droop controlled MG can be found in [27] in which the authors utilized the multi agent cooperative control in a distributed manner for achieving energy balance. While accounting for the local information, a MAS based EMS is designed in [28] for stable operation of MG at high altitude. Also, a MAS based approach for the distributed energy management of microgrid can be found in [29]. The authors in [30] proposed a multi agent control concept by utilizing heuristic intelligent optimization for minimizing power consumption and attaining a high level of comfort in a smart building. Intelligent control and management for smart energy

efficient buildings can be found in [31]. Authors in [32] developed distributed coordinated control strategies based on multi agent system for large power systems. For satisfying the requirement of a remote area, an autonomous polygeneration microgrid concept was introduced in [33]. Wherein the authors used grey prediction algorithm along with multi agent system for intelligent energy management. For a grid-connected microgrid, an agent based energy management system using improved genetic algorithm was presented in [34]. The authors in [35] have proposed a self-organizing agent based framework for resolving the basic control and monitoring problems of an MG. A MAS based optimal MG control using fully distributed diffusion strategy is presented in [36], in which the authors adopted an optimization based MAS for the economic dispatch of DERs. The authors in [37] introduced a fully distributed online optimal energy management solution for smart grids with the help of a MAS. A two-level architecture for DER management for multiple MGs using MAS can also be found in [38]. The authors in [39] demonstrated a MAS control strategy that can enable the transition of an MG from the grid connected to the islanded mode in response to a fault that occurred in the system in the simulation environment. All the aforesaid research concluded that MAS based EMS could yield better efficiency and can also manage complex DGs efficaciously due to the competence of MAS that can give numerous key advantages to the system as proclaimed in [11, 33, 40].In [41], the authors suggested that distributed coordination can be implemented by utilizing a MAS with distributed energy system and should be coupled with hardware to find the entire agent based solution for distributed energy resource management. Also, the authors have suggested that more intelligent MG operation can be achieved by incorporating load forecasting, Renewable Energy Source (RES) power production forecasting, resource scheduling and DSM into the MG modeling in future. Also, most of the research mainly addressed the energy management functionality for MGs by utilizing the multi agent system. However, the self-healing capability is equally important in case of a smart MG for flexible and resilient operation during an outage. A scanty amount of research in the field of MG energy management with self-healing capabilities has thus been found.

1.3 Literature Review

The power system is presently experiencing vital changes: it is advancing from a centralized structure to a decentralized one, primarily because of the enormous advancement of distributed renewable energy sources, so future power system

obliges new control strategies. These systems must have the capacity to withstand new requirements, for example, the exceedingly disseminated nature, the irregularity of renewable energy sources and the restricted data transfer capacity for communications. Multi Agent Systems (MAS) have attributes that meet these prerequisites. A certain degree of distributed or collective intelligence can be accomplished through the connection of these agents with one another, participating or contending to achieve their objectives. This section introduces the outline of the fundamental ideas of MAS and its different platforms. Also, it provides a comprehensive survey of the power system applications in which MAS technique has been applied. For each power system application, technical details are also discussed. This section also details the review of forecasting models used for PV, wind and load forecasting.

Agent based frameworks have been actualized in the field of power system engineering, having been deployed as a new approach for control and coordination in the recent years. Adopted from the computer sciences, the wide utilization of agent based innovative applications in this specialized area has brought about an uncertain use and requires an elucidation over the thoughts pertaining to on "Agents" and 'multi-agent systems'; this is especially apparent in the current smart power system research projects. The properties of agents' adaptable self-sufficiency, reactivity, distributed nature have been exploited to justify the utilization of agents' innovative ability to solve problems as diverse as Distribution System Management with DGs, Electric Vehicle Management, Energy Management System and Control, Generation Expansion Planning, Micro Grid, On-Line Transient Stability Enhancement, Fault Detection, Protection and Self-healing and many more related to electricity market and Smart Grid. Besides this, the innovation is developing to the point where the first MAS frameworks are currently being relocated from the lab to the utility, permitting industry to accelerate involvement in the utilization of MAS furthermore to assess its viability [42].

Although it is not mandatory to blindly implement Multi Agent System (MAS) in any complex problem we find, the proficient features of MAS sway many researchers to build them for various grounds of engineering. Before implementation of any algorithm, it is crucial that one should know whether it will be useful in the given situation and is it more efficient than its alternatives. The concept of MAS is applied in those situations where different tasks have to be performed by different persons/ organizations (also called agents) which supposedly store private information not to be exposed to partner agents and possess some individual goals/benefits to be fulfilled. Myriads of the real life instances exhibiting system

of agents can be thought of. Suppose the task is to organize a cultural event at some institute. This task can be divided into modular subtasks like the arrangement of caterer service, auditoriums, sound systems, conducting versatile cultural events, exhibitions, stage performances, handling finance, transportation, accommodation, technical aid, marketing and publicity tasks, entire management, etc. Unquestionably, these subtasks will have to be allotted to different individuals or groups of people. Now, imagine that all these tasks were to be performed by a single person. This explains the difference between a single agent system and a Multi Agent System. The advantage of time optimization is quite certain. The parallel processing reduces the work burden on individual agent. The modularity of MAS makes it easier for a central body to assign tasks to different agents, manage them and coordinate with them. More number of agents can be added as the number of subtasks increases. This feature of MAS is termed as Scalability. All these features together make it very convenient to program such a system. There are chances that an agent may fail to provide some information. However, MAS can be made more robust by creating backup agents which can deliver the same service if the primary agent fails, just like when the person whom we call is not there to respond, we send a voice message instead.

1.3.1 Multi Agent System (MAS)

1.3.1.1 Basic Concept

The role of an agent becomes very important. Many authors have provided various definitions of the term Agent. According to Wooldridge's definition, an agent signifies a computer system which possesses the capability to make critical decisions based on circumstances which will help it to hike towards its objective [43]. With time, the concept of agent is becoming stronger and more advanced, highlighting not only the characteristics of the agent but the environment too. [14] have beautifully explained the elusive and seemingly incongruent concepts regarding agent and its environment. They have described the autonomous behavior of an agent as the ability to plan action based on the situational analysis. Another point covered was ambiguity in the distinctive identification of agents and non-agents. Consequently, we need a set of characteristic features to delineate an agent. [44] has proved to be a worthy contribution in discussing various notions of the agent as claimed by different researchers throughout the world. It brought substantial clarity which prevents a program to be mistaken as an agent by eradicating various

misconceptions embedded as flaws in previously claimed definitions. According to [44], if simple mechanism of sensing input and producing output is followed, then an agent is no different from a computer program. Even with the inclusion of features of being autonomous, reactive, social and pro-active, the distinction between an agent and a program remains ambiguous. Also, the authors defined an autonomous agent as the one which: Lies within, persistently senses input signals from and acts on its environment. Throughout its life, works towards its motive.

The ability to persevere actions towards self-owned objectives makes an agent autonomous. A computer program may become active only when it is called, but an autonomous agent perseveres taking input from its environment to realize its agenda. Although we may be building MAS on computational grounds, highly adept agent system can only be obtained if we bring this concept close to the real world. A different perspective can be perceived from the work of [45] who have proposed to replace typical Artificial Intelligence (AI) agents with Adaptive Intelligent System (AIS) due to the cause that the latter is adaptable to a class of niches (environment) just like real-world agents (human beings), rather than being restricted to a strictly defined niche. To support their idea, they present an architecture for their AIS agent named Guardian which is designed to take care of patients inside Intensive Care Unit (ICU). It possesses dynamic nature, concerning its changing agenda or control mode in accordance with signal feed it takes from its patient, ensured by various reasoning and diagnosis it performs in parallel to normal data acquisition. The intellectual contribution of perspective towards changing notions facilitates many practitioners to realize and evaluate the concepts for accomplishing greater efficiency and advancement. The perpetual works on the most recent notions of MAS are one step ahead towards Artificial Intelligence.

A multi-agent system is the collection of several agents interacting with each other. A group of computational entities that can operate without human intervention (Autonomous), interact with each other (sociality), perceive and react to its environment (re-activity), exhibit goal-oriented behavior by taking initiatives (pro-activity) are called agents [39].

1.3.1.2 MAS Design

The different methodologies for the design of MAS are presented in [46, 47, 48] and their fundamentals are same. By developing or extending traditional software engineering approaches and knowledge engineering approaches, the design

methodologies have emerged for the specification and design of multi-agent systems. Generally, there are three phases of the design of a multi agent system, i.e., conceptualization, analysis, and design. The problem to be solved is specified in the conceptualization phase, analyzed in the analysis phase and the results of the analysis phase are used to produce agents and their communication strategy. Figure 1.1 shows the typical stages of multi agent design. In the design process, the output from each stage is used in the subsequent stages.

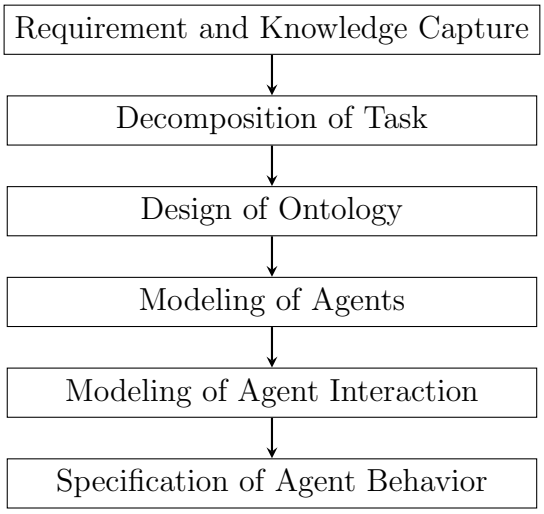

Figure 1.1: Design Stages of MAS

This methodology begins with system requirement specification and capturing of knowledge to fulfill those requirements. During task decomposition stage, the specified requirement and captured knowledge are transformed into the hierarchy of tasks and subtasks. Next stage is the designed vocabulary of agent communication called ontology. Modeling of agent uses the task hierarchy and ontology to identify a group of autonomous agents with the abilities to perform the tasks. The outcome of this stage is a set of agents and specific tasks that the agents should perform. After the agent modeling, the agent interaction must be defined.

For the development of MAS number of issues are associated, and the same should be identified and addressed carefully. In [49] explained the issues with the following agent-oriented software methodologies presented in [50, 51, 52, 53] and also the authors suggested an alternative MAS methodology to overcome some of the key issues addressed. In [54] surveys of multi agent system development, key issues and why recent researchers are giving specific attention towards MAS has been addressed. Based on this state of the art the authors identified the key areas to work that are integration techniques for design and code, to extent agent-oriented programing language for covering the specific aspects that are social concepts and

modeling environment which is currently missing. In current state of art, the implementation is done entirely manually from the design that may lead to the design less useful in future.

1.3.1.3 Different MAS Architectures

The Cooperative Distributed Problem Solving System (CDPS) is the process of developing a number of distributed agents by decomposing a complex problem to simpler subproblems. Each agent may have the capability of solving problems independently, but may have deficiencies in expertise, resources and information are to solve the problem by themselves. In CDPS the agents exchange their expertise, informations and resources to solve the sub-problem (local) cooperatively and then uses the results to solve the global problem. Once the number of agents is identified then overall control scheme needs to be developed to achieve the global objectives.

There are different MAS architecture namely centralized, distributed and hierarchical has been found in literature, also the different architecture shows their own benefits and confines. The distributed control manages a complex problem in a manner that it places its computational resources and capabilities by using different interconnected agents whole over the network. The centralized system collects informations at a central point and take the decisions at the single point, thus having an advantage of openness and flexibility. But a centralized framework might be tormented by constraints, execution bottlenecks, or critical failures, a decentralized MAS does not experience the effects of the " single point of failure " issue connected with complex network [55], [56].

- **Centralized**:

  Centralized approaches are mostly for ordinary part and have a tendency to be insufficient for future power system as a result of inadequacies in robustness, openness and flexibility. In centralized approach the control centre have full monopoly to take decision and send control signal to the agents accordingly to act up on any particular abnormalities. Figure 1.2 shows the agent communication with control centre in centralized design. In centralized design, every one of the agents send their information to a control centre and sit tight for the Instructions/control signal. Instructions will be sent back to corresponding agents to act to reduce/rectify the effect of the abnormalities. An example of centralized scheme is proposed in [57] and in

which the authors developed a plan for the distribution of teams of robots in a coordinated manner has been addressed. Also a centralized planning engine that uses the multi agents planning system can be found in [58, 59].

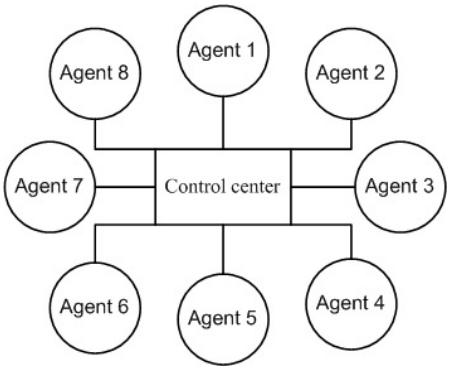

Figure 1.2: Centralized MAS Architecture

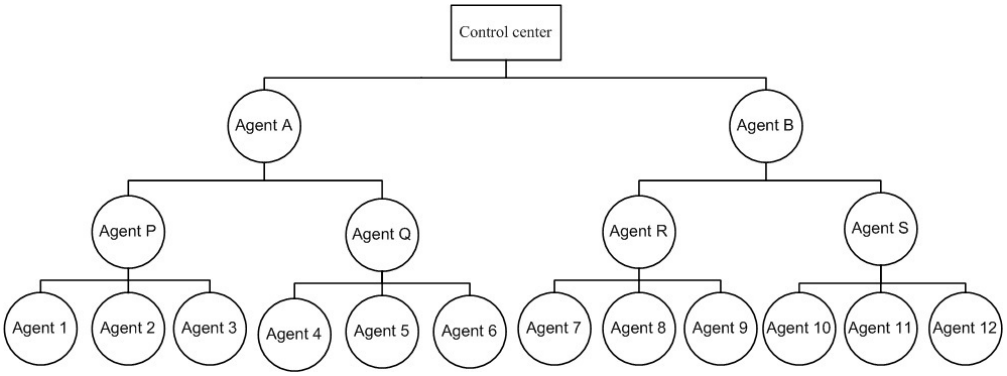

Figure 1.3: Hierarchical MAS Architecture

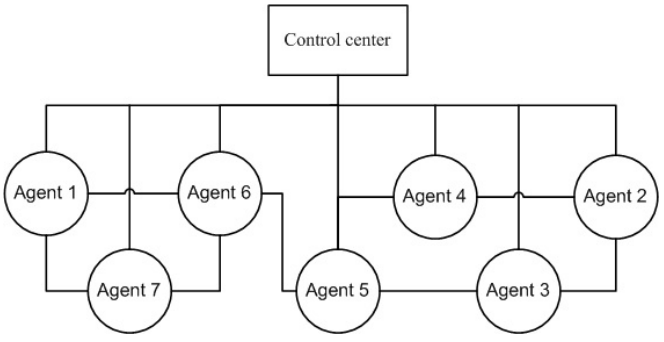

Figure 1.4: Distributed MAS Architecture

- **Hierarchical**:

  In this design, agents are working in distinctive levels of decision making. Agent's levels from high to low are control center, Agents (A, B), Agents

(P, Q, R, S) and the agent (1-12) as shown in Figure 1.3. Agent (A,B) is responsible for gathering informations from Agents (P, Q, R, S) also to give control signal to Agents (P, Q, R, S) form control center. Agents (P, Q, R, S) is having a duty to collect information from Agents (1-12) and give the same information to Agents (A, B), also pass control signal to agents (1-12). In this approach the decision making power is given only to higher level agents and lower level agents can only able to communicate with higher level agents. The main disadvantage of this architecture is that the failure of higher level agents can cause critical conditions in all lower level agents. Some examples of the hierarchical multiagent system can be found in [60, 61, 62].

- **Distributed**:

  Decentralized methodologies are more powerful and adaptable as opposed to centralized ones however the burden with the decentralized systems is not coming to the global optimal solutions in all situations since the agents correspondences are simply constrained to neighbours. In this approach, all agents are in the same level of usefulness and speak with the neighbours to a predetermined neighbourhood as in Figure 1.4. In this design agents attempt to settle on optimal decision based on the local condition and on account of a glitch of any agents, different agents can keep working. Agent's connection to control center is simply considered as a supervisory observing. In the event that the control agent additionally assumes a part in decision making, this design could be considered as hybrid architecture too.

  The decentralized architecture has been widely claimed by the researchers in the literature due to the inherent advantages of the decentralized system over centralized such as [63, 64], that include the lesser need of communication requirement, higher fault tolerance, better scalability etc. In this control strategy, there is no central controller and single point process, and the agents will share the informations each other to reach the goal. This nature of distributed MAS control reduces both communication requirements and allows systems under distributed control to scale well in terms of the number of agents deployed. The decentralized control system is unaware of the task performed by another system at the premises due to the deficiency of central controller this may encourage the redundant system operation. Fault tolerance is created as a side effect of this task redundancy. The examples of this kind of system can be found in [65, 66, 20].

1.3.1.4 Advantages of MAS

The multi agent system has following advantages [67]

- **Extesibility :** number of agents working on a problem can be altered.
- **Robustness:** ability to tolerate uncertainty due to the suitable information exchanged among agents.
- **Maintainability:** It is easy to maintain multiple component-agents because of its modularity.
- **Flexibility:** Agents with different abilities can adaptively organize to solve the current problem.
- **Learning of agents:** Agents update their rules to provide better performance.
- **Reuse:** Functionally specific agents can be reused in different agent teams to solve different problems.
- Provides solutions in situations where expertise is spatially and temporally distributed.
- Ability to distribute computational resources and capabilities across a network of interconnected agents.
- In multiple legacy system MAS allows interconnection and interoperation.
- MAS efficiently retrieves, filters, and globally coordinates information from sources that are spatially distributed.

1.3.2 Different MAS Platforms

An agent platform is an environment where agents live, similar to the universe for human beings. The main functions of agent platform are to ensure communication that is reliable, provide multiple communication protocols, languages, and communication media. Several agent based modeling toolkits have been developed by agent based modeling community to support individuals to develop their own agent based applications. More and more such toolkits are appearing, and each toolkit has an assortment of qualities. In literature, different authors have used different platforms like JADE, SWARM, ZEUS and many more for implementing

Multi Agent System for power system applications as shown in Table 1.1. NA denotes that the platform has not been addressed by authors in their article. Table 1.2 provides a more detailed comparison of different MAS platforms in terms of power system application and specific domain, the underlying programming language, licensing the tools and their developers.

Table 1.1: Different MAS platform

Author	Platform
[67] ; [15] ; [68]; [69]; [70]; [71]; [23]; [72]; [20]; [73]; [74]; [75]; [41]; [16]; [22]; [76]; [77]; [78]; [79]; [80]; [21]; [81]; [82]; [83]; [84]; [85]; [67]; [86]; [87]; [88]; [89]; [90]; [91]; [92];	JADE
[17]; [93]; [94]	ETMSP+matlab
[95]; [40]	Matlab/Simulink
[96]; [97]	EMTDC
[98]; [99]	Visual C++
[100]; [101]	C++Builder environment
[39] ;[102]	ZEUS
[103]	PSAT package in MATLAB
[104]	EPOCHS + PSCAD
[105]	IDEAS + Tcl/T
[106]	EPOCHS+EMTDC
[107]	EMTP
[108]	SWARM
[109]; [110]; [111]; [112]; [113]; [114]; [115]; [116]; [117]; [118]; [119]; [120]; [121]; [122]; [123]; [124]; [125] ; [126];[127];	NA

Table 1.2: Comparison of MAS platforms

Platform	Application(s)	Primary Domain	License	Programming Language	Remarks	Developer
JADE	-Micro Grid, EV Management System, Fault Detection, Protection and Self-healing, EMS and Control-Distribution System Management with DGs.	Distributed applications composed of autonomous entities.	LGPL	Java	-Independence and asynchronous processing-Safer and better tolerance -Reducing the network load	Telecom Italia Lab [128]
SWARM	-Electric Vehicle Management System	General purpose agent based	GPL	-Java, Objective-C	-Adaptable	Swarm Development Group [129]
ZEUS	-Micro Grid	Distributed multi-agent simulations	Open source (read license)	Visual editors and code gen	-Agents are deliberative, goal-directed, versatile, truthful.	BTexact [130]
EMTDC	-Fault detection, Protection and Self-healing		End User License Agreement (EULA)		-The power of EMTDC is greatly enhanced by its GUI called PSCAD	Manitoba HVDC Research Centre [131]
EPOCHS	-Fault Detection, Protection and Self-healing	distributed simulation platform	GPL			[132]

1.3.3 MAS Applications to the Power System

This section details the applications of the MAS technique to power system problems. The themes addressed in this section include those presented by [14], along with some new areas under evolution. In addition, technical particulars are explained for each application to allow the bibliophile to accomplish related experiments and solve problems of the same features. Table 1.3 explains some practical applications of multi agent systems in the literature in the different field of power engineering. Table 1.4 gives the bibliography survey of the application of MAS technique to power system by technical areas.

1.3.3.1 Distribution System Management with DGs

Distribution Network (DN) is the last step in the distribution of electricity to end users [121]. Classically, the bulk generation is the only one energy solution to the DN, and the power flow direction strictly follows from central generation to end user [78]. Emerging Distributed Generator (DG) is the alternative power resource in DN usually located near to the load [88, 133] and have some advantages like it can fulfill loads with no transmission system, reduced power loss, and cost [134]. But in other hands due to the intermittent nature of DERs like wind, solar most of the DG can only able to provide intermittent power to the network and their output is very difficult to control. So the increased DG penetration may also change the distribution system power flow from unidirectional to bidirectional [135].Therefore, conventional methods may fails to manage the electricity dispatch in a DN with a large number of DG penetration due to the lack of flexibility and decision making [120] and become an important power engineering research issue.

The authors in [136] explains the functional objectives of MAS that are balancing of demand and supply, reduce power usage cost and allow DGs to supply more power in DN along with constraints (Cable, Generator, Busbar, Component). Also some related publications reflects cost minimization [74], voltage and current limitation [73] and load maximization [137]. [92] proposed a decentralized MAS based approach combining all [73, 74, 136, 137] considerations to solve above-said problem with five types of agents namely Substation Agent (SA), Bus Agent (BA), Feeder Agent (FA), Load Agent (LA) and Generation Agent GA) to model the key electric components in a DN.

Reference [83] reviewed the impact of high-level photovoltaic penetration in Perth Solar City project and investigated the potential issues caused by voltage regu-

lation, then suggested that more agents will give better performance. [124] have applied a three-agent (i.e. Regulator agent, DG agent, Capacitor agent) based approach to study voltage regulation in unbalanced distribution feeder with DG penetration and showed that MAS based technique could overcome the traditional control techniques limitations caused by one-way communication with other components and insufficient information of DGs.

The authors in [138] proposed a MAS based control system for the distribution system, which can be able to correct voltages violations globally, avoid feeder congestion and manage the operation of reactive power devices. Also, [139] developed a hybrid MAS based control strategy for the reconfiguration of distribution system with DGs. The main function of MAS control in this scheme is to locate and detects the faults, accordingly decide the optimal reconfiguration plans to restore the de-energized loads and regulate the node voltage finally. The authors assigned the responsibilities of agents in two layers. i.e., at first level (agents at load bus) can only limited freedom, to communicate only with its feeder agents and next neighbor load agents and second layer agents can exchange their knowledge to each other. The main advantage of the proposed control system is that for moderate communication infrastructure, the control system failure can be reduced.

Reference [140] explained A goal-based holonic multi agent system (HMAS) for the management of active DN with the integration of rooftop PVs in large scale. The first role associated with HMAS is control of reactive power at PV installations at individual houses for ensuring the optimal operation. Secondly, the authors concentrated on state estimation of system measurement received from the smart meter installed at houses.

Using a MAS, [141] presented the modeling of intelligent control center controlling DGs. They utilized the MAS here because of extensibility, autonomy and reduced maintenance for providing management and intelligent control in a grid. Controlled DG islanding based service restoration scheme with the help of decentralized MAS can be found in [142]. It explores the effect of V2G capability of EVs for service restoration. Flexibility (to perform under different DG and EV penetration), Scalability (capability to restore service for both large and small systems) and robustness (perform effectively for single and multiple fault situations) are the main advantages claimed for the proposed method. The Distributed coordinated control of DGs in the Energy Internet with the help of MAS can found in [143].

1.3.3.2 Electric Vehicle management system

In upcoming years it is expected that there is a significant intensification in the share of Electric Vehicles (EVs) and it can affect the power system normal operation undesirably due to the uncontrolled charging, particularly at the distribution level. Numerous studies have publicized that dumb charging [144] can result in new peak loads that can lead to an excursion of feeder voltage and equipment overloads [145, 146, 147], predominantly at the coincidence of new demand and maximum demand of rest of the loads. So co-ordination of electric vehicle charging becomes a key research attention. Several centralized control concepts have been proposed [148, 149, 150, 151] for EV charging, but it can be only able to perform effectively for a restricted number of EVs. The centralized management cannot outperform for bulky EV crews due to the deficiency of communication technologies and significant computational resources for processing a substantial amount of local information from a central point.

Reference [118] suggested the type of agents which is required for the microgrid market operation and technical operation with EV. And they introduced a concept of Mobile agent technology to integrate the characteristics and mobility of EVs. [119] also proposed a distributed intelligent approach without disturbing the advantages of centralized control on EV charging by considering the large number of EVs and with their owners preference and ensuring the efficient network operation. The main properties of this approach are automatic decision taking agents based on global (network state) and local (EV owners preferences and charging infrastructure parameters) environment. It has been shown that this distributed approach distribute EV energy requirements by valley filling during off-peak hours resulting to the increased load factor and reduced energy loss also the computation time of this method is nearly independent of the number of EV crews.

The authors in [112] taken an initial benchmarking step for DSM with PHEV using multi agent system and quality of solution compared with the quadratic programming scheduler solution and obtained 95 percent efficiency. The authors implemented the above-said problem in realistic scenario distribution grid, Belgian electricity provider Nuon. In this, they considered two types of agents, i.e. transformer agents and PHEV agents, and they work with each other in coordination to provide charging power. Here, the main function of PHEV agents is to charge the individual battery on time, transformer to flatten the load of its transformer and avoid overloading in the system. Related work by considering four agents namely PHEV Agent, TF Agent, Load Agent and Grid Agent has been done [75]

by using a decentralized MAS with the combination of Evolutionary Algorithm (EA) and a Linear Programming (LP) for DN management with PHEVs. This also shows that the proposed decentralized approach is scalable and can adapt to unpredictable and incomplete information while the arithmetical results not much dull than that of the central scheduler.

Reference [113] proposed a MAS-market-based control strategy for EV charging which incorporates distribution transformer, voltage constraints, and the performance is analyzed on a prevailing three-phase four-wire distribution grid. This MAS-market based method outperforms by minimum charging cost for EV crews, without altering the network state with utmost customer prosperity. Reactive voltage control helps to support more EVs to charge at the same time during off-peak periods before the critical voltage restrictions and also considered special attention towards the neutral shift. [82] considered voltage constraints but for minimizing the cost of charging the EVs need fully comprehensive search to find the combination of schedules.

The authors in [125] developed a MAS based system for reducing the cost and the peak hour overloading by switching consumer load and controlling PHEV according to the battery SOC. The results improve the efficacy for permitting EVs during peak hours and customer cost reduction. [123] introduced two methodologies, the first one QP based scheduling and the later based on MAS-market coordination by considering virtual market bidding to obtain optimum market prize to satisfy supply and demand. They have done this experiment by selecting residential area comprising of 63 houses and found that reduced peak loads, grid voltage fluctuations and variability in load with controlled charging. Finally, this method falls to be a benchmark for the entirely distributed market-based MAS against the optimal QP results.

In order to reduce the greenhouse, emissions EV is one of the main solutions but a shortage of research regarding charging profiles of EVs has been found. [86] proposed control and management of EV charging using smart and distributed MAS in which designed MAS function is used to achieve better voltage control of DN.In literature, [87, 108] contributed charging station modeling along with modeling of EVs and [119, 75] charging and discharging characteristics of the fleet of EVS. Nevertheless, the EVs considered in these study are mainly private vehicles and also developed MAS in those studies are concentrated on specific problems only. But [68] proposed a new framework for overcoming the deficiencies of [75, 87, 108, 119] by considering existing as well as new agents also different type of EV. Reference

[90] implemented an approach in two steps. In the first step, they considered different uncontrolled EV penetration and analyzed that uncontrolled penetration results in stability issues in the system. Later they proposed MAS based scheduled charging and observed improvement in system stability. An EV coordination mechanism in the distributed manner can be found in [152]. Uncontrolled charging of EVs can lead to severe stress on the power system, [153] explored a MAS based control mechanism that only needs information exchange among agents for the charging rate control of PEVs.

1.3.3.3 Electricity Market

The creative ability of energy industry players are coordinated on what may be done in this information-rich world, yet the way ahead is not clear. By what means should new markets be organized? In what capacity would the data trade be actualized adaptably so that it empowers great decision-making and develops with the business sector and innovation changes? What may the change look like as existing systems get supplanted with new methodologies after some time? What regulation and strategy build should be set up to guarantee dependable administration and a strong framework for the security of the country's economy? To address these questions prior to implementation, the analysis must be supported by simulation. To date, the thorough recreation of the technical accepts of running the framework have been isolated from market simulators [154, 155, 156]. Likewise, the market-based system moves the ideal control model far from centralized power toward appropriated, independent decision making [157]. Appropriately outlined, the outcome can give more prominent efficiencies and unwavering quality of operation, yet it will likewise be a framework with an alternate type of consistency, a system that carries on additional with determined limits such climate, a framework that requires the use of complex framework hypothesis to discover emergent behavior conduct and direct it in a helpful way.

The authors in [122] proposed a market model based on agents in which contributors correspond to storage power plants along with generation power plants. The proposed model uses multi-step optimization to maximize the profit by finding bidding curve in contrast to the agents utilizing heuristics and trial and error approach. Also, the authors used a prize adjuster during the calculation of profit based on an hourly price forward curve (HPFC) which considers the participant to take into account his market power.

For studying the market participant behavior, [109] motivated towards multi-layer MAS architecture. In the first layer renewable power producers and wholesale market players which optimize the bidding/offering strategies have been modeled, and in second layer consumers including PHEV owners and DR program participator are modeled as independent agents. To increase the benefit though retaining welfare is the main objective of a responsive customer. The authors have also used incomplete information game theory algorithm for modeling the interactions between market players in real and day ahead markets.

Reference [158] proposed a MAS-game theory based reverse auction model for microgrid market operation considering renewable and conventional DER. The authors utilized the properties of MAS for monitoring, controlling and performing reverse auction process for DERs and a competitive game-theory reverse auction model was examined to plan the DER unit commitment with one day ahead market approach for the 24 h of the day. Also, the proposed model realistically implemented on Florida International University smart grid test system and found that it can be actualized in the current electric utility grid as new as new assets of the system are added.

1.3.3.4 Generation expansion planning

As an example, California and Australia have already adopted deregulation and restructuring, which lead to significant changes in electricity market i.e., more decentralization and negotiation freedoms have caused original system replacement. So generation expansion planning problem should be considered seriously.In literature it has been found that some researchers have used Distributed Artificial Intelligence (DAI) for negotiation and bargaining [159, 160, 161] and some have developed and proposed game theory based approaches [162].

[105] introduced a MAS based approach for taking an intelligent decision towards coalition formation and cost allocation for electric utility industry in a fully distributed manner. For the healthy investment for generation expansion (GE), different methodologies have been adopted, but there are only limited tools available to investigate the effect of these incentives. [163] developed a MAS based toolbox understanding aftermath of different mechanisms for promoting GE. The authors proved that the developed agent based solution could enable flexible framework, also regulatory authorities to accomplish comprehensive assessments of different methodologies in the specific power system.

1.3.3.5 On-Line Transient Stability Enhancement

For decades, scholars in the power system region have dedicated an extraordinary push to discover extensive dynamic, decentralized strategies to control the instability of the system. To do so obliges examination of the new framework state and blend of a suitable framework reconfiguration. Such investigation must be performed sufficiently quick that the disturbances do not prompt falling arrangements of occasions that will prompt disastrous disappointments and system blackout. On the off chance that where transient stability is an issue, the routine techniques for soundness examination, by a period area iterative procedure, are dreadfully moderate [164].This has driven, researchers to investigate quick direct routines to study the transient stability of power system [165]. [94] proposed MAS based online transient stability strategy by considering two types of agent namely a prediction agent and a control agent. The main function of the prediction agent is to predict power system instability by using a robotic ball-catching algorithm and the control agent act according to the output of the prediction agent to rectify the instability problem if it is there. [93] also proposed MAS based approach for improving transient stability of the system. Here the authors have considered an agent called tracker agent having the function to track rotor angle for identifying transient instability of the system. Tracking agent uses off-line time domain analysis to develop lookup tables of obliged quick valving. Also, the tracking agent utilizes two sub-agents, the first sub-agent is assigned to decide whether fast valving is required for every operating conditions and disturbance whereas the second one is to determine the approximate mechanical power reduction to stabilize the system by comparing the electrical power for each generator before and after the occurrence of disturbance. The function of control agent is turbine fast valving. Hence the author proves MAS can determine PS instability and establish stability. [103] concentrated on developing a MAS based distributed control for large-scale transient stability enhancement of the power system. Initial, MAS model structure is developed by utilizing Wide Area Measurements (WAMs). Besides, the fuzzy technique is acquainted in every agent mode for improving the power system transient stability as an online modification. The intelligent optimization control for the entire system is acknowledged through the tuning among every agent according to fuzzy rules, and finally, the authors proved by simulation results that coordinated distributed control using WA signals is more efficient than distributed control.

1.3.3.6 Smart Grid

MAS innovation has been perceived as a promising new worldview of operation, planning, and design of power grid. MAS utilizes a gathering of heterogeneous and disseminated canny operators which interact with one another and their surroundings to accomplish specific results. Agents exchange data with neighbors and with brought together controller if vital, assemble information from the environment, and may be able to perform psychological figuring out how to adjust to changes in the system [166]. In this manner, MAS give a typical correspondence interface to all framework segments with self-sufficient control activities in a dispersed and decentralized way. It offers a powerful method for serving as the platform for demonstrating self-governing choice making elements and can be utilized to realize smart grid/microgrid ideas for planning and operations.

The authors in [167] addressed the main interfacing issues of MAS simulations in smart grid applications. The complexity of the power system is increasing because of the highest penetration of the renewable energy and leads to the new PS environment. A bottom-up-agent based methodology has the capability to handle the new environment, such that the system reliability can be kept up and expenses reduced. Be that as it may, this methodology prompts conceivable conflicting interest between keeping up secure network operation and the market requirements. [77] proposed a methodology to understand the conflicting interest to accomplish complete optimal performance in the power supply system. The strategy is taking into account a cooperative game theory to ideally distribute resources from every local actor, i.e., system administrators, dynamic makers, and buyers. Through this methodology, agent based capacities, for encouraging both system administrations and vitality markets, can be incorporated and composed. Different MAS based reactive power control strategies in the smart grid have been found in [76, 80, 117, 127] and they try to solve the problem in a distributed manner by decomposing real optimization objective. In fact, all the methods are not fully distributed in a sense some specialized agent exchange information to coordinate the other agents also leads to system inflexibility and still suffer from single point failure. To overcome the above-mentioned disadvantages [116] have introduced a fully distributed technique which does not need any specialized agent for coordination.

The increased penetration of intermittent DERs in DN increases the need for resource management of smart grid in an effective manner. The main motivations of installing DERs are low carbon-based generation and increased revenue for the

resource owner. The availability of DERs highly desponds on the time and day, many environmental factors. [168] introduced completely distributed MAS based algorithm for volt/var control in the smart grid. In which shunt capacitors and voltage regulators are controlled by intelligent agents in a coordinated way to fix the optimal settings for the whole system.

1.3.3.7 Fault detection and Protection

Communication and decision making, play a crucial role in protection, fault detection, and self-healing of the power system. The prompt advancement in communication technology leads thoughtfulness towards protection, fault detection and self-healing in researchers. A decentralized approach can serve better fault detection and protection control for a power network with recurrent changes due to load variation and fault. [99] also explained a MAS based power system protection coordination in distribution feeder in which the overcurrent relay (OCR) functions as a device agent that detects and calculates fault and maximum load current. If any change happens, then it automatically corrects the parameter by coordinating with adjacent agents. Hence, the application of MAS for protection of power system has been justified well.

The authors in [104] presented an agent based Wide Area (WA) primary and backup protection by using IEEE 14 bus system aggregation with fiber-optic Ethernet network. For the purpose of protection, authors have developed a new platform called Electric Power and Communication Synchronizing Simulator (EPOCHS) and used as a platform to combine simulators from different domains. The simulation results show that the performance of agents, concerning the power and communication networks by considering traffic congestion, breaker failure, link losses and agent failure, is superior to the conventional scheme.

For series compensated lines [91] proposed MAS based WA backup protection in which they used agents in such a way that within the protected area, the relay operating procedure of neighboring substations would be organized by each agent by keeping the conventional distance protection principle normally. [106] used MAS based approach for smart grid restoration with Distributed Energy Storage (DES) support. [111] also explained WABP using WA communication network in which WABP algorithm is designed to detect the fault and heal it suddenly by collecting and exchanging the information from WA agents. The main advantage of this method is that it can avoid extensive blackouts due to the fast fault detecting

property.[98] introduced MAS based WA current differential protection scheme by considering power system topological variations.

Reference [72] introduced an agent based concept for understanding and identifying, how grid performance can be improved. The authors have firstly focused on self-healing problem by taking preventive measures using intelligent agents by activating/deactivating control signals according to the situations faced during.

The authors in [70] presented a MAS based self-healing approach by utilizing microgrid agents interacting each other during emergency condition and taking control decision. The simulation results show that the power system self-healing is difficult, but the agent concept to the power system can make power system self-healing easy. Also [67] presented a centralized multi agent power system with superconducting fault current limiter (SFCL) in which they used the property of SFCL to reduce the fault current and an intelligent MAS for detecting the outage and sending control signals to CBs to introduce the SFCL in the circuit during an outage. A study of the self-healing operation of numerous microgrids with MAS transient stability platform is also found [85].

Reference [126] has addressed a MAS based distributed control system for Navy Shipboard Power Systems (SPS) by utilizing less number of human activities while having intelligent self-reconfiguration of the power system under the different scenario. They have mainly concentrated to achieve fault detection, and that reconfiguration of SPS should be done with less response time compared to the human-operated system. Also, [79] implemented a graph theory and mathematical programming based MAS approach for power system reconfiguration and fault detection.

The authors in [114] introduced a case based reasoning MAS for power system protection (PSP), the main advantage of this system is that it can perform well even for incomplete information according to the experience in intelligent participation. Also due to the distributed nature of the proposed MAS it can possess reliability, reusability, and robustness. However [110] developed a relay agent to trip CB during the outage for PSP and results show that relay agent can easily isolate any zone at all extreme condition of the system. Also for multi-terminal lines MAS based distance protection [96] and by the use of communication network, MAS based current differential protection [97] are also found in the literature. For DG system, [107] explored a distributed MAS based high impedance fault (HIF) detection, load shedding and fault location scheme by using the concept explained in [110].

1.3.3.8 Energy Management System and Control

Due to the characteristics such as bidirectional power flows, multi generators, multipurpose infrastructures of microgrids [169] EMS in microgrid leads to new challenges. For tackling these challenges some researchers have focused on EMS-MG (Energy Management System for Microgrid). [81] proposed a MAS based EMS-MG and also tested the effectiveness of the proposed structure in the laboratory with the single and multiple storage systems. [41] developed a MAS based market structure for an MG and validated the negotiation capability of the developed structure separately using power world simulator. [40] introduced MAS EMS-MG developed in Matlab/Simulink but because of the lack of simulation platform the agents developed for market negotiation was simple, and gatherings of the EMS were limited. Also, [100] simulated MAS based EMS-MG digitally for real microgrid so that the efficiency/effectiveness of the control strategies can be validated before implementing it to a real physical system. In literature, two main approaches have been found, namely, Centralized EMS-MG (CEMS-MG) and decentralized EMS-MG (DEMS-MG) [170, 171].The centralized EMS architecture for microgrids has been applied to optimize power scheduling [172, 173, 174, 175], operating costs [176, 177], load sharing [178, 179, 180], and life cycle of storage units [181]. All these studies show CEMS-MG has benefits like complete system operation observability and precise optimization algorithm applicability convenience, but there are shortcomings like the requirement of more computational facilities, higher communication cost and deficiency of flexibility.

In DEMS-MG approach, the obligation and tasks are generally apportioned to the DERs' controllers, and the main function is to act together to manage and optimize the flexible and reliable operation of an MG [182]. The main advantages of DEMS-MG approaches found in the literature are the reduction in information to be exchanged and lesser need of expensive communication networks. In literature, it has also been found that for distributed control mainly used MAS due to its self-mutual action/reaction properties and also utilizes the above advantages. Publication [115] addresses on MAS applications in the control and scheduling of DERs in microgrids. [71], a MAS framework delivered to qualify mutual organization among various agents performing optimal energy exchange between the DERs and the local loads, as well as the main grid. A hybrid EMS-MG system by considering both centralized and distributed control has been implemented by [101]. [95] has implemented MAS to Hybrid energy systems (HES) and shown the agent behavior to prove that the proposed controller can act well enough towards

alteration in system configurations. Also, that the authors have used fuzzy logic to take an intelligent decision is one of the main outstanding contributions in this paper. [89] also explained (MAS) solution to energy management in a dispersed hybrid renewable energy generation system using JADE platform. [84] explored a MAS based EMS to control the fuel cell array very effectively for the purpose of minimizing cost while satisfying the demand. Also, the authors presented that there is no special adaptation required for better performance for MPSOM algorithm to the same problem. They have also diverted to the readers that, in future, one can develop EMS with the capacity to control according to the performance and ability to start and stop fuel cell automatically will help in further cost savings and the MAS implementation leads to the high degree of freedom and flexibility even with sudden system structure alterations.

1.3.3.9 Microgrid

A microgrid is a controllable unit composed of distributed energy resources, storage, loads and control devices. The operation and control of microgrid is the way to guarantee the security and stability of the power grid. [102] designed and implemented monitoring and control of the microgrid based on IP and MAS in Matlab and ZEUS platform and shown the feasibility of MAS based control strategy. [39] demonstrated a MAS in the simulation environment to control distribution smart grid, and shown MAS can enable, smooth transition from grid-connected mode to island mode during the fault condition. [15] presented real-time operation of the microgrid with the help of MAS in which they have considered different DER agents, load agents, energy storage system agents. Simulation studies shown that the MAS can manage DERs and loads in real time in both grid-connected and islanded mode.

DER can be made adaptable and hearty with a coordination methodology that considers effectively including or evacuating energy resources. An energy node can extend as interest expands and can change configuration effortlessly. [41] suggested that the distributed coordination, a potential technique to understand these advantages, can be executed by utilizing MAS. It is conceivable to apply a distributed coordination way to deal with facilitating DES (distributed energy system) at the key level. DES is likewise self-sorting out, permitting agents to be included or uprooted whenever with no reliance on a particular agent. By utilizing this, distributed coordination appears like a conceivable procedure to understand the advantages of DES. At last, the idea of MAS based distributed coordination

should be joined with a real hardware framework to show a complete agent based solution for DER management. Keeping in mind the end goal to accomplish it, the future exploration will be centered around intelligent Micro Grid operations such as forecasting of load, RES power production forecast, economic resource scheduling and DSM, which can be added on this Micro Grid modeling. Also [16] created a MAS that amplifies the power generation of local DG and minimizes the operational expense of microgrid subject to system and units constraints for microgrid during the islanded mode.

Authors in [20] implemented MAS based microgrid energy market with DGs and price sensitive loads in consideration. In which scheduling and market coordination have been done as a task assigned to the DG agents and prize sensitive load agents either maximize DG or load surpluses or both. Due to the high penetration of DER, the connection of power converters to the electrical network has been boosted, and it permits for the formulation of MG and local networks when main grid failure occurs due to any reason. But it leads to overcurrent transients due to the connection/disconnection of MG, and it is undesirable. In order to solve this issue [17] introduced an intelligent connection agent (ICT) having a task of purposeful disconnection and reconnection of the main grid according to the grid condition. Also, the authors have shown the simulated and experimental results.

Reference [21] introduced MAS-grid control as a solution for todays power system for maintaining dynamic as well as adequate power balance in changing system conditions. [22] presented MAS for real-time operation of MG which mainly focuses on DSM and generation scheduling. The authors have mainly considered two types of agents i.e. firstly schedule coordinator agent is having two duties like a day ahead and real-time scheduling. The day ahead scheduling is done here for finding the hourly DER from day ahead market. Whereas real-time scheduling updates the power settings of the DER by utilizing the day ahead scheduled data and feedback from RTDS. And the second agent i.e. DSM agent accomplishes load shifting before the day-ahead scheduling, and also curtailment of the load in real-time whenever it is possible and needed. [23] proposed a hybrid control scheme which is based on MAS to improve the economic and environmental benefits and also for ensuring secure voltages. The developed control scheme composed of different levels of agent architecture namely top-level energy management agent, several interlevel control agents, and bottom level unit control agents to accomplish the aim of smart control. Real-Time Microgrid Power Management and Control with Distributed Agents can be found in [69].

For improving the security and stability of microgrid, [24] proposed a MAS based two hierarchal distributed control scheme. In [24] the upper-level agent is assigned with the duty to develop switching control strategies for ensuring the microgrid security and the lower level agents are designed for decentralized continuous control for assuring unit system stability and showed the effectiveness of proposed scheme by simulation. Also in [25] developed a two-layer MAS based control structure for islanded microgrid and shown, with the help of agent based control strategy the output power supplied by the DG can able to fulfill the load requirements of the microgrid.

Under uncertain communication topologies, [26] introduced a pinning based cooperative control strategy for autonomous microgrid, which uses the MAS technology. In this only less fraction of pinned agents is directly controlled by simple feedback controllers, whereas MAS synchronization of all other DG agents is done by distributed communication coupling among pinned agents. A fully distributed microgrid control which eliminates the need of central controller and difficult communication topology, reduces the requirement of controllers by controlling less fraction of pinned agents, also can meet the requirements of plug and play operations and line switches for a microgrid are the main highlights of this work. In a droop controlled microgrid for improving frequency and reliability, [27] proposed dynamic energy level balancing strategies between distributed storage devices in which the authors have used MAS cooperative control in a distributed fashion for modifying power output of droop controlled storage devices for achieving the balanced energy state. Also, [183] developed MAS based control schemes for managing the power-sharing between the energy storage devices distributed in a DC microgrid. This system can overcome the advantages offered by the hybrid energy storage system without any need of a central controller. And in [184] introduced a unified distributed control strategy for different operating modes of DC microgrid, without bus voltage signaling or mode detection mechanisms that are normally needed for distributed control schemes. A comprehensive economic power transaction of the multiple MGs network with MAS can be found in [185]. [186] introduced a MAS that can effectively manage the DERs connection/disconnection by using a plug and play algorithm so as to reduce the mismatching of demand and supply balance and also limit the power drawn from utility grid during peak hours in DN. Also, state of the art on holonic structure based MAS for reactive power dispatch in smart grid can be found in [187].

Table 1.3: Practical Applications of MAS to Power System

Product Name	Application(s)	Remarks	Author
ARCHON(AR-chitecture for Co-operative Heterogeneous ON-line systems)	Distribution network fault diagnosis	ARCHON was supported by Iberdrola, and has been deployed in a control room in Bilbao [188]	[189]
PEDA (Protection Engineering Diagnostic Agents)	Post-fault analysis	A number of the PEDA agents were deployed in the UK with SP Power Systems [42]. The deployment leads to understanding the software challenges of MAS required for an industrial system needing new technologies and approaches for achieving stability and maintainability.	[190]
COMMAS(COndition Monitoring Multi-Agent System)	Gas turbine start-up sequences. Transformer condition monitoring. Dissolved gas analysis of historical data and PD analysis of lab samples. Deployed on-site for HVDC reactor monitoring. Deployed on a wireless sensor network for transformer monitoring.	Second practical implementation deployed with National Grid	[191] [192] [193] [194] [195]

SPID (Strategic Power Infrastructure Defence)	Network Reconfiguration. Generating a restoration plan after an incident.	System was created to identify and resolve the types of hidden failure of components that can leave the system vulnerable to cascading events.	[196] [197]
IntelliTEAM II	Automatic Restoration System (restoration plan after isolation of a faulted line section)	The system has been deployed with the ENMAX Power Corporation in Canada on key circuits	[198] [199]
PowerMatcher	Demand management in congested or constrained networks	First test had control agents with five devices in 2006 to reduce supply and demand imbalance. The second field test used five micro-CHP devices as a virtual power plant in 2007 for reducing the peak load of the local network. The third and largest test is PowerMatcher City with agents deployed with 100 controllable devices split across 30 households and two laboratories.	[120] [200]
AuRA-NMS(Autonomous Regional Active Network Management System)	Congestion management	Field trial can be found in [201]	[202]
INTEGRAL	Distributed control of electrical networks	Performance was tested on a LV laboratory-based test network,i.e. sized to represent a real 20 kV DN in France [203].	[204]

Table 1.4: Application of MAS to Power Systems by Technical Areas

Distribution System Management with DGs
[136]; [121]; [124]; [73]; [74]; [120]; [78]; [83]; [92]; [88] [138]; [139]; [140]; [141]; [142]; [143] .
Electric Vehicle management system
[136] [68]; [108]; [118]; [119]; [75]; [123]; [82]; [125]; [86]; [87]; [112]; [152]; [168].
Electricity Market
[122]; [109]; [158].
EMS and Control
[71]; [95]; [40]; [41]; [100]; [101]; [81]; [84]; [89] ; [115]
Generation expansion planning
[105]; [163].
Micro Grid
[15]; [69]; [23]; [20]; [21]; [41]; [16]; [22]; [81]; [39]; [17]; [102]; [24]; [25]; [26]; [183]; [27]; [184]; [185] .
On-Line Transient Stability Enhancement
[103]; [93]; [94].
Fault detection, Protection and Self-healing
[70]; [96]; [97]; [72]; [104]; [126]; [99]; [79]; [106]; [85]; [98]; [67]; [110]; [111]; [114]; [107]; [91].
Smart Grid
[76]; [127]; [80]; [77]; [116]; [117]; [168]; [186]; [187] .

1.3.4 Review on RES Forecasting

The short-term power prediction methods of PV and wind are broadly classified into physical and statistical methods. The physical methods involve the forecasting established by physical equations by PV and wind generation process along with the weather data [205]. The statistical methods utilize the historical power data to forecast the upcoming PV and wind generations [206, 207, 208]. Traditionally, lin-

ear and nonlinear autoregression approaches have been used for forecasting. The increase in nonlinearities in the data made the researchers to doubt the accuracy of such models and think about alternative models. Nowadays, the researchers in the field of PV and wind prediction are concentrated towards the artificial intelligence techniques due to its inherent capability to track the complex nonlinearities in the system. The artificial intelligence model includes fuzzy logic methods [209], artificial neural network (ANN) [210, 211] and support vector machine (SVM) [212], etc. Reference [213] used Evolutionary Programming (EP) and Particle Swarm Optimization (PSO) algorithm for tuning the hyperparameters of the SVM for improving the accuracy SVM based wind speed forecasting model. The authors in [214] proposed a hybrid forecasting model by using fuzzy information granulation and SVM, In which the authors have used fuzzy information granulation for refining the data, and after that, SVM uses that for forecasting. A hybrid forecasting model developed by combining three algorithms, i.e., wavelet transform (WT), genetic algorithm (GA) and SVM can be found in [215].The self-adaptive data-driven neural network can approximate any arbitrary continuous function to any given accuracy without needing large knowledge on the structural relationship [216]. The fuzzy logic can also be used for the same with the greatest accuracy [217]. The performance of the neural network and fuzzy logic models are good enough as compared to autoregression approaches and has been implemented in various engineering problems [218, 219]. An expert system with rule-based forecasting approach by incorporating weight extrapolation methods and utilizing the features of time series can be found in [220].The forecast by weather information is difficult because the accurate measurement and availability of weather data are expensive. Moreover, the measurement errors induce information to the forecasting model and may lead to inaccurate forecast [221]. As a dynamic system, the wind has a relationship with its former values at any time [222]. So, an accurate and simple forecasting model by using historical data is required.

1.3.5 Review on Load Forecasting

Electric load forecasting is the practice used to forecast upcoming electric load using known historical load and historical, current and forecasted weather information. Load forecasting is normally carried out to help planners in creating decision strategies with regards to unit commitment, interchange evaluation, hydro-thermal co-ordination and security assessments [223]. Due to these reasons, electrical demand forecasting has turned into one of the key research areas in power engineer-

ing. The short-term to long-term load forecasts are required with different lead times for power industry because nowadays the privatization and deregulation has been adopted by the power systems in many countries. The electricity has been transformed into a commodity to be marketed and purchased at market prices. Since the load forecasts perform a significant part in the structure of those prices, so load forecasting has become vital for the supply industry. The cost-effectiveness of the system is directly dependent on the load forecasting accuracy [224]. Load forecasting is primarily classified into four categories based on time: long term, medium term, short term and very short-term load forecasting [225, 226, 227]. Out of these Short Term Load Forecasting (STLF) is more important in efficient decision making process [228] and also the importance of STLF explained in detail can be found in [229].A small increase ($\approx 1\%$) of forecasting error can lead to an increase of operating cost of 10 million pounds for an electric utility in the UK [230] is a magnificent example of LF significance.

There are a lot of load forecasting(LF) methods that can be found in literature and simply be classified as conventional regression models, AI-based models, Computational Intelligence(CI) models, bioinspired and hybrid models [231, 232, 233, 234]. In the past few decades, different techniques combined with neural network architectures have been most frequently used. The main problems associated with neural network models are overfitting and the curse of dimensionality, which reduces the forecasting accuracy. Grey Index Models [235],[236] are applied when the information about datasets and its cause factors is incomplete. Most of the traditional load prediction models are single neural network based and may pervert the mapping of input and output. In literature, [237] presents a cooperative co-evolutionary (Co-Co) approach for load and market clearing price forecasting of the next day which can overcome the abovementioned limitations by multiple networks [238]. Also, [239] introduced a hybrid forecasting model that integrates several artificial neural networks and model selection for load forecasting. [240] studied the importance of load profiling on LF with neural network and investigated the importance of different input by the use of the concept of partial derivatives to understand the relevance of including this type of data in the input space. A combination of improved harmony search algorithm and refined exponentially weighted fuzzy time series for LF can be found in [241]. The authors in [234] used improved grey dynamic model for STLF. [242] proposed a novel recurrent extreme learning machine (RELM) technique for LF. In [243] proposed a new two-step algorithm, in the first step the author's used wavelet transform (WT) and an artificial neural network (ANN) for primary forecasting of next 24 hours load.

In the second step for improving the accuracy of the primary forecast, a similar-hour method and adaptive neural fuzzy inference system (ANFIS) is employed. In [244] gives two methods to forecast load demand and price from the historical data and are based on principal component analysis and nonparametric models with functional both response and covariate. Moreover, the nonparametric suggestion is prolonged to integrate, in a linear way, exogenous scalar covariates. A clustering based load forecasting model is represented in [245]. Fractal interpretation and wavelet analysis based load forecasting model is introduced in [246]. In this model, first the authors used multi-resolution wavelet to analyze the self-similarity of the historical load data and then calculated the vertical scaling factors in Iterative Function System (IFS) using Hurst parameters values and remaining parameters of affine transformation can be calculated using vertical scaling factor. For tackling the uncertainties present in LF, a new random fuzzy neural network is proposed in [247]. In [248], the performance of aggregation algorithms is examined for load forecasting based on neural network.

A generalized neural network with the integration of fuzzy logic and wavelet transform for STLF is proposed in [249] to overcome the inherent limitations of ANN models. Support Vector Regression in [250], comes up with an idea to use the determining part of the given information, i.e., support vectors, which are obtained with the help of an epsilon-tube performing bandwidth selection. The drawback of this method is that it offers single bandwidth selection throughout the data points, and thus cannot accommodate all possible situations. Bayesian Multivariate Linear Spline (BMLS) approach outperforms by making use of variable bandwidth. Moreover, it offers advantages like, it uses local and piecewise linear models, it is highly interpretable and the procedure of disintegration of design space into the linear region [251, 252].

1.4 Research Gaps

Most of the aforesaid research concluded that multi agent based energy management could yield better efficiency and can also manage complex DGs efficaciously due to the competence of multi agent system (MAS).

- In the centralized scheme, a microgrid central controller is used to optimize the economic power dispatch for DERs and storage system. As the number of components in the microgrid increases, the central controller faces certain

issues like the requirement of large measurements and it also increases the complexities in solving the optimization problem.

- A major concern with the centralized scheme is the chance of single point failure in the system that can lead to a complete system failure which questions the reliability of the system.
- Due to the high penetration of renewable energy resources, it is challenging to provide a reliable, consistent power supply for local customers, because of the unpredictable and intermittent nature of these renewable energy resources.
- The electricity load demand also changes due to the season effect and human behavior which results in difficulties in energy management.
- An intelligent microgrid operation would be required which incorporates load forecasting, Renewable Energy Source (RES) power production forecasting and resource scheduling into the microgrid modeling in future.
- Most of the research mainly addressed the energy management functionality for MGs by utilizing the multi agent system. However, the self-healing capability is also equally important in case of a smart microgrid for flexible and resilient operation during an outage. A scanty amount of research in the field of microgrid energy management with self-healing capabilities has thus been found.

1.5 Research Objectives

In view of the above discussions, this work proposes a new multi agent based architecture for energy management in a smart microgrid with self-healing capabilities as illustrated in Figure 1.5.

For developing the proposed architecture following objectives have been formulated:

1. To develop a microgrid test bed for studying the performance of the proposed multi agent based architecture for microgrid energy management.
2. To propose an accurate renewable energy source (RES) forecasting model for the development of RES forecasting agent for proposed microgrid energy management.

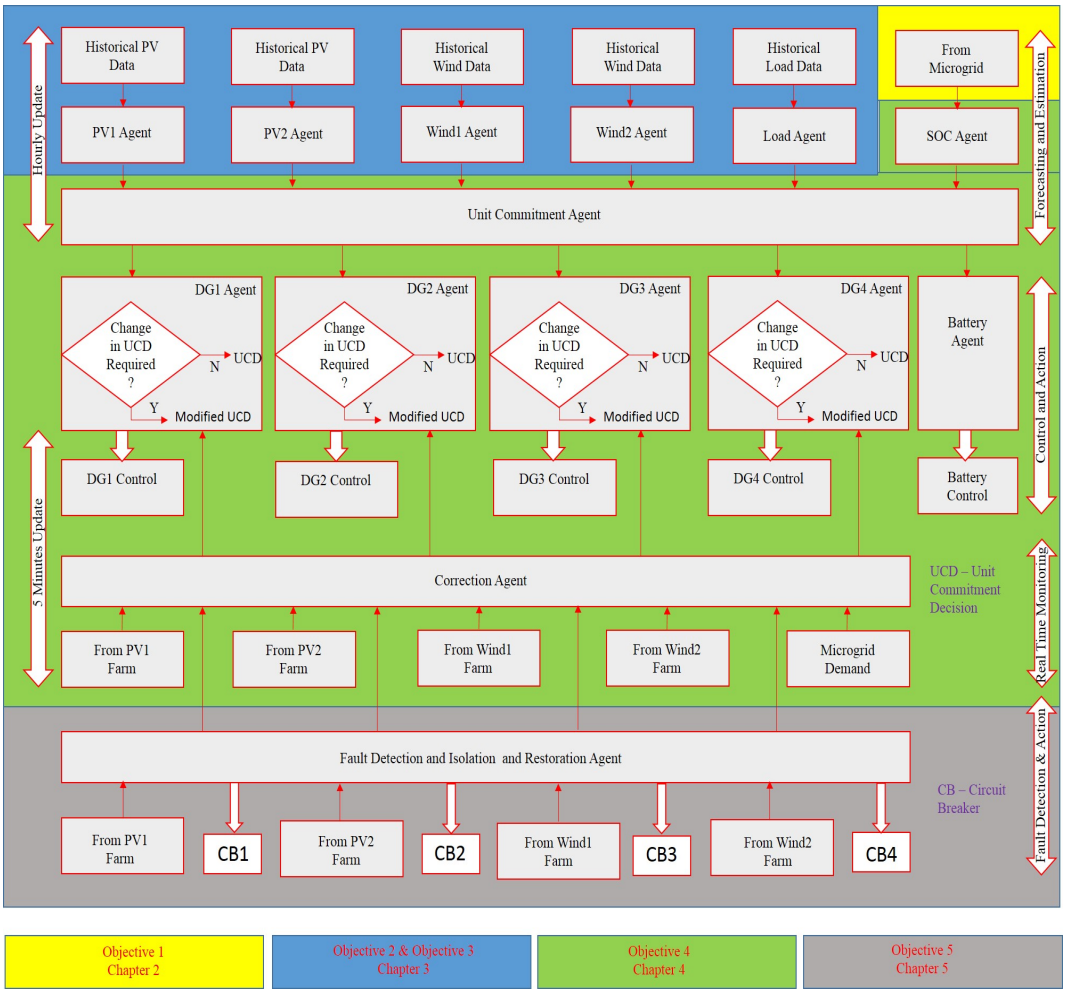

Figure 1.5: Proposed MAS based architecture for energy management in a smart microgrid with self-healing capabilities

3. To propose an accurate load forecasting model for the development of load forecasting agent for proposed microgrid energy management.

4. To develop control strategies for optimal energy management operation in the microgrid.

5. To propose a new self-healing scheme for the pro-active restoration of microgrid during the fault.

1.6 Thesis Organization

This Ph.D. thesis consists of six chapters, including introduction and conclusions. Figure 1.6 provides the organization of the thesis in the form of a block diagram highlighting the significant portions covered in each chapter.

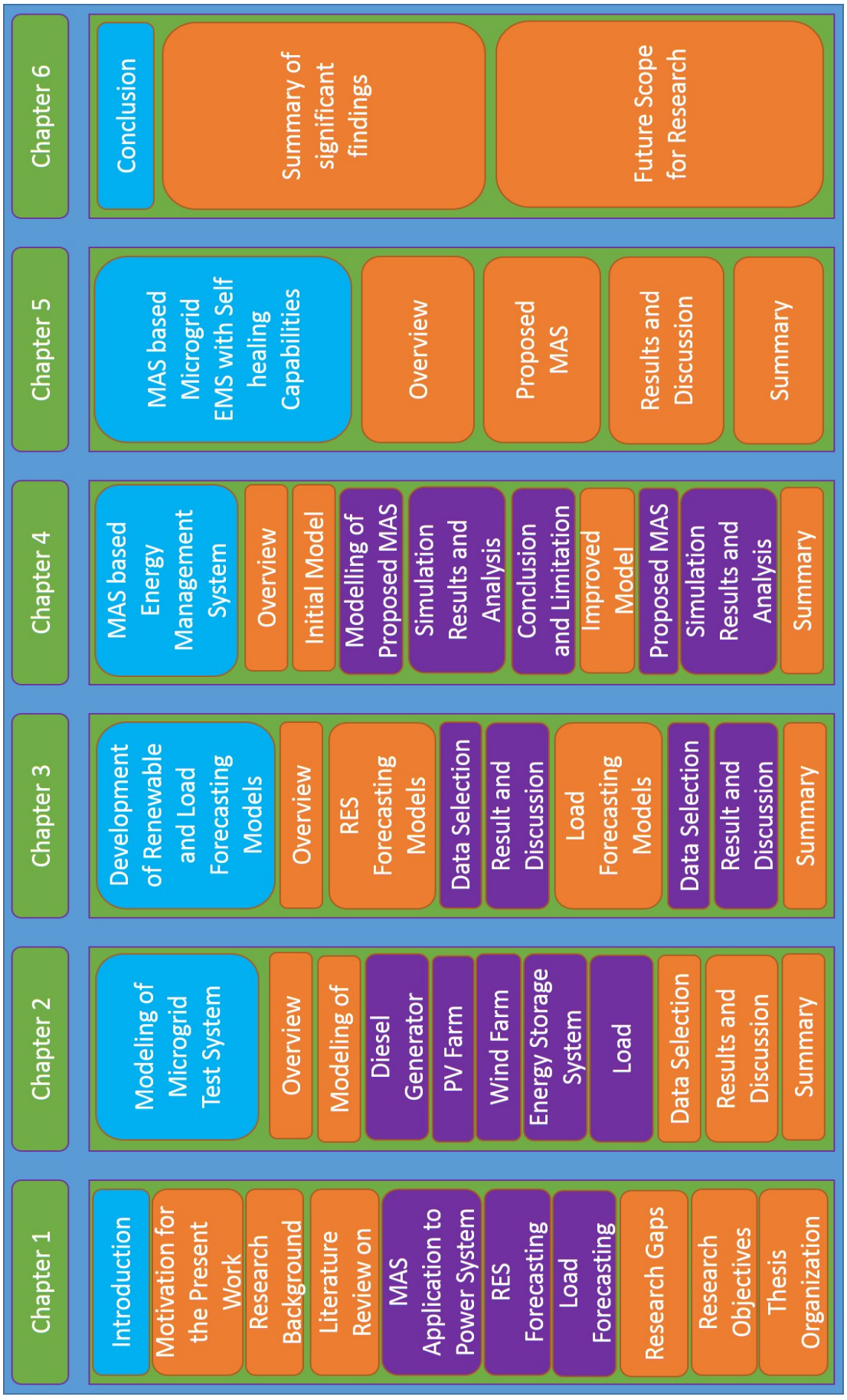

Figure 1.6: Thesis Organization

Chapter 2

Modeling of Microgrid Test System

2.1 Overview

This chapter develops a microgrid (MG) test system comprises of diesel generators, wind farms, PV farm, loads and a battery storage system. It also covers the detailed modeling of each component in the microgrid, i.e., diesel generators, wind farms, PV farm, loads and a battery storage system. The microgrid test system developed in this chapter is further utilized to study the effectiveness of multi agent based microgrid energy management in this work.

2.2 Microgrid Modeling

Figure 2.1 shows the schematic diagram of the microgrid model used to study the effectiveness and applicability of the proposed energy management system. The microgrid is developed in Matlab Simulink with phasor-mode simulation. The primary reason for using the phasor-mode simulation is its faster run-time. The microgrid comprises of four diesel generators, two wind farms, two PV farms, energy storage and loads. The diesel generator is used in the microgrid is for providing base power. Table 2.1 shows the parameters used to model each component of the microgrid. The detailed modeling of each component of the microgrid has been discussed in the following sub-sections.

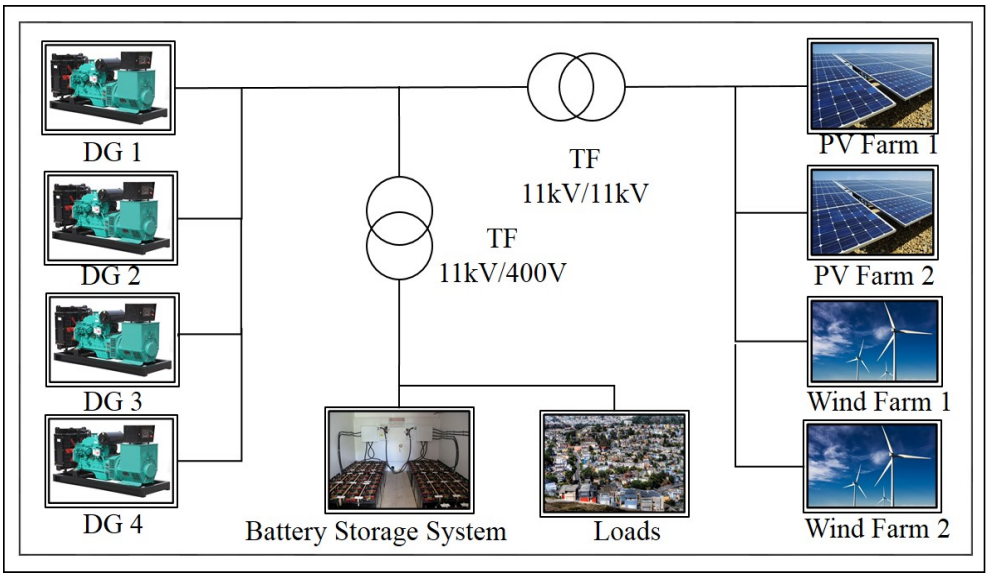

Figure 2.1: Proposed Microgrid Model

Table 2.1: Simulation Parameters

Component	**Description**	**Specification**
Diesel Generator	DG1	2.5 MW
	DG2	1000 kW
	DG3	500 kW
	DG4	500 kW
PV System	Efficiency	10 %
	Nominal Power Output	250kW
	Area	5000 m^2
Wind Farm	Nominal Power Output	250 kW
	Cut in wind speed	2.5 m/s
	Rated wind speed	7.5 m/s
	Cut out wind speed	11 m/s
Battery Storage	Nominal Voltage	400 V
	Battery Capacity	10800 Ah
	Efficiency	90 %

2.2.1 Diesel Generator Modelling

The diesel engine generator in the microgrid is represented by a synchronous machine block operating in generator mode having a diesel engine governor system, and an excitation system. The governor system consists of an actuator and a control system modeled using transfer functions. The inputs to the governor are the reference speed and the actual speed. The difference in reference speed and actual speed is given to the controller, and then the controlled output is provided to the actuator. The output of the governor is the mechanical power to the synchronous

machine working in generator mode. The controller and actuator are modeled using the transfer function as given in Eq .(2.1) and Eq.(2.2) [253].

$$T_c = \frac{k\,(1 + T_1 s)}{1 + T_2 s + T_2 T_3 s^2} \tag{2.1}$$

Where,

T_c - Controller transfer function.

T_1, T_2, T_3- Regulator time constants in seconds.

k-Gain

$$T_A = \frac{(1 + T_4 s)}{[s(1 + T_5 s)(1 + T_6 s)]} \tag{2.2}$$

Where,

T_A - Actuator transfer function

T_4, T_5, T_6- Actuator time constants

The excitation system is modeled using the transfer function represented in Eq.(2.3) [253]

$$\frac{V_{fd}}{V_{ro}} = \frac{1}{K + sT_e} \tag{2.3}$$

Where,

V_{fd} - Exciter voltage

V_{ro} - Regulator volatge

K - Gain

T_e - Time constant in seconds.

The overall efficiency of diesel generator can be expressed as Eq.(2.4)

$$\eta_{overall} = \eta_{BT} * \eta_{Gen} \tag{2.4}$$

Where, η_{BT}- Brake thermal efficiency.

η_{Gen}- Generator efficiency.

2.2.2 PV Modelling

The power output of the modeled PV farm depends on solar irradiance, PV panel efficiency and total solar panel area. The power output relationship is modeled as represented in Eq.(2.5).

$$P_{pv} = IP_f A_{pv} \eta_{pv} \tag{2.5}$$

Where,

I- Solar irradiance in W/m^2.

P_f- Partial shading factor.

A_{pv}- Total solar panel area in m^2.

η_{pv}- Efficiency of PV panel (approximately 10 %).

2.2.3 Wind Farm Modelling

The power available from an electric wind generator can be represented as in Eq. (2.6) [254] and is proportional to the cube of wind velocity. Hence, a small change in wind velocity can produce large variation in energy generated and in the cost of generation.

$$P_W \propto V_w^3 \tag{2.6}$$

Where,

V_w- Average wind velocity in m/s.

The wind turbine will produce nominal power when wind speed reaches its nominal value. Though when the wind speed increases above maximum wind speed, the wind turbine isolates itself from the grid and stay offline until the wind speed returns to its nominal value. The power output from the wind farm is modeled as represented in Eq. (2.7).

$$P_{wind} = \begin{cases} V_{wind}^3 \frac{P_{Nom}}{V_{Nom}^3} & ; V_{wind} \leq V_{Nom} \\ V_{Nom}^3 \frac{P_{Nom}}{V_{Nom}^3} & ; V_{Nom} \leq V_{wind} < V_{Max} \\ 0; \quad V_{wind} \geq V_{Max} \end{cases} \tag{2.7}$$

Where,

V_{wind} - Actual wind speed in m/s.

V_{Nom} - Nominal wind speed in m/s.

V_{max} - Maximum wind speed in m/s.

P_{wind}- Wind power output in kW.

P_{Nom}- Nominal wind power output in kW.

2.2.4 Energy Storage System Modelling

An energy storage system is required for providing auxiliary services during power mismatch in the microgrid [254]. The energy storage system for the microgrid is modeled in such a way that it can store energy during excess power production from renewable sources and is also able to supply to meet load requirements of the microgrid during a power shortage. Also, the battery control in the proposed model is constrained in a manner that the battery will charge only when there is an excess power production from the distributed renewable energy resources, not from the diesel generators. The battery is modeled according to the characteristics of deep cycle lead acid batteries, and battery dynamics are represented as in Eq.(2.8) and Eq.(2.9) [253].

$$B_{SOC} = 100[1 - (\frac{1}{Q_B}) \int_0^t i_B(t)dt] \tag{2.8}$$

$$B_{AH} = \frac{1}{3600} \int_0^t i_B(t)dt \tag{2.9}$$

Where,

B_{SOC}- State of charge of battery in %.

Q_B- Maximum battery capacity in ampere hour

i_B- Battery current in ampere.

B_{AH}- Battery ampere hour.

2.2.5 Load Modelling

Load model consists of two types of loads, commercial loads, and residential load. The commercial load is indicated using the asynchronous machine with the capacity of 0.2 MW to incorporate the effect of inductive loads like air conditioner, refrigerator, heating loads in the microgrid. The residential load is modeled using the real 24-hour variations in load at the Tioman Island with one hour span utilizing a lookup table.

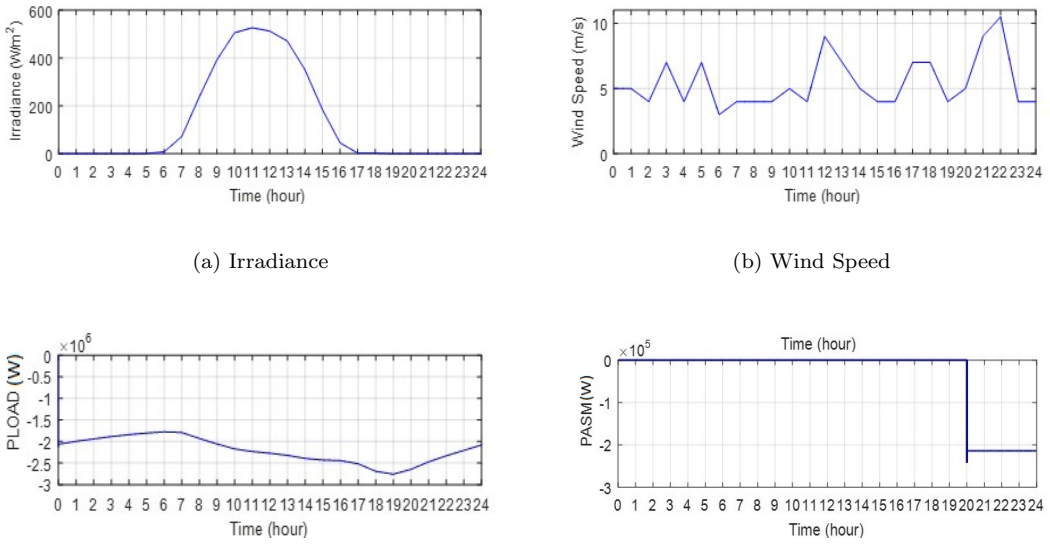

(a) Irradiance

(b) Wind Speed

(c) Residential Load Profile

(d) Commercial Load

Figure 2.2: Irradiance, Wind Speed and Loads used for Simulation

2.3 Data Selection

The performance of the proposed model is evaluated based on data collected from Tioman Island. The Tioman Island is the resort island in the South China Sea within the east coast of Peninsular Malaysia, located at $104°10'24''E$ longitude and $2°47'47''N$ latitude. The solar irradiation profile and wind speed used for the simulation study are shown in Figure 2.2(a) and Figure 2.2(b) respectively [255]. The irradiation profile follows a typical pattern with the maximum irradiation ($526.99\ W/m^2$) occurring during the middle of the day. The wind speed varies with several peaks and troughs significantly throughout the day. Since the simulation is based on the data collected from the Tioman island resort, the load follows a

distinct profile due to tourist activities. The load demand of the island at the beginning of the day is minimum, and it gradually increases and meets the peak by evening and drops at night as shown in Figure 2.2(c). The load profile data used for the simulation is extracted from [253] and the maximum and minimum load values are 2.75 MW, and 1.77 MW respectively found. Also, Figure 2.2(d) shows the commercial load profile used in the simulation case study.

2.4 Results and Discussion

The model shown in Figure 2.1 is simulated for 24 hours duration to analyze the performance of the microgrid model.

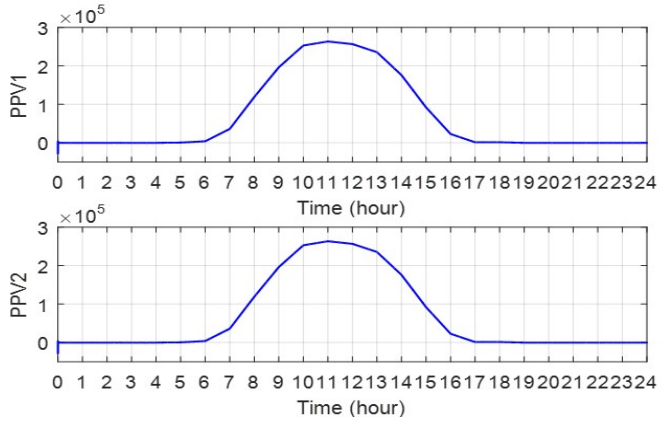

Figure 2.3: Power Output of PV Farm

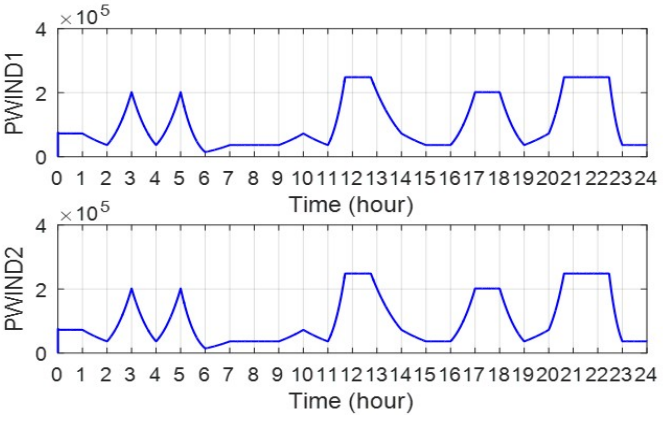

Figure 2.4: Power Output of Wind Farm

Figure 2.3 shows the output power generated from PV farm1 and PV farm 2 respectively as PPV1 and PPV2 in watts. It is clear from both waveforms that the solar power follows the irradiance pattern represented in Figure 2.2(a). Figure

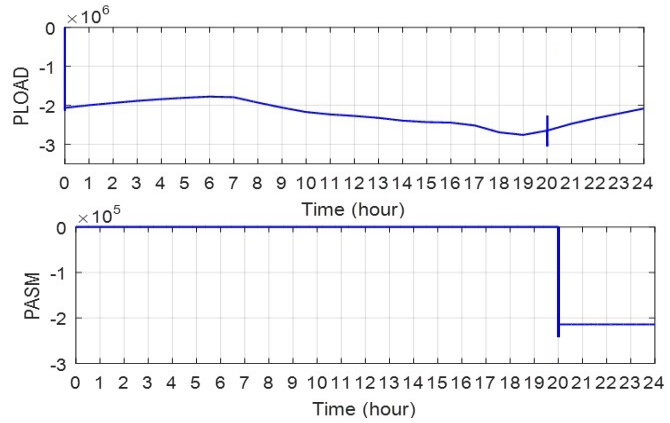

Figure 2.5: Load requirement of microgrid

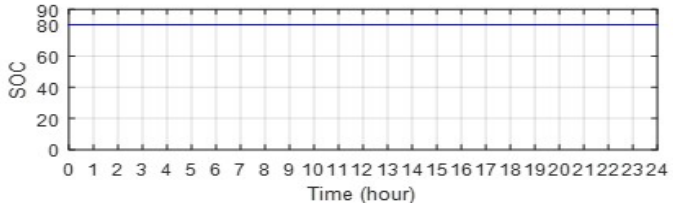

Figure 2.6: Battery SOC

2.4 displays the output power of wind farm 1 and wind farm 2 respectively as PWIND1 and PWIND2 in watts. As the wind power output is proportional to the cube of the wind velocity, it trails the pattern of wind speed represented in Figure 2.2(b). The load demand of the system in watts is shown in Figure 2.5. Where the PLOAD represents the residential load demand, and the PASM represents the commercial load demand in the system. Figure 2.6 shows the state of charge of the battery in % during 24 hours simulation. In Figure 2.6 the state of charge of the battery is constant because the battery control action is not performed since there is no excess power requirement in the system as all the diesel generators are active. The battery is not charged throughout the simulation because the battery controller is constrained that the battery will charge whenever there is an excess power produced by renewable distributed energy resources. The output power provided by diesel generators in watts to meet the load demand of the microgrid is presented in Figure 2.7. Which shows the power produced by the diesel generator 1, diesel generator 2, diesel generator 3 and diesel generator 4 (PDG1-PDG4) respectively.

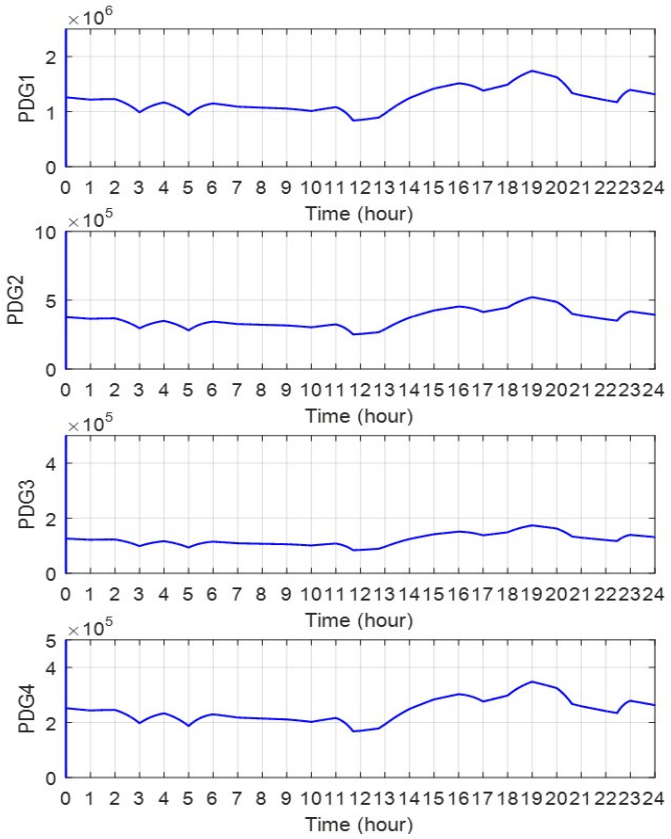

Figure 2.7: Power Output of Diesel Generators

2.5 Chapter Summary

In this chapter, a microgrid test system has been modeled by incorporating diesel generator, PV farm, wind farm, battery, residential and commercial loads. The simulation for 24 hours scenario has been carried out to analyze the performance of the microgrid model developed. The simulation results are shown to justify the effectiveness and to analyze the performance of the system model for further studies. The model developed in this chapter is utilized in chapter 4 for the development of multi agent based autonomous energy management system and chapter 5 for a multi agent based energy management with self-healing capability.

Chapter 3

Development of Renewable and Load Forecasting Models

3.1 Overview

Due to the high penetration of renewable energy resources, it is challenging to provide a reliable, consistent power supply for local customers, because of the unpredictable and intermittent nature of these renewable energy resources. Moreover, the electricity load demand also changes due to the season effect and human behavior. Accordingly, an accurate forecasting of power generation and load demand are required to solve unit commitment and schedule the operation of energy storage devices. Therefore, this chapter discusses the different renewable (PV and wind) forecasting models and load forecasting models. Initially, this chapter discusses the adaptive neuro fuzzy inference system (ANFIS) based forecasting models for PV and wind output power forecasting. Later, linear time series (LTS), support vector regression (SVR) and Bayesian Multivariate Linear Spline Model (BMLS) load forecasting models. The performance of the developed models have been analyzed using different indices, and the model which gives the better performance is utilized further for developing the respective forecasting agents for proposed multi agent based microgrid energy management system.

3.2 PV and Wind Forecasting Model

A review on the short-term power prediction methods of PV and wind are provided in section 1.3.4. The accuracy of ANN models are proven to be higher as compared to other short term prediction models for PV and wind prediction [256]. Even though the ANN models have the capabilities of nonlinear modeling, it possesses some disadvantages that it is considered as a black box and rules are not easily explicable[257]. These rules can be recognized by the implementation of fuzzy logic, but the number of variables associated with it is large and make it complex in dealing [258]. This work utilizes an ANFIS based forecasting model for the wind and PV generation forecasting. ANFIS model utilizes the principles of both neural network and fuzzy logic. Neural networks are included in the class of supervised learning algorithms which uses historical data to predict the upcoming values. Whereas in fuzzy logic the control signal is produced from firing the rule base. The rule base is random in nature and extracted from historical data. This leads to the random controller output. The advantage of using ANFIS prediction model is that it makes the rule base more realistic and adaptable to the situation by the use of the neural network. The capability of fuzzy logic to approximate a nonlinear function by its intelligence in developing if-then rules makes this hybrid technique to be a universal estimator [259].

3.2.1 Basic Structure of ANFIS

Adaptive Neuro Fuzzy Inference System (ANFIS) is a technique that is developed by the hybridization of the fuzzy inference system and neural networks by effectively utilizing the advantages of two cutting-edge technologies. The fuzzy logic inherently incorporates the uncertainty and fuzziness of the system that is being modeled. On the other hand, the neural network introduces the intelligence of adaptability in the model [260]. The fuzzy inference system that considered to model maps

1. Input to input membership function (MF)
2. Input MF to associated rules
3. Rules to output characteristics
4. Output characteristics to output MF

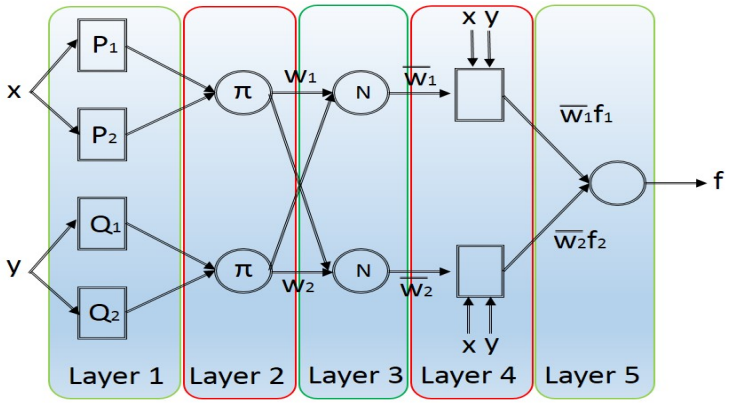

Figure 3.1: Basic Structure of ANFIS

5. Output MF to final output or associated decision.

For the better understanding of the structure of the ANFIS consider a fuzzy inference system with one output and two inputs. The rule base comprises the fuzzy if-then rules of Takagi and Sugenos type as in [261] are.

If x is P and y is Q, then z is f(x,y)

Where ,

P and Q - fuzzy sets in the antecedents.

z=f(x,y) - crisp function in the consequent.

Generally, the f(x,y) is considered to be a polynomial function for a given input variables x and y. However, it is not necessary that to consider it as a polynomial function always, can be any function that can describe the output of the system inside the fuzzy region provided by the antecedent. A zero order Sugeno fuzzy model is achieved when treating the f(x,y) as a constant and can be considered to be a distinct case of Mamdani fuzzy inference system [262] where every rule consequent is described by a fuzzy singleton. When considering f(x,y) is to be a first-order polynomial a first-order Sugeno fuzzy model is achieved. The rules of a first order two rule Sugeno fuzzy inference system can be expressed as follows.

1. IF x is P_1 and y is Q_1 THEN $f1 = k_1x + l_1y + m_1$
2. IF x is P_2 and y is Q_2 THEN $f2 = k_2x + l_2y + m_2$

Here, the output of each rule is a linear combination of input variable along with the addition of a constant in the inference system. The final output is the weighted

average of each rule's output. The Figure 3.1 shows the equivalent ANFIS structure.

The each layer in the structure is briefly explained as follows

Layer 1: Each node i in the layer is adaptive with a node function

$$N_i^1 = \mu P_i(x) \tag{3.1}$$

Where,

μP_i- Membership function of P_i.

x - input to the i_{th} node.

P_i - linguistic variable related to node function.

Generally, $\mu P_i(x)$ is considered to be

$$\mu P_i(x) = \frac{1}{1 + [(\frac{x-c_i}{a_i})^2]^{b_i})} \tag{3.2}$$

Or

$$\mu P_i(x) = exp\left\{-(\frac{x - c_i}{a_i})^2\right\} \tag{3.3}$$

Where,

a_i, b_i, c_i- set of premise parameters.

Layer 2: This layer calculates the firing strength w_i of the particular node and produces an output corresponding to the product of incoming signals to that node represented as in

$$N_i^2 = w_i = \mu P_i(x) * \mu Q_i(y), i = 1, 2 \tag{3.4}$$

Layer 3: This layer calculates the normalized firing strength of the i_{th} node rule i.e. the ratio of firing strength of the particular rule to the sum of firing strength of all incoming rules in the node.

$$N_i^3 = \bar{w_i} = \frac{w_i}{w_1 + w_2}, i = 1, 2 \tag{3.5}$$

Layer 4: The each node in this layer is an adaptive node with a node function expressed as.

$$N_i^4 = \bar{w_i} f_i = \bar{w_i}(k_i x + l_i y + m_i) \tag{3.6}$$

Where,

k_i, l_i, m_i- set of consequent parameters.

$\bar{w_i}$- Output from the layer 3.

Layer 5: This layer calculates the final output as the summation of all the incoming signals in that node.

$$N_i^5 = \sum_i \bar{w_i} f_i = \frac{\sum_i w_i f_i}{\sum_i w_i} \tag{3.7}$$

3.2.2 Learning Algorithm

The overall output can be represented as a linear combination of consequent parameters with the given values of premise parameters in the ANFIS structure. i.e.

$$f = \frac{w_1}{w_1 + w_2} f_1 + \frac{w_2}{w_1 + w_2} f_2 \tag{3.8}$$

$$f = \bar{w_1} f_1 + \bar{w_2} f_2 \tag{3.9}$$

$$f = \bar{w_1}(k_1 x + l_1 y + m_1) + \bar{w_2}(k_2 x + l_2 y + m_2) \tag{3.10}$$

$$\begin{aligned} f = (\bar{w_1} x)k_1 + (\bar{w_1} y)l_1 + (\bar{w_1})m_1 + (\bar{w_2} x)k_2 \\ +(\bar{w_2} y)l_2 + (\bar{w_2})m_2 \end{aligned} \tag{3.11}$$

Where,

f- linear in the consequent parameters $(k_1, l_1, m_1, k_2, l_2, m_2)$

These parameters will change through the learning process. A gradient vector facilitates the adjustment or computation of these parameters. Also, it represents the degree of measure to which the FIS is modeling the input-output data for a dispensed set of parameters. Further, any of the optimization techniques can be used to adjust the associated parameter by reducing the difference in sum of squares of actual and desired outputs. This work used the backpropagation algorithm and a hybrid (hybridization of backpropagation and least squares estimation) algorithm presented in [263]. The first step in the process of model development is to create an initial fuzzy inference system (FIS) with the help of the extracted rules from the input-output data of the system which is considered to be modeled. After that, the initial fuzzy model developed is fine-tuned using the neural network and achieved the final ANFIS model of the system. The different existing models developed

Table 3.1: Different ANFIS based Models

Model	**FIS generation method**	**Optimization**
1	Grid Partitioning [264, 265]	backpropagation (BP)
2	Subtractive Clustering [266]	backpropagation (BP)
3	FCM Clustering [267]	backpropagation (BP)
4	Grid Partitioning [264, 265]	Hybrid
5	Subtractive Clustering [266]	Hybrid
6	FCM Clustering [267]	Hybrid

by the combinations of different initial FIS generation methods and optimization algorithms are represented in Table 3.1.

3.2.3 Development of Initial Fuzzy Model

Different methods can be used to develop the initial fuzzy model. In this work, the initial fuzzy model has been modeled using grid portioning [264, 265], subtractive clustering [266] and fuzzy c means (FCM) clustering [267] and the details are as follows.

3.2.3.1 Grid Partitioning Technique

This partition strategy used when the number of membership functions and inputs are less [264, 265]. The number of fuzzy IF-THEN rule for 'n' input and 'm' membership functions can be represented as in Eq. (3.12).

$$Fuzzy_{nRule} = m^n \tag{3.12}$$

The membership functions can be any, but the degree of membership function information is used for the further processing can lead to the loss of the considerable amount of information during the process of fuzzification. This can be identified as a nonlinear transformation of the input. In case of the trapezoidal or triangular membership function, the information may be the loss at the point where the slope is zero, where the function is not differentiable. Thus a fuzzy system with trapezoidal or triangular membership function can face issues in learning from data. Therefore the membership functions like Gaussian or bell function can be used to avoid this issue due to the smoothness of the function [260]. So, this work considers five inputs and two Gaussian membership function and a total of 32 (2^5) rules.

3.2.3.2 Subtractive Clustering Technique

Subtractive Clustering Technique helps to locate the cluster centers of input-output data pairs, as each cluster center is a sign of the existence of a rule. Which also supports in finding the rules which are distributed in the input-output space as well as in determining the values of the premise parameters. It also helps in finding the initial values that are closely related to input values facilitate the quick convergence of the model while training with the neural network. In this technique, the capability of each input-output data points is considered as a function of Euclidian distances from the remaining data points. The data point with a threshold more than a preset value is treated as cluster centers. The initial fuzzy model can be extracted after determining the cluster center as in [268].

Consider 'n' data points $D = \{x_1, x_2, x_3.., x_n\}$ in M dimensional space. The data points are considered to be normalized in all dimensions so as to be bounded by a unit hypercube. Each data points are treated to be a possible cluster center. The capability of a data point x_i to be a cluster center is measured by

$$C_i = \sum_{j=1}^{n} e^{-\alpha \|x_i - x_j\|^2} \tag{3.13}$$

Where,

$$\alpha = \frac{4}{r_a^2} \tag{3.14}$$

$\|x_i - x_j\|$- Euclidean distance r_a- Influence Radius that effectively define the neighborhood.

The data points exterior to the influence radius have little influence on C_i. After calculating the C_i for all the data points, the data points with highest C_i is considered as the first cluster center. Let x_{1^*}, and C_{1^*} are the location of first cluster center and its capability value respectively. Then the capability of each data point x_i is modified by the equation as in

$$C_i = C_i - C_{1^*} e^{-\beta \|x_i - x_{1^*}\|^2} \tag{3.15}$$

Where,

$$\beta = \frac{4}{r_b^2} \tag{3.16}$$

r_b- Influence Radius that effectively define the neighborhood. Generally, r_b=1.25r_a [268].

After updating the capabilities of all data points according to Eq. (3.15), the data points with the highest remaining capability are considered to be the second cluster center. The capabilities of each data point are further minimized accordingly. Typically, the capabilities of each data points are updated as in Eq. (3.17) after obtaining k_{th} cluster center.

$$C_i = C_i - C_{k^*} e^{-\beta \|x_i - x_{k^*}\|^2} \tag{3.17}$$

Where, x_{k^*} represents the location of k_{th} cluster center and $C_{k^*}$is its value. Repeat the process until the stopping criterion is achieved. Each cluster center derived from the above procedure is the representation of data point that describes the characteristics of the input-output behavior of the system that is intended to be modeled. Thus the cluster center can be treated as the basis of a rule that can describe the behavior of the system.

Let $x_{1^*}, x_{2^*}, x_{3^*}.., x_{c^*}$ set of c clusters in M dimensional space. First N dimensions represents the input variables and reaming $M - N$ dimensions represents the respective output variables. Each cluster center x_{i^*} is decomposed into two component vectors y_{i^*}, the location of cluster center in the input space and z_{i^*}, the location of cluster center in output space respectively. Thus x_{i^*} can be symbolically represented as

$$x_{i^*} = [y_{i^*}; z_{i^*}] \tag{3.18}$$

Where, every cluster center x_{i^*} is considered as a representation of fuzzy rule. i.e.

IF the input is near y_{i^*} THEN output is near to z_{i^*}.

The degree of membership of a rule i for a given input vector y can be computed as in

$$\mu_i = e^{-\alpha \|y - y_{i^*}\|^2} \tag{3.19}$$

Where α is a constant defined as by Eq. (3.14), and the output vector is measured as in

$$z = \frac{\sum_{i=1}^{c} \mu_i z_{i^*}}{\sum_{-i=1}^{c} \mu_i} \tag{3.20}$$

This computational scheme can be observed in terms of FIS using fuzzy IF-THEN rules as

IF Y_1 is A_{i1} and Y_2 is A_{i2} .... THEN Z_1 is B_{i1} Z_2 is B_{i2} ....

Where, Y and Z are input and output variable respectively and the A and B corresponds to the membership function associated with i^{th} rule for j^{th} input/output.

$$A_{ij}(Yj) = e^{-0.5(\frac{Y_j - y_{ij*}}{\sigma_{ij}})^2} \tag{3.21}$$

$$B_{ij} = z^*_{ij} \tag{3.22}$$

Where y^*_{ij} and z^*_{ij} are j^{th} elements of y^*_i and z^*_i respectively and $\sigma^2_{ij} = \frac{1}{2\alpha}$ [268].

3.2.3.3 Fuzzy C Means Clustering

The fuzzy clustering associates each data point with each cluster using a membership function. The data point with similar properties are assigned with a higher degree of membership, and dissimilar properties are assigned with a lower degree of membership [269]. This clustering technique is based on the minimization of the objective function represented in Eq. (3.23).

Algorithm 3.1 Fuzzy C Means Clustering algorithm

1: Initialize no of cluster as k
2: Calculate μ_{ij} for all i,j from Eq. (3.24)
3: **for** `<Until termination criteria is met>` **do**
4: `Calculate Cluster centers` V_j
5: `Update` μ_{ij} `for all i,j`
6: **end for**

$$J_k = \sum_{i=1}^{k} \sum_{j=1}^{c_j} \mu_{ij}^m (||X_i - V_j||)^2 \tag{3.23}$$

$$l < m < \infty$$

Where the degree of membership of X_i in the cluster k^{th} is represented by μ_{ij}. Eq. (3.24) and Eq. (3.25) presents the degree of membership μ_{ij} and cluster center V_j respectively and m is a real number more than one. The algorithm for fuzzy C means is presented in Algorithm 3.1

$$\mu_{ij} = \frac{1}{\sum_{p=1}^{k} \left(\frac{||X_i - V_j||}{||X_i - V_p||} \right)^{\frac{2}{m-1}}} \tag{3.24}$$

$$V_j = \frac{\sum_{i=1}^{N} \mu_{ij}^{m} X_i}{\sum_{i=1}^{N} \mu_{ij}^{m}} \tag{3.25}$$

In this algorithm, the relation between data points to each cluster is established using a membership function which characterizes the fuzzy behavior of the algorithm. The more details of the fuzzy c mean clustering can be found in [267].

3.2.4 Data Selection

The performance of the proposed model is evaluated based on the average hourly PV and wind output power data collected from Tioman Island for the year 2011 [255]. The pre-processing of the data is important to achieve the higher forecasting accuracy. The preprocessing of the data has been performed using the step 1 to 11 illustrated in algorithm 3.2. Then the pre-processed data is given to the developed ANFIS as mentioned in the algorithm 3.2 step 12 to 26. The algorithm 3.2 represents the complete model implementation. The 15 days hourly PV and wind output power values have been used for the model implementation. For example to forecast the value for January 15^{th}, the hourly values of January 1^{st} to January 15^{th} is used. In which the January 15^{th} is used as a testing target, and the remaining values are used for model building and training. Respectively all different days in 2011 have been predicted.

3.2.5 Results and Discussions

The forecasted value of PV and wind output power by the proposed model is compared with actual PV, and wind output power values and error has been calculated. The indices used for the performance evaluations of the proposed model are Mean Absolute Error (MAE), Mean Square Error (MSE), Root Mean Square Error (RMSE) and Mean Relative Error (MRE) in % as represented in Eq. (3.26) - Eq. (3.29) respectively.

$$Mean\ Absolute\ Error\ (MAE) = \frac{1}{N} \sum_{i=1}^{N} |Q_i - Y_i| \tag{3.26}$$

$$Mean\ Square\ Error\ (MSE) = \frac{1}{N} \sum_{i=1}^{N} (Q_i - Y_i)^2 \tag{3.27}$$

Algorithm 3.2 Data Pre-processing and Model implementation

1: Input historical data (x)(historical PV output power or Historical wind output power.
2: Calculate the length of the data L.
3: Initialize delay D=1:5
4: Calculate maximum delay MaxD
5: Calculate range of values R=MaxD+1 to L
6: **for** `<All delay D>` **do**
7: Sort model inputs X=[X;x(:,(R-D))]
8: **end for**
9: Sort Model Targets Y=x(:,R)
10: Calculate the input to the ANFIS X= transpose of X
11: Calculate the Targets to the ANFIS Y= transpose of Y
12: Calculate the length of X i.e. K
13: Provide Training index
14: Generate Training inputs
15: Generate Training Targets
16: Execute ANFIS model with Training inputs and Targets
17: Provide Testing index
18: Generate Testing inputs
19: Provide testing inputs to the trained ANFIS
20: Input Testing Targets
21: Perform Testing
22: Calculate MAE using Eq.(3.26)
23: Calculate MSE using Eq.(3.27)
24: Calculate RMSE using Eq.(3.28)
25: Calculate MRE using Eq.(3.29)
26: Analyze the model performance

$$Root\ Mean\ Square\ Error\ (RMSE) = \sqrt{\frac{1}{N}\sum_{i=1}^{N}(Q_i - Y_i)^2} \tag{3.28}$$

$$Mean\ Relative\ Error\ (MRE)\ in\ \% = \frac{1}{N}\sum_{i=1}^{N}\frac{|Q_i - Y_i|}{Wtotal} * 100 \tag{3.29}$$

Where, Q_i- Predicted Value, Y_i- Actual Value, $Wtotal$= Total generation capacity (500 kW for PV & 250 kW for wind)

3.2.5.1 Performance Analysis: PV Forecasting

The solar irradiation follows a typical pattern having the maximum irradiation at the middle of the day.

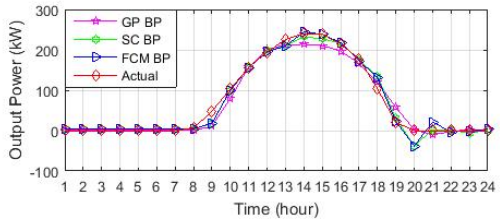

(a) Performance Plot of January 15

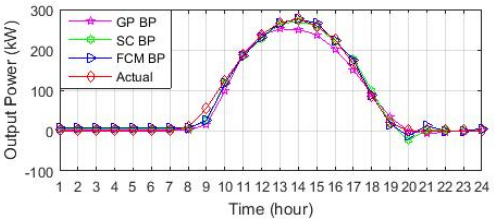

(b) Performance Plot of February 24

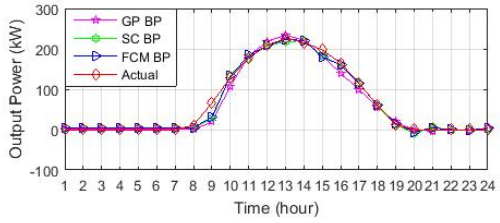

(c) Performance Plot of March 18

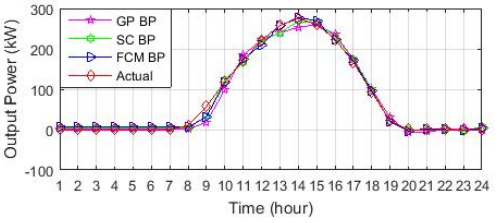

(d) Performance Plot of April 27

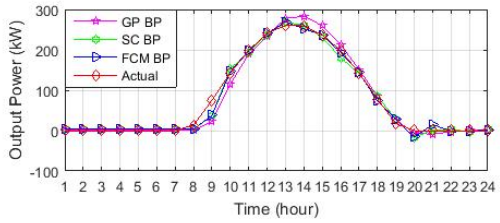

(e) Performance Plot of May 17

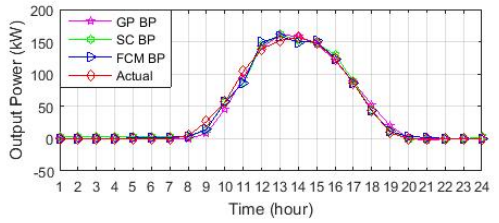

(f) Performance Plot of June 21

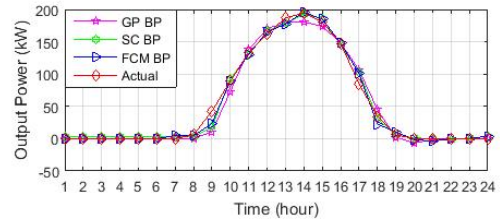

(g) Performance Plot of July 23

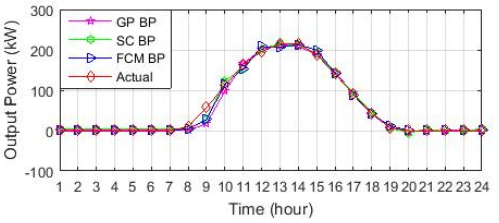

(h) Performance Plot of August 15

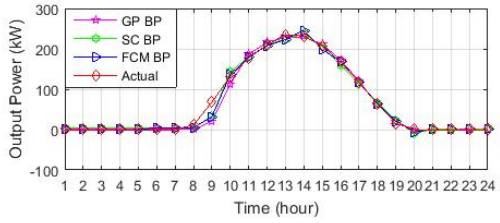

(i) Performance Plot of September 05

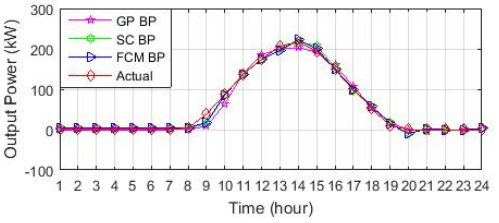

(j) Performance Plot of October 2

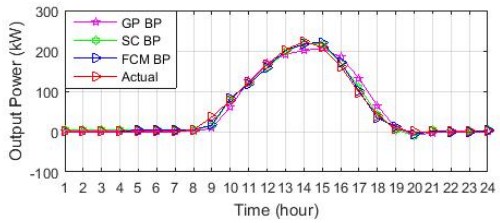

(k) Performance Plot of November 14

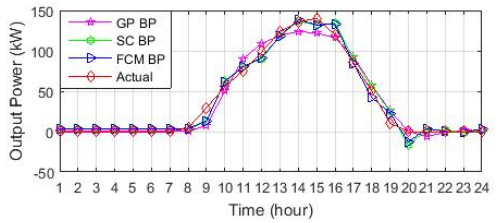

(l) Performance Plot of December 08

Figure 3.2: Performance Plot of PV Forecasting with Backpropogation Algorithm

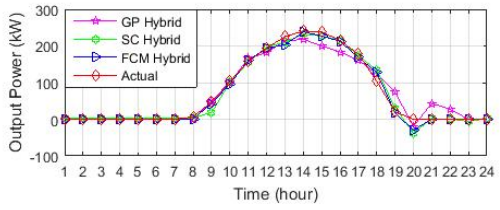

(a) Performance Plot of January 15

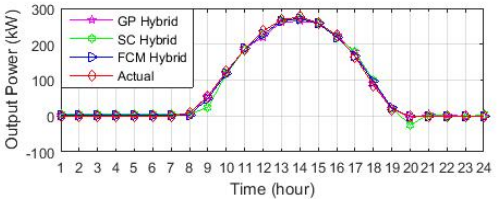

(b) Performance Plot of February 24

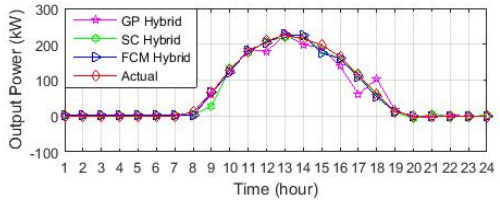

(c) Performance Plot of March 18

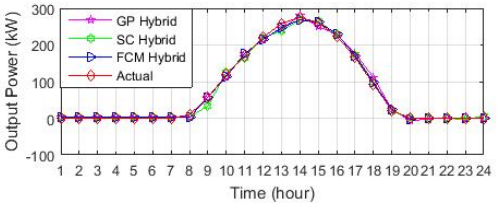

(d) Performance Plot of April 27

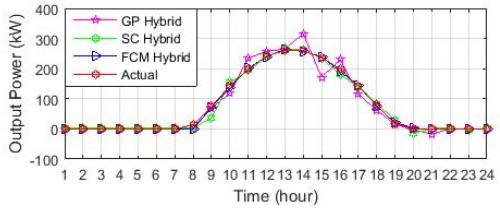

(e) Performance Plot of May 17

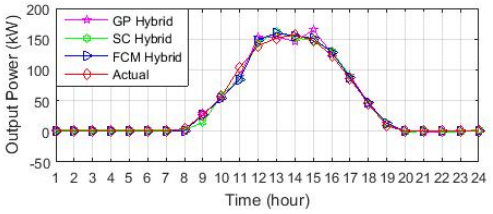

(f) Performance Plot of June 21

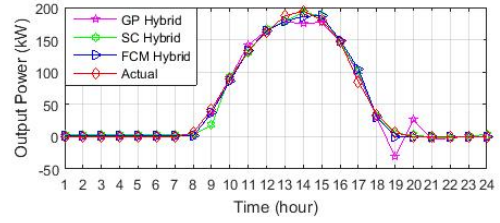

(g) Performance Plot of July 23

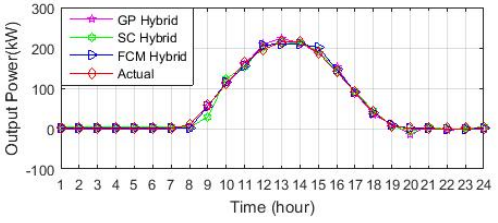

(h) Performance Plot of August 15

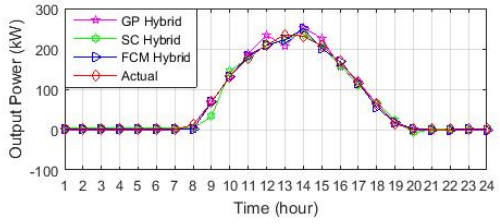

(i) Performance Plot of September 05

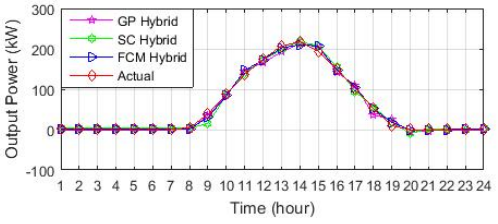

(j) Performance Plot of October 2

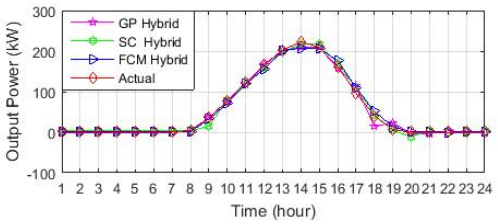

(k) Performance Plot of November 14

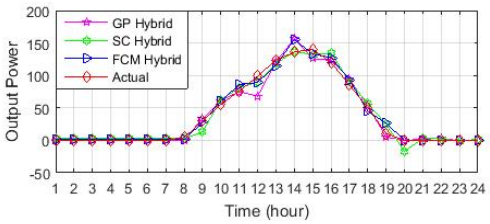

(l) Performance Plot of December 08

Figure 3.3: Performance Plot of PV Forecasting with Hybrid Algorithm

Table 3.2: Performance of different models for PV forecasting

	Algorithm	**Hybrid Optimization**			**Backpropagation**		
	Indices	***GP***	***SC***	***FCM***	***GP***	***SC***	***FCM***
	MSE	414.1685	168.8988	99.2330	246.2968	169.4644	167.4012
	RMSE	20.3511	12.9961	9.9616	15.6938	13.0178	12.9384
Jan 15	***MAE***	13.4444	8.2632	5.6700	10.1639	8.3315	7.9723
	MRE %	2.6889	1.6526	1.1340	2.0328	1.6663	1.5945
	MSE	35.1057	98.4337	17.2885	200.2514	98.0572	73.3942
	RMSE	5.9250	9.9214	4.1579	14.1510	9.9024	8.5670
Feb 24	***MAE***	3.8841	6.8132	3.1067	8.8350	6.7796	6.1077
	MRE %	0.7768	1.3626	0.6213	1.7670	1.3559	1.2215
	MSE	282.8570	86.6859	35.7337	173.7549	89.1504	79.5422
	RMSE	16.8184	9.3105	5.9778	13.1816	9.4419	8.9186
March 18	***MAE***	9.3655	5.5760	3.4523	7.5857	5.6160	5.5862
	MRE %	1.8731	1.1152	0.6905	1.5171	1.1232	1.1172
	MSE	45.5058	56.6618	18.7890	139.4561	57.5152	48.6022
	RMSE	6.7458	7.5274	4.3346	11.8092	7.5839	6.9715
April 27	***MAE***	4.7293	5.5039	3.1425	7.1750	5.5556	5.1592
	MRE %	0.9459	1.1008	0.6285	1.4350	1.1111	1.0318
	MSE	512.4110	109.3600	14.5305	240.7384	113.7673	99.2802
	RMSE	22.6365	10.4575	3.8119	15.5157	10.6662	9.9639
May 17	***MAE***	13.6904	6.8591	2.6667	9.6782	7.1114	6.4063
	MRE %	2.7381	1.3718	0.5333	1.9356	1.4223	1.2813
	MSE	38.5889	32.4876	26.9697	36.4005	32.3215	30.0152
	RMSE	6.2120	5.6998	5.1932	6.0333	5.6852	5.4786
June 21	***MAE***	3.8091	3.9307	2.9154	3.6237	3.9434	3.0680
	MRE %	0.7618	0.7861	0.5831	0.7247	0.7887	0.6136
	MSE	119.4234	47.8320	30.5203	97.1439	50.0240	39.8767
	RMSE	10.9281	6.9161	5.5245	9.8562	7.0728	6.3148
July 23	***MAE***	6.2863	4.5158	3.3901	5.8895	4.5904	3.6687
	MRE %	1.2573	0.9032	0.6780	1.1779	0.9181	0.7337
	MSE	34.3296	56.7724	24.5266	81.8138	57.6744	58.4467
	RMSE	5.8591	7.5347	4.9524	9.0451	7.5944	7.6450
August 15	***MAE***	4.0547	5.0913	3.2453	3.8320	5.1802	3.7592
	MRE %	0.8109	1.0183	0.6491	0.7664	1.0360	0.7518

	MSE	100.8984	84.4111	31.9667	126.0273	84.5177	81.1620
	RMSE	10.0448	9.1875	5.6539	11.2262	9.1934	9.0090
Sept 05	***MAE***	5.7276	5.9288	3.2620	5.1275	5.9872	4.6665
	MRE %	1.1455	1.1858	0.6524	1.0255	1.1974	0.9333
	MSE	52.1534	50.0090	22.6523	84.0985	50.4685	38.5652
	RMSE	7.2217	7.0717	4.7594	9.1705	7.1041	6.2101
Oct 02	***MAE***	5.1636	5.0426	3.1525	5.0188	5.0837	4.5780
	MRE %	1.0327	1.0085	0.6305	1.0038	1.0167	0.9156
	MSE	66.3426	48.4473	43.5114	170.9419	49.0401	41.9304
	RMSE	8.1451	6.9604	6.5963	13.0745	7.0029	6.4754
Nov 14	***MAE***	4.6323	5.2391	4.3218	7.8662	5.2673	4.6218
	MRE %	0.9265	1.0478	0.8644	1.5732	1.0535	0.9244
	MSE	75.0902	57.5521	47.5614	73.4156	57.0869	48.3927
	RMSE	8.6655	7.5863	6.8965	8.5683	7.5556	6.9565
Dec 8	***MAE***	4.7718	5.8271	4.5601	5.6613	5.7906	5.5517
	MRE %	0.9544	1.1654	0.9120	1.1323	1.1581	1.1103

The Figure 3.2(a) - Figure 3.2(l) show the foretasted and actual PV output power values of randomly selected days January 21, February 18, March 08, April 12, May 27, June 26, July 03, August 06, September 07, October 12, November 02 and December 21 respectively for initial FIS generation methods (grid portioning, subtractive clustering and fuzzy c mean clustering) and backpropagation optimization algorithm based model. Also, the Figure 3.3(a) - Figure 3.3(l) show the foretasted and actual PV output power values of randomly selected days January 21, February 18, March 08, April 12, May 27, June 26, July 03, August 06, September 07, October 12, November 02 and December 21 respectively for initial FIS generation methods (grid portioning, subtractive clustering and fuzzy c mean clustering) and hybrid optimization algorithm based model. Table 3.2 shows the performance of ANFIS model with PV output power forecasting in terms of different indices (i.e. mean absolute error, mean square error, root mean square error and mean relative error as represented by Eq. (3.26) - Eq. (3.29)). From the table it is clear that the ANFIS model with initial FIS generation based on the Fuzzy C Means clustering and backpropagation algorithm based model provides better accuracy as compared to grid partitioning and subtractive clustering based model. Also, the ANFIS model with initial FIS generation based on the Fuzzy C Means clustering and hybrid optimization based model outperform the models with initial FIS gen-

Table 3.3: Average model performance for PV forecasting

Algorithm	**Hybrid Optimization**			**Backpropagation**		
Indices	***GP***	***SC***	***FCM***	***GP***	***SC***	***FCM***
MSE	148.0729	74.79598	34.44026	139.1949	75.7573	67.21741
RMSE	10.79609	8.430783	5.651667	11.44378	8.48505	7.954067
MAE	6.629925	5.7159	3.573783	6.704733	5.769742	5.095467
MRE %	1.325992	1.143175	0.714758	1.340942	1.153942	1.019083

eration based on the grid partitioning, subtractive clustering and back propagation optimization based models. Table 3.3 represents the average model performance of the different proposed models with PV output power forecasting. It is clear from the Table 3.3 that with a backpropagation based optimization algorithm, initial FIS generation using fuzzy c means clustering (FCM) provide better accuracy. Also in case of hybrid algorithm based model, initial FIS generation using FCM shows better accuracy. Comparing the results of all the six model developed the FCM based hybrid optimization based model gives better performance as shown in Table 3.3. Thus FCM based hybrid optimization based ANFIS model is utilized further in this study for developing PV forecasting agent for the proposed multi agent based energy management system.

3.2.5.2 Performance Analysis: Wind Forecasting

The wind speed follows the pattern having several ups and downs throughout the day. The Figure 3.4(a) - Figure 3.4(l) show the foretasted and actual wind output power values of randomly selected days January 21, February 18, March 08, April 12, May 27, June 26, July 03, August 06, September 07, October 12, November 02 and December 21 respectively for initial FIS generation methods (grid portioning, subtractive clustering and fuzzy c mean clustering) and backpropagation optimization algorithm based model. Also, the Figure 3.5(a) - Figure 3.5(l) show the foretasted and actual wind output power values of randomly selected days January 21, February 18, March 08, April 12, May 27, June 26, July 03, August 06, September 07, October 12, November 02 and December 21 respectively for initial FIS generation methods (grid portioning, subtractive clustering and fuzzy c mean clustering) and hybrid optimization algorithm based model. Table 3.4 respectively show the numerical results obtained by grid portioning, subtractive clustering and fuzzy c mean clustering (initial FIS generation methods) and backpropagation, hybrid optimization algorithm based ANFIS model for different randomly selected days respectively for wind forecast.

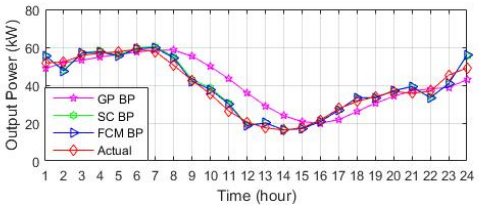

(a) Performance Plot of January 21

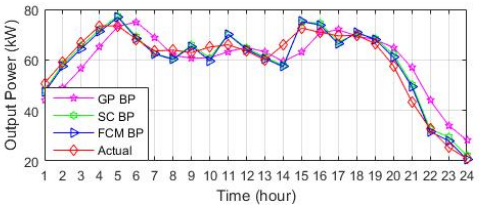

(b) Performance Plot of February 18

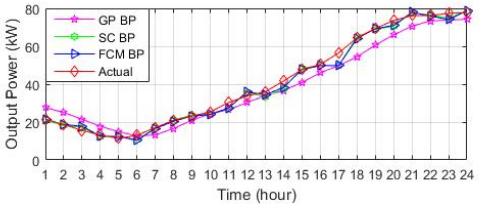

(c) Performance Plot of March 08

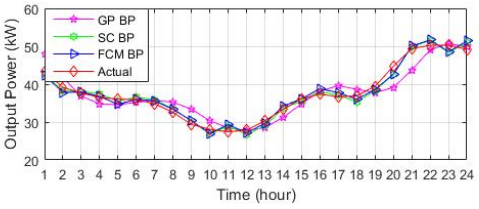

(d) Performance Plot of April 12

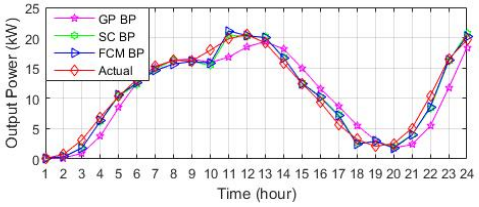

(e) Performance Plot of May 27

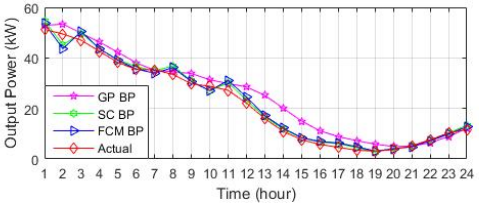

(f) Performance Plot of June 26

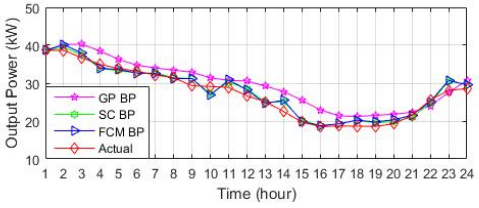

(g) Performance Plot of July 03

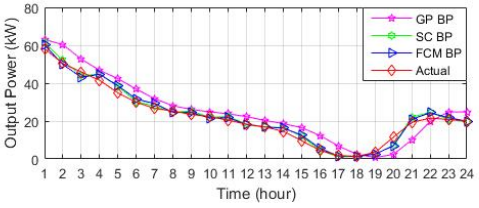

(h) Performance Plot of August 06

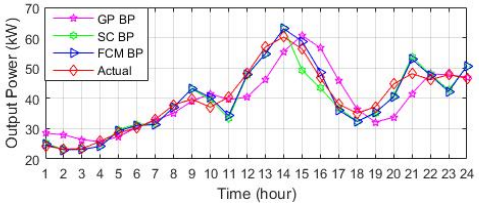

(i) Performance Plot of September 07

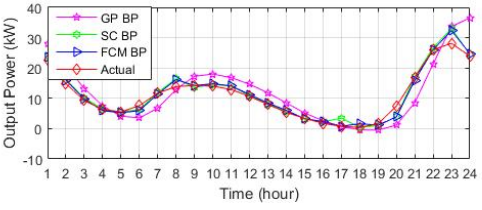

(j) Performance Plot of October 12

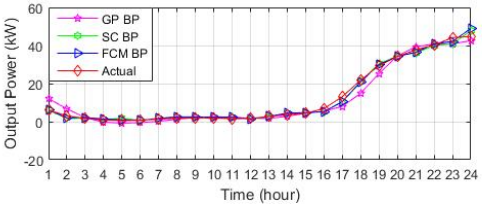

(k) Performance Plot of November 02

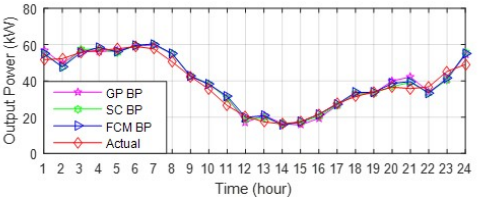

(l) Performance Plot of December 21

Figure 3.4: Performance Plot of Wind Forecasting with BP algorithm

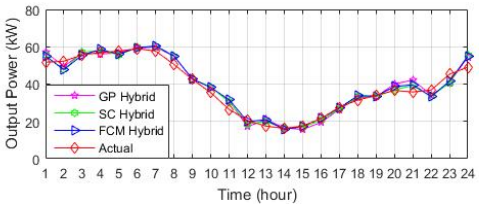

(a) Performance Plot of January 21

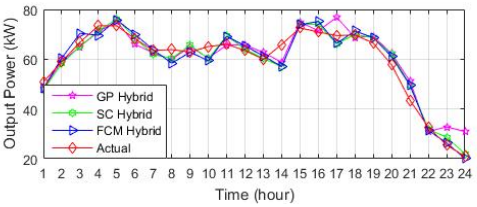

(b) Performance Plot of February 18

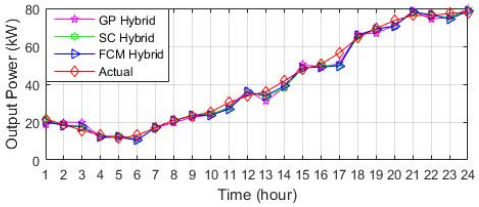

(c) Performance Plot of March 08

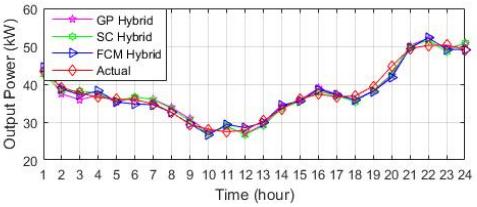

(d) Performance Plot of April 12

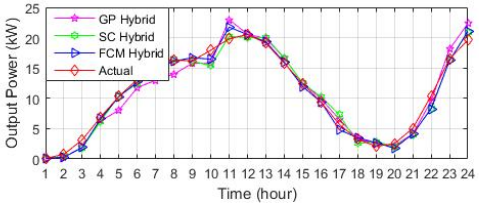

(e) Performance Plot of May 27

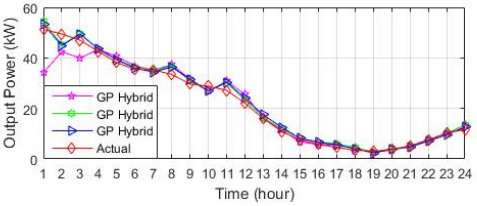

(f) Performance Plot of June 26

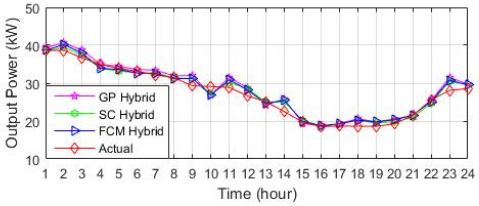

(g) Performance Plot of July 03

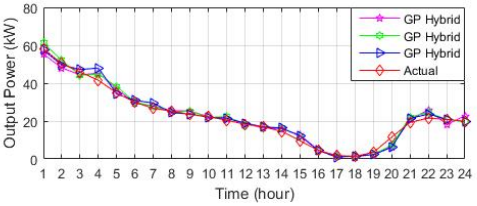

(h) Performance Plot of August 06

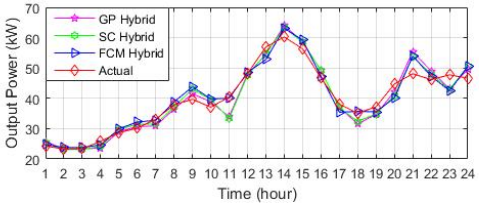

(i) Performance Plot of September 07

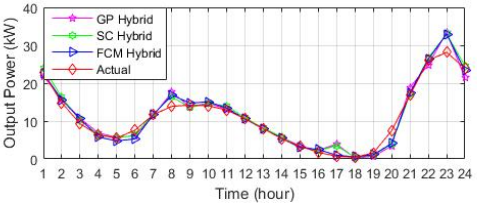

(j) Performance Plot of October 12

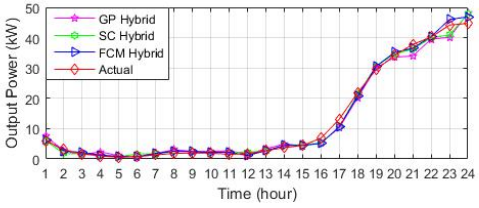

(k) Performance Plot of November 02

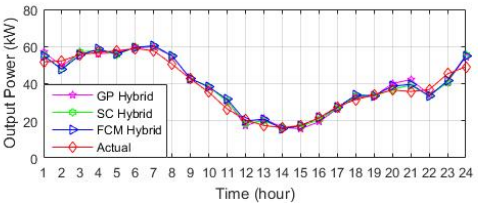

(l) Performance Plot of December 21

Figure 3.5: Performance Plot of Wind Forecasting with Hybrid algorithm

Table 3.4: Performance of different models for wind forecasting

	Algorithm	**Hybrid Optimization**			**Backpropagation**		
	Indices	***GP***	***SC***	***FCM***	***GP***	***SC***	***FCM***
	MSE	9.8948	8.0625	7.9502	56.5785	8.2297	8.1693
	RMSE	3.1456	2.8395	2.8196	7.5219	2.8688	2.8582
Jan 21	***MAE***	2.5798	2.2938	2.2447	5.6586	2.3221	2.2454
	MRE %	1.0319	0.9175	0.8979	2.2634	0.9288	0.8982
	MSE	18.0900	11.2062	10.8230	44.8025	11.9505	11.0138
	RMSE	4.2532	3.3476	3.2898	6.6935	3.4570	3.3187
Feb 18	***MAE***	3.3393	2.7221	2.6005	5.5096	2.7813	2.7136
	MRE %	1.3357	1.0888	1.0402	2.2038	1.1125	1.0854
	MSE	6.8827	4.5711	4.9357	27.0812	4.7794	4.5527
	RMSE	2.6235	2.1380	2.2216	5.2040	2.1862	2.1337
March 8	***MAE***	2.2934	1.5589	1.6736	4.6721	1.5958	1.4896
	MRE %	0.9174	0.6236	0.6694	1.8688	0.6383	0.5958
	MSE	1.5487	1.2976	1.3852	6.4915	1.2778	1.3498
	RMSE	1.2445	1.1391	1.1769	2.5478	1.1304	1.1618
April 12	***MAE***	1.1391	1.0319	0.9428	2.0377	1.0229	1.0120
	MRE %	0.4556	0.4128	0.3771	0.8151	0.4092	0.4048
	MSE	2.0169	0.9608	0.7530	5.2392	0.9763	0.8640
	RMSE	1.4202	0.9802	0.8678	2.2889	0.9881	0.9295
May 27	***MAE***	1.0998	0.7558	0.6329	1.8368	0.7693	0.7645
	MRE %	0.4399	0.3023	0.2531	0.7347	0.3077	0.3058
	MSE	18.9175	3.1872	3.0607	18.0279	3.2521	4.1456
	RMSE	4.3494	1.7853	1.7495	4.2459	1.8034	2.0361
June 26	***MAE***	2.3713	1.3851	1.4105	3.4198	1.4048	1.5449
	MRE %	0.9485	0.5541	0.5642	1.3679	0.5619	0.6180
	MSE	2.7372	1.4395	1.4152	8.9122	1.4652	1.8270
	RMSE	1.6544	1.1998	1.1896	2.9853	1.2104	1.3517
July 3	***MAE***	1.3080	0.9707	0.7139	2.6508	0.9778	1.0577
	MRE %	0.5232	0.3883	0.2856	1.0603	0.3911	0.4231
	MSE	4.6853	3.8536	4.3771	31.6073	3.9370	3.9397
	RMSE	2.1646	1.9631	2.0921	5.6220	1.9842	1.9849
August 6	***MAE***	1.6841	1.4899	1.3673	5.0797	1.5208	1.5499
	MRE %	0.6736	0.5960	0.5469	2.0319	0.6083	0.6200

	MSE	8.8036	8.6113	7.3310	27.2143	10.5437	8.1817
	RMSE	2.9671	2.9345	2.7076	5.2167	3.2471	2.8604
Sept 07	***MAE***	2.3621	2.4007	2.1140	3.9344	2.6212	2.3367
	MRE %	0.9448	0.9603	0.8456	1.5738	1.0485	0.9347
	MSE	3.6899	2.4971	2.3022	22.2102	2.2257	1.9839
	RMSE	1.9209	1.5802	1.5173	4.7128	1.4919	1.4085
Oct 12	***MAE***	1.3090	1.0413	0.9424	3.8555	0.9967	0.9525
	MRE %	0.5236	0.4165	0.3770	1.5422	0.3987	0.3810
	MSE	2.7519	1.5705	1.0568	7.1434	1.6062	1.6345
	RMSE	1.6589	1.2532	1.0280	2.6727	1.2674	1.2785
Nov 2	***MAE***	1.2163	0.8801	0.7714	1.8772	0.8858	0.8681
	MRE %	0.4865	0.3521	0.3086	0.7509	0.3543	0.3472
	MSE	47.4641	14.8951	12.5053	328.2101	26.2276	13.5648
	RMSE	6.8894	3.8594	3.5363	18.1166	5.1213	3.6830
Dec 21	***MAE***	5.4925	2.8857	2.7208	15.4093	4.2629	2.8299
	MRE %	2.1970	1.1543	1.0883	6.1637	1.7052	1.1319

Table 3.5: Average model performance for wind forecasting

Algorithm	**Hybrid Optimization**			**Backpropagation**		
Indices	***GP***	***SC***	***FCM***	***GP***	***SC***	***FCM***
MSE	10.62355	5.179375	4.824617	48.62653	6.3726	5.102233
RMSE	2.857642	2.084992	2.016342	5.652342	2.229683	2.08375
MAE	2.182892	1.618	1.511233	4.661792	1.76345	1.613733
MRE %	0.873142	0.647217	0.604492	1.864708	0.705375	0.645492

The average performance of the model has also been shown in Table 3.5. From Table 3.5 it is has been found that with a backpropagation based optimization algorithm, initial FIS generation using fuzzy c mean clustering (FCM) provide better accuracy. Also in case of hybrid algorithm based model, initial FIS generation using FCM shows better accuracy. Comparing the results of all the six model developed the FCM based hybrid optimization-based ANFIS model gives better performance as shown in Table 3.5. Thus in this case also FCM based hybrid optimization based ANFIS model is utilized further in this study for developing wind forecasting agent for the proposed multi agent based energy management system.

3.3 Load Forecasting Models

A brief review of different models used for the load forecasting is provided in section 1.3.5. This section describes the load forecasting models used to forecast the upcoming loads in the microgrid in this work. The three load forecasting models namely Linear Time Series Model (LTS) [270], Support Vector Regression Model (SVR) [271] and Bayesian Multivariate Linear Spline Model (BMLS) [251] are explored in this work. The details of each model are explained in the further sections. The performance of the different model is evaluated based on the monthly average hourly load consumption data extracted from [272] (Tioman Island) for the year 2009, 2010 and 2011.

3.3.1 Linear Time Series Models (LTS)

3.3.1.1 One Day Linear Time Series Model

A uni-variate model that uses monthly average hourly load data S_K and forecast the monthly average hourly load data S_{K+1} of the next month, for an equal interval of time and represented by the Eq. (3.30) [270].

$$S_{K+1}(n) = p + q * S_K(n) \tag{3.30}$$

$$G = \begin{bmatrix} p \\ q \end{bmatrix} = \begin{bmatrix} H^T & H \end{bmatrix}^{-1} . H^T . S_K \tag{3.31}$$

$$H = \begin{bmatrix} 1 & S_K(1) \\ 1 & S_K(2) \\ 1 & S_K(3) \\ : & : \\ 1 & S_K(n) \end{bmatrix} \quad S_K = \begin{bmatrix} S_K(1) \\ S_K(2) \\ S_K(3) \\ : \\ S_K(n) \end{bmatrix} \tag{3.32}$$

Where, S_K represents monthly average hourly load data of month K, S_{K+1} represents monthly average hourly load data of month K+1, n represents number of hours (24 hour) and p and q are model parameters.

3.3.1.2 Two Day Linear Time Series Model

A multivariate model which uses monthly average hourly load data of month S_K and monthly average hourly load data of month S_{K-1}, then forecast the monthly

average hourly load data of month S_{K+1}, for an equal interval of time and represented by the Eq. (3.33) [270].

$$S_{K+1}(n) = p + q * S_K(n) + r * S_{K-1}(n) \tag{3.33}$$

$$G = \begin{bmatrix} p \\ q \\ r \end{bmatrix} = \begin{bmatrix} H^T & H \end{bmatrix}^{-1} . H^T . S_K \tag{3.34}$$

$$H = \begin{bmatrix} 1 & S_K(1) & S_{K-1}(1) \\ 1 & S_K(2) & S_{K-1}(2) \\ 1 & S_K(3) & S_{K-1}(3) \\ : & : & : \\ 1 & S_K(n) & S_{K-1}(n) \end{bmatrix} S_K = \begin{bmatrix} S_K(1) \\ S_K(2) \\ S_K(3) \\ : \\ S_K(n) \end{bmatrix} \tag{3.35}$$

Where, S_K, S_{K-1} represents monthly average hourly load data of month K and monthly average hourly load data of month K-1 respectively, S_{K+1} represents monthly average hourly load data of month K+1, n represents number of hours (24 hours) and p, q and r are model parameters.

3.3.1.3 Three day Linear Time Series Model

Also, a multivariate model which uses monthly average hourly load data of month S_K, monthly average hourly load data of month S_{K-1} and monthly average hourly load data of month S_{K-2}, then forecast the monthly average hourly load data of month S_{K+1}, for an equal interval of time and represented by the Eq. (3.36) [270].

$$\begin{aligned} S_{K+1}(n) &= p + q * S_K(n) + \\ & r * S_{K-1}(n) + s * S_{K-2}(n) \end{aligned} \tag{3.36}$$

$$G = \begin{bmatrix} p \\ q \\ r \\ s \end{bmatrix} = \begin{bmatrix} H^T & H \end{bmatrix}^{-1} . H^T . S_k \tag{3.37}$$

$$H = \begin{bmatrix} 1 & S_K(1) & S_{K-1}(1) & S_{K-2}(1) \\ 1 & S_K(2) & S_{K-1}(2) & S_{K-2}(2) \\ 1 & S_K(3) & S_{K-1}(3) & S_{K-2}(3) \\ : & : & : & \\ 1 & S_K(n) & S_{K-1}(n) & S_{K-2}(n) \end{bmatrix} \tag{3.38}$$

Where, monthly average hourly load data of month S_K, monthly average hourly load data of month S_{K-1} and monthly average hourly load data of month S_{K-2} respectively, and forecast monthly average hourly load data of month S_{K+1}, n represents number of hours (24 hour) and p, q, r and s are model parameters.

3.3.2 Support Vector Regression Model (SVR)

Support Vector Machines (SVM) are supervised learning models with associated learning algorithms that evaluate data and identify patterns which can be used for regression analysis and classification.Under the application of classification, a set of training examples in which each is marked as belonging to one of the specified categories is given. Training algorithm builds a model that allocates new examples into one category or the other, creating it a non-probabilistic binary linear classifier. An SVM model is an illustration of the examples as points in space which is mapped so that the examples of the distinct categories are divided by a clear gap that is as wide as possible. New examples are then mapped into that same space and forecast to be belonged to a category based on which side of the gap they fall in. Like linear classification, Support Vector Machines can efficiently perform a non-linear classification using the kernel trick which is implicitly mapping their inputs into high-dimensional feature spaces [273]. A version of SVM for regression was proposed in 1996 by Vladimir N. Vapnik, Harris Drucker, Christopher J. C. Burges, Linda Kaufman and Alexander J. Smola. This method is called Support Vector Regression (SVR). The model made by support vector classification depends only on a subset of the training data, training points that lie beyond the margin is independent of the cost function for building the model. Similarly, the model produced by SVR depends only on a subset of the training data. The cost function for building the model ignores any training data close to the model prediction [274, 275].The idea behind SVR is to map nonlinearly the original data x into a higher dimensional feature space [271].

Consider a set of data

$$G = \{(x_i, d_i)\}_{i=1}^{N} \tag{3.39}$$

where, x_i, d_i and N are input vector, actual values and number of data pattern respectievely. The SVR function is given by Eq.(3.40)

$$Y = f(x) = W\psi(x) + b \tag{3.40}$$

Where, $\psi(x)$ is the feature which is obtained by nonlinear mapping of input space.

The coefficients W and b are calculated by minimizing the regularized risk function which is given by Eq.(3.41),

$$R(C) = (C/N)\sum_{i=1}^{N} L_\epsilon(d_i, y_i) + \frac{|W^2|}{2} \tag{3.41}$$

where,

$$L_\epsilon(d, y) = \begin{bmatrix} 0 & if|d-y| <= \epsilon \\ |d-y| - \epsilon & otherwise \end{bmatrix} \tag{3.42}$$

C and ϵ are prescribed parameters .

This function creates a tube which has error less than ϵ. $L_\epsilon(d, y)$ is called the ϵ insensitive loss function. If the forecasted values are within the ϵ tube, the loss function become zero. The flatness of the function is measured by the second term $|W^2|/2$ [271]. C is the trade-off between empirical risk and model flatness, the user can define both of these parameters C and ϵ. There are two slack variables μ and μ^*, which represent the distance from the actual values to the corresponding boundary values of ϵ- tube [276]. The Eq. (3.41) can be written as

$$minR(W, \mu, \mu^*) = \frac{|W^2|}{2} + C(\sum_{i=1}^{N}(\mu_i + {\mu^*}_i)) \tag{3.43}$$

With constraints,

$$W\psi(x_i) + b - d_i \leq \epsilon + {\mu^*}_i \tag{3.44}$$

$$d_i - W\psi(x_i) - b \leq \epsilon + \mu_i \tag{3.45}$$

$$\mu_i, {\mu^*}_i \geq 0 \tag{3.46}$$

where i= 1, 2, 3.....N

Primal lagrangian equation is used for solving this constrained optimization problem, which is in the form of

$$\begin{aligned} L(W, b, \mu_i, \mu_i^*, \alpha_i, \alpha_i^*, \beta_i, \beta_i^*) = \frac{|W^2|}{2} + C(\sum_{i=1}^{N}(\mu_i + {\mu^*}_i) \\ - \sum_{i}^{N} \beta_i(W\psi(x_i) + b - d_i + \epsilon + {\mu^*}_i) \\ - \sum_{i}^{N} {\beta^*}_i(d_i - W\psi(x_i) - b + \epsilon + {\mu^*}_i) - \sum_{i}^{N}(\alpha_i\mu_i + \alpha^*{\mu^*}_i) \end{aligned} \tag{3.47}$$

This equation is maximized with respect to nonnegative lagrangian multipliers $\alpha_i, \alpha_i^*, \beta_i$ and β_i^*, minimized with respect to the primal variables W, b, μ_i and μ_i^*, which leads to the equations

$$\frac{\partial L}{\partial W} = W - \sum_i^N (\beta_i - \beta_i^*)\psi(x_i) = 0 \tag{3.48}$$

$$\frac{\partial L}{\partial b} = \sum_i^N (\beta_i - \beta_i^*) = 0 \tag{3.49}$$

$$\frac{\partial L}{\partial \mu_i} = C - \beta_i - \alpha_i = 0 \tag{3.50}$$

$$\frac{\partial L}{\partial \mu_i^*} = C - \beta_i^* - \alpha_i^* = 0 \tag{3.51}$$

The application of Karush-Khun-Tucker conditions, the substitution of previous Eq. (3.48) to Eq. (3.51) into Eq. (3.47) and the kernel $K(x_i, x_j) = \psi(x_i * x_j$ gives the dual Lagrangian equation

$$\begin{aligned} D(\beta_i, \beta_i^*) = \sum_i^N d_i(\beta_i - \beta_i^*) - \sum_i^N \epsilon(\beta_i + \beta_i^*) - \\ \frac{1}{2}\sum_i^N \sum_j^N (\beta_i - \beta_i^*)(\beta_j - \beta_j^*)K(x_i, x_j) \end{aligned} \tag{3.52}$$

Subject to the constraints,

$$\sum_i^N (\beta_i - \beta_i^*) = 0 \tag{3.53}$$

$$0 \leq \beta_i \leq 0 \tag{3.54}$$

$$0 \leq \beta_i^* \leq 0 \tag{3.55}$$

$$\beta_i * \beta_i^* = 0 \tag{3.56}$$

There are different type of kernel functions like Gaussian kernel, polynomial kernel, laplacian kernel ,exponential kernel,l Cauchy kernel and generalised T- student kernel etc which are presently used for non-linear mapping. From these kernels, Gaussian kernel gives best performance for load forecasting [277].Gaussian function is created by composing the exponential function with a concave quadratic function. The Gaussian functions are thus those functions whose logarithm is a concave quadratic function.

$$K(x_i, x_j) = Ae^{-(x_i - x_j)^2/\sigma^2} \tag{3.57}$$

Where A is the amplitude (for load forecasting we have taken that as 1), x_i and x_j are two input vectors, σ is the standard deviation or Gaussian RMS width. The optimization of lagrangian multipliers β_i and β_i^* can be calculated by quadratic programming. The maximization quadratic function for the above equation is given by in Eq. (3.58).

$$Max(\beta) = -0.5\beta^T H\beta + f^T\beta \tag{3.58}$$

which is subject to the same constraints. Where H is the hessian matrix given by Eq. (3.59).

$$H = \begin{bmatrix} h & -h \\ -h & h \end{bmatrix} \tag{3.59}$$

$$h(i,j) = K({x_i}^T, x_j) + 1 \tag{3.60}$$

$$f = \begin{bmatrix} \epsilon - y_1 & \epsilon - y_2 & .... & \epsilon - y_n & \epsilon + y_1 & .... & \epsilon + y_n \end{bmatrix} \tag{3.61}$$

Where $y_1, y_2.....y_n$ are the training stage output values.

The regression hyperplane optimal desired weight vector is given by Eq. (3.62).

$$W = \sum_{i}^{N} (\beta_i - \beta_i^*)\psi(x) \tag{3.62}$$

If β_i is in between 0 and C, the co-efficient b is given by Eq. (3.63).

$$b = y_i - W\psi(x) - \epsilon \tag{3.63}$$

If β_i^* is in between 0 and C, the co-efficient b is given by Eq. (3.64).

$$b = y_i - W\psi(x) + \epsilon \tag{3.64}$$

The predicted value Q is given by Eq. (3.65).

$$Q = \sum_{i}^{N} (\beta_i - \beta_i^*)K(x_i, x_j) + b \tag{3.65}$$

3.3.2.1 Data Selection

The year 2009, 2010 and 2011 values are used for model building and implementation.

- Training input: Monthly average hourly load data of month k of the year 2009 and monthly average hourly load data of month k-1 of the year 2009 and monthly average hourly load data of month k-1 of the year 2010.
- Training output: Forecasted values of the monthly average load values of month k of the year 2010.
- Testing input: Monthly average hourly load data of month k of the year 2010 and monthly average hourly load data of month k-1 of the year 2010 and monthly average hourly load data of month k-1 of the year 2011.
- Testing output: Forecasted values of the monthly average load values of month k of the year 2011.

3.3.3 Bayesian Multivariate Linear Spline Model (BMLS)

Bayesian Multivariate Linear Spline Model (BMLS), it presents a basis function approach using a multivariate linear spline for modeling the piecewise linear structure. Bayes' local linear model, having distributions on prediction and on local linear parameters, is obtained by integration over the posterior model space. The local variable parameters vary smoothly over the design space. The lower order splines can remove the irrelevant covariates and determine the relatively important ones from the rest. The averaging creates smooth mean regression surfaces. The model can automatically determine the bandwidth at each design point due to its random selection of location and number of splines [251, 252].

3.3.3.1 Piecewise Linear Regression

Regression of a variable K on set of p input variables Q, with observed data parings $H = \{(k_1, q_1), ... (k_n, q_n)\}$ can represent as represented in Eq. (3.66)

$$k_i = f(q_i) + \varepsilon_i \tag{3.66}$$

where,

- $f-$ True regression function
- ε_i- Gaussian noise coefficient($\sim N(0, \sigma^2)$)
- $q_i - i^{th}$ row of the design matrix Q

  i.e. $q_i = \{1, q_{i1}, q_{i2}, ..., q_{ip}\}$, inducing intercept term.

The true regression function f can be replaced by an approximate regression function $\hat{f}$, which is defined as piecewise linear over design space Q. The basis function approach using multivariate linear spline is adopted here to model piecewise linear structure [251]. Basis function generalizes the univariate linear spline to multivariate and is given by,

$$\hat{f}(q_i) = \beta_0 + \sum_{j=1}^{t} \beta_j (q_i.\mu_j) \tag{3.67}$$

where,

- $\beta = \{\beta_0, ...\beta_k\}^{'}$ are regression coefficients
- $\mu = \{\mu_{j0}, ...\mu_{jp}\}$ are basis parameters.
- $(q_i.\mu_j) = max(0, q_i.\mu_j)$
- j - Spline number (1,2,...t)
- $i-$ Sample number

3.3.3.2 Bayesian Framework

The classical piecewise linear models use single optimized parameters according to cross-validation score or penalized likelihood, and also those models fail to accommodate the uncertainty of parameter values, which results into a non-smooth regression surface. In Bayesian approach, the probability distribution of parameters is used instead of a single optimized set of parameters. Regression coefficients (β), basis function parameters (μ), number of spline (t) and noise variance (σ^2) are required for a particular Bayesian structure, $M = \{t, \mu, \beta, \sigma^2\}$. Prior distribution on the model space $p(M)$ are updated to posterior distribution using Bayes rule as in Eq. (3.68).

$$p(M|H) = \frac{p(H|M)p(M)}{p(H)} \tag{3.68}$$

Expectations can be used to represent point prediction under the model space as shown in Eq. (3.69)

$$E\left[k_i|q_i\right] = \int \hat{f}_M(q_i)p(M|H)dM \tag{3.69}$$

where $\hat{f}_M$ is $\hat{f}$ with model structure M. The likelihood and priors required for Bayesian analysis are explained in section 3.3.3.3. Analytical methods for finding posterior distribution is complex and time consuming, so this work uses Markov Chain Monte Carlo (MCMC) sampling technique [278] for the calculation of posterior distribution explained in section 3.3.3.4.

3.3.3.3 Bayesian Model

According to the assumed Gaussian noise Eq. (3.66), the model log likelihood can be expressed as

$$l(M|H) = -nlog\sigma - \frac{1}{2\sigma^2}\sum_{1}^{n}[k_i - \hat{f}_M(q_i)]^2 + a \tag{3.70}$$

where, a is tuning constant.

For a nonlinear basis space by adopting the conjugate Normal Inverse-Gamma priors for β and σ^2 Eq. (3.71), model can be treated as linear regression.

$$p(\beta, \sigma^2|t) = N_{t+1}(\beta|0, \sigma^2\lambda I_{t+1})IGa(\sigma^2|\tau_1, \tau_2) \tag{3.71}$$

Where λ is constant, I represents an identity matrix of dimension $d \times d$ and zero is assigned to prior mean of β. The gradient of the planes are determined by β and large gradients results sharp-rough surfaces. Inside the basis space μ, β and σ^2 posterior distribution can be expressed as Eq. (3.72).

$$p(\beta|H, \mu/\sigma^2, t) = N_{t+1}(\beta|\hat{\beta}, V)IGa(\sigma^2|\hat{\tau}_1, \hat{\tau}_2) \tag{3.72}$$

Where V, $\hat{\tau_1}, \hat{\tau_2}$ and $\hat{\beta}$ are the posterior updates from the prior.

$$\hat{\beta} = V(S^{'}K) \tag{3.73}$$

$$V = (\lambda^{-1}I_{t+1} + S^{'}S)^{-1} \tag{3.74}$$

$$\hat{\tau_1} = \tau_1 + n/2 \tag{3.75}$$

$$\hat{\tau_2} = \tau_2 + \frac{1}{2}(K^{'}K - \hat{\beta}^{'}V^{-1}\hat{\beta}) \tag{3.76}$$

and S is $n \times (t+1)$ spline design matrix

$$S = \begin{pmatrix} 1 & (q_1.\mu_1)_+ & \cdots & (q_1.\mu_t)_+ \\ 1 & (q_2.\mu_1)_+ & \cdots & (q_2.\mu_t)_+ \\ \vdots & \vdots & \vdots & \vdots \\ 1 & (q_n.\mu_1)_+ & \cdots & (q_n.\mu_t)_+ \end{pmatrix} \tag{3.77}$$

By fixing some of the elements of μ_{j-0} to zero, covariate selection can be induced into the model. This aligns the plane orthogonal to respective covariates. Integer interaction variable (z_j)calculates the number of non-zero elements μ_{j-0} for all basis functions. $\gamma_j = (\gamma_{j1}, \gamma_{j2}....., \gamma_{jp})$ is the indicator vector used in such a way that $\gamma_{jd} = 1$ if the d^{th} elements of μ_{j-0} is non-zero else $\gamma_{jd} = 0$. Hence,

$$z_j = \sum_{d=1}^{p} \gamma_{jd} \tag{3.78}$$

For each z_j, allocate a uniform prior $U[1, 2, ...Z]$, here Z is the maximum interaction permissible for each basis. The indicated vector uniform prior is adopted with respect to z_j and also the j^{th} spline alignment is uniformly rotated in the z_j dimensional covariate space denoted by γ_j.

Plane position is controlled by the first element of μ_{j0} in each basis. The μ_{j0} in each basis can be selected in such a way that atleast one data point is found on plane. The prior specification is on number of bases which is considered to be uniform and is $p(t) = U(0, ..., \infty)$. The joint prior can be written in factorized form on the model space as

$$\begin{aligned} p(t, \beta, \mu, \sigma^2, z, \gamma) = p(\beta|\sigma^2, t)p(\sigma^2) \\ p(\mu|z, \gamma, t)p(\gamma|z, t)p(z|t)p(t) \end{aligned} \tag{3.79}$$

Where,

- $p(\beta|\sigma^2, t)p(\sigma^2)$ is considered Normal Inverse Gamma with other all priors uniform.

The distribution of β and σ^2 is conditioned on data. The corresponding parameters are in the standard form however the posterior distribution of the other parameters are complex in nature. Therefore to derive inference, it is required to move towards simulation based parameters on full model space as in section 3.3.3.4.

3.3.3.4 Sampling from posterior distribution

For deriving the inference regarding marginal densities like mean regression surface or predictive distribution, sample form posterior density is used. As the number of pieces *a priori* is unknown, the conventional Markov Chain Monte Carlo (MCMC) simulations are impractical. This work uses the sampling method explained in [279]. At time T the state of Markov chain is represented by $M_T = \{\beta, \sigma^2, \mu, t, z, \gamma\}$. The sampler chooses any of the proposal with equal probability i.e. (Add, Remove, Alter) a basis function (plane) from/in the model by changing the position or orientation of the plane at each iteration. Procedure of adding a basis function to the model is explained in algorithm 3.3.

Algorithm 3.3 Basis Function Management

1: Initialize new basis function to 0, $\mu_j = \gamma_j = (0, ..., 0)$, here $j = t + 1$
2: From the prior $z_j \sim U\,[1, ..., Z]$ draw the interaction level.
3: Randomly select z_j elements γ_j and set the value =1.
4: Draw the values form Gamma(1,1) distribution corresponding to the elements of μ_{j-0}.
5: Normalize and square root all elements of the μ_{j-0} and then reverse the sign with $\frac{1}{2}$ probability.
6: Randomly select a data point form data set, say q_i & set $\mu_{j0} = -\sum_{d=1}^{p} q_{id}\mu_{jd}$.
7: From the full conditional densities in(7)draw the values for β & σ^2

The steps 2-5 guarantee that the rotation of new plane is uniform in the z_j, dimensions denoted by γ_j and orthogonal to all covariates. Step 6 ensures that atleast one data point is found on the boundary of new plane. There are two methods to alter a plane i.e. either changing the orientation or changing the position by randomly selecting one say(μ_j). For altering a basis function by changing the orientation, step 3,4 5 and 7 and by changing the position step 6 and 7 in algorithm 3.3 is used. For removal randomly select a plane and delete it, then after redraw β & σ^2 from Eq. (3.72).

$M_T^* = \{\beta^*, (\sigma^2)^*, \mu^*, t^*, z^*, \gamma^*\}$ represent new state after the proposed changes. The acceptance probability of the proposed changes is represented by,

$$O(M_T, M_T^*) = min\left\{1, \frac{p(M_T^*|H)Z(M_T^*, M_T)}{p(M_T|H)Z(M_T, M_T^*)}\right\} \tag{3.80}$$

where,

- $p(M|H)$- Posterior probability of M
- $Z(M_T^*, M_T)$-Probability of the movement M to M^*

After acceptance the new chain element,$M_{T+1} = M_T^*$ otherwise, $M_{T+1} = M_T$. After considering the move proposal and model prior,

$$O(M, M^*) = min\left\{1, \frac{p(H|t^*, \mu^*, z^*, \gamma^*)}{p(H|t, \mu, z, \gamma)}\right\} \tag{3.81}$$

where,

$p(H|t, \mu, z, \gamma)$-Marginal likelihood,
$\frac{p(H|t^*,\mu^*,z^*,\gamma^*)}{p(H|t,\mu,z,\gamma)} = \frac{\lambda^{-t^*/2}|V^*|^{1/2}}{\lambda^{-t/2}|V|^{1/2}}\left(\frac{\hat{\tau_2}}{\hat{\tau_2^*}}\right)^{\hat{\tau}_1}$- penalty factor.

Penalty factor in the MCMC removes the prior requirement of number splines by keeping it as a variable. Required number of samples close to the stationary equilibrium are iterated by MCMC. These samples drawn from the Posterior model space are called as BMLS model. Each sample generates piecewise linear surfaces and smooth regression surface is created by averaging of these linear surfaces.

3.3.3.5 Data Selection and Methodology

The performance of the model is evaluated based on the monthly average hourly load consumption data extracted from [272] (Tioman Island) for the year 2009, 2010 and 2011. The load demand of the Island is classified into commercial, municipal and residential loads. The commercial load includes resorts, hotels, schools, buddings, etc. requiring electricity to power lights, fan, AC, heating loads meanwhile the residential loads requiring electricity to power lights and fans and municipal loads to power street lights. The methodology used for the simulation is explained in different steps and is represented by,

1. Calculate model parameters prior distribution from training inputs and training outputs
    - Training inputs: 2010 $(i-1)^{th}$ monthly average hourly load data, 2009 i^{th}, $(i-1)^{th}$ and $(i+1)^{th}$ monthly average hourly load data.
    - Training outputs: 2010 i^{th} monthly average hourly load data .
2. Update prior distribution to posterior distribution using Bayes rule.

3. Select model samples close to the stationary equilibrium using MCMC algorithm.

4. Take the average of all the model parameter samples and add all splines to get the complete model structure.

5. Apply test inputs to the developed model structure for the forecasted values.

   - Test inputs: 2011 $(i-1)^{th}$ monthly average hourly load data, 2010 i^{th}, $(i-1^{th}$ and $(i+1)^{th}$ monthly average hourly load data.
   - Forecasted day: 2011 i^{th} monthly average hourly load data

6. Compare the forecasted values with actual data for the error evaluation.

3.3.4 Results and Discussions

The forecasted value of load by the developed model is compared with actual load values and error has been calculated. The indices used for the performance evaluations of the developed model are mean average error (MAE), maximum error (MAX E) in % and mean absolute percentage error (MAPE). The calculation of error has been done by simply taking the difference between the forecasted and actual values for each data point. Figure 3.6(a) - Figure 3.6(l) give the performance plots of different models for the month January to December respectively. The Eq. (3.82) - Eq. (3.85) is used for the calculation of MAE, MAPE and maximum error.

$$E = Y - Q \tag{3.82}$$

where, Y = actual output

Q = predicted value

Mean average error has been calculated by taking the mean of absolute error.

$$MAE = E_A/N \tag{3.83}$$

$$E_A = E_1 + E_2 + E_3.....E_n \tag{3.84}$$

where $E_1, E_2...E_n$ are absolute values of individual errors. Percentage error (PE) is calculated by dividing absolute value of error by corresponding actual value and then multiplying the result by 100.

Mean absolute percentage error is the mean of percentage error (PE)

$$MAPE = (1/N)\sum PE \tag{3.85}$$

The seasonal variations in the island are one of the main factors which affect the consumer load profile variations, and the same can be classified into four seasons:

1. northeast monsoon (NEM) season: From November to February
2. southwest monsoon (SWM) season: From May to August
3. first inter monsoon (FIM) season: From March to April
4. second inter monsoon (SIM) season: From September to October

The occupancy of the tourists in the island is highly affected by the NEM season compared to all another season. The tourists do not prefer to visit the island during NEM season due to the high wind speed and heavy rainfall. Thus the island exhibits two distinct load profiles in a year (i.e., NEM season and non-NEM season). From Figure 3.6(a) - Figure 3.6(l) it can be found that the maximum load consumption of the island is found around 20:00 hours and the minimum load consumption occur at 7.00 hours irrespective of all the season. The reason can be well justified by the fact that most of the tourist activities on the island are generally start from morning 7:00 am to evening 7:00 pm. The lower demand during this interval is due to most of the electrical appliances are switched off during tourist activities. After 7:00 pm the tourists return to their respective places and the electrical appliances come into action, hence gradually the electric power consumption increases and reaches the peak. The average maximum load during NEM and non-NEM seasons are approximately 1,019 kW, 1,509 kW and average minimum load 668 kW and 948 kW are respectively. Figure 3.6(k), Figure 3.6(l), Figure 3.6(a) and Figure 3.6(b) represent the forecasted (LTS, SVR, and BMLS) and actual load of NEM season respectively. During this period the electric load consumption is less due to the reason that the fewer frequencies of tourist activities as explained. Figure 3.6(c) and Figure 3.6(d) represent the FIM season, Figure 3.6(e) - Figure 3.6(h) represent SWM and Figure 3.6(i) and Figure 3.6(j)) represent SIM season respectively.

Being a stochastic method, each sample may offer a different value, but average smoothening of amply large samples reduces the chances of fluctuation from the ought to be predicted value. The sources of error may be the wrong selection of

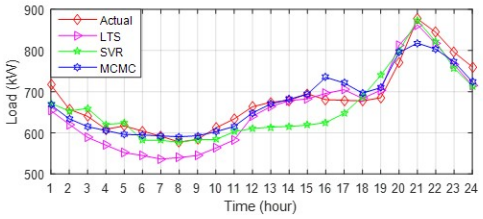

(a) Performance Plot of January

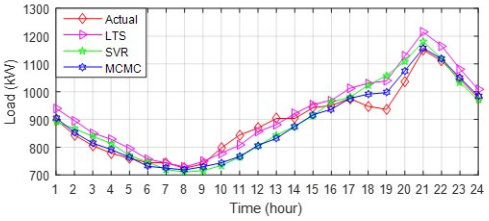

(b) Performance Plot of February

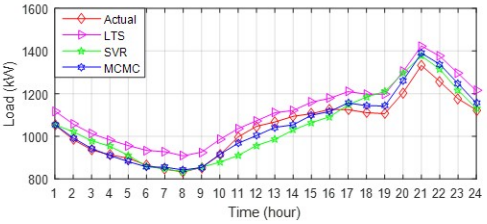

(c) Performance Plot of March

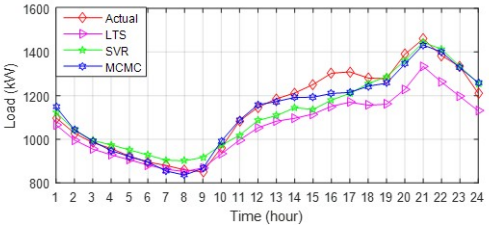

(d) Performance Plot of April

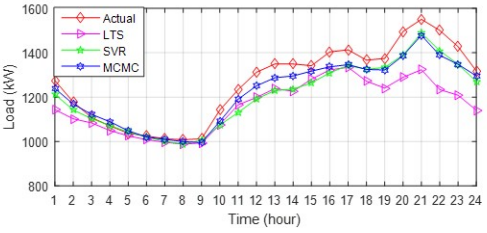

(e) Performance Plot of May

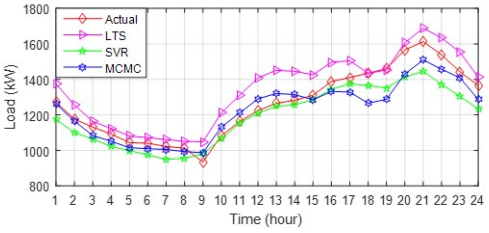

(f) Performance Plot of June

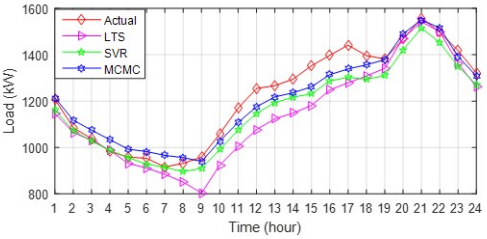

(g) Performance Plot of July

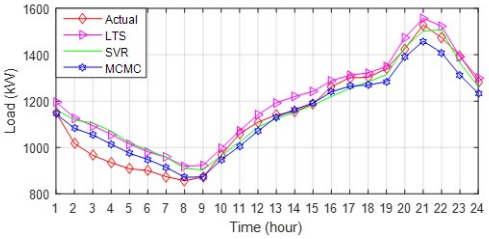

(h) Performance Plot of August

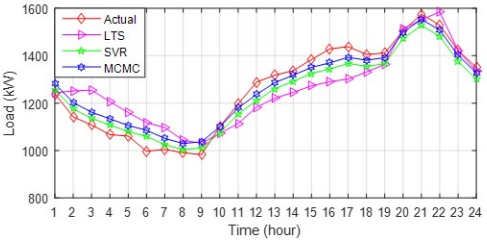

(i) Performance Plot of September

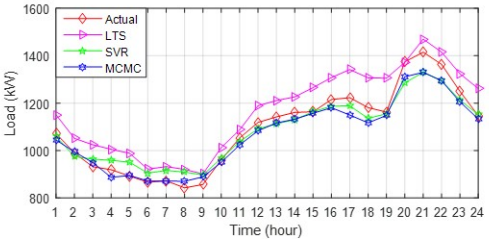

(j) Performance Plot of October

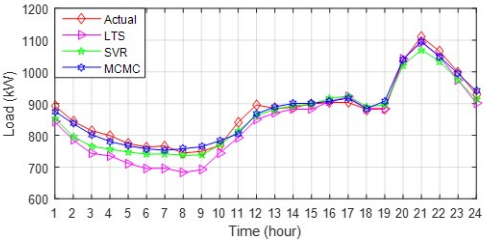

(k) Performance Plot of November

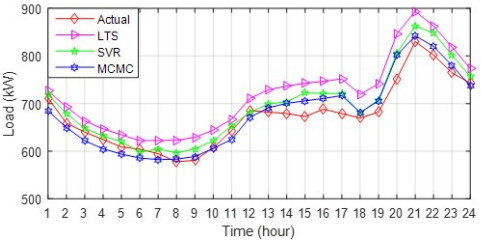

(l) Performance Plot of December

Figure 3.6: Performance Plot of LTS, SVR and BMLS Load Forecasting Model

Table 3.6: MAE, MAX E and MAPE of Different Model for Different Months

	LTS			SVR			BMLS		
	MAE	***MAX E***	***MAPE***	***MAE***	***MAX E***	***MAPE***	***MAE***	***MAX E***	***MAPE***
Jan	34.0620	10.5326	5.1806	30.2010	10.9173	4.3907	21.9098	7.9877	3.0920
Feb	37.0960	10.9541	4.0181	35.1872	12.9785	3.9613	24.7617	9.1853	2.8108
March	72.3802	10.0670	6.9917	42.4504	9.3656	3.9367	25.7788	6.4209	2.3025
April	79.8864	11.6334	6.4851	43.0454	9.4683	3.7951	28.0341	7.1809	2.3728
May	98.3771	17.7771	7.2408	57.7965	9.1542	4.3226	43.3817	7.4799	3.2116
June	83.6967	15.0644	6.7608	71.6898	10.8073	5.4915	60.1882	11.7945	4.5505
July	81.0461	16.1512	6.7050	58.4768	9.6742	4.5674	40.4311	7.1064	3.3658
Aug	52.0331	13.2833	5.0699	45.5071	14.4999	4.4894	41.3729	9.0928	3.6933
Sept	76.4034	13.3021	6.3328	43.6301	6.2573	3.4125	37.1301	8.8648	3.1449
Oct	75.9605	12.2838	7.1129	35.5177	7.8975	3.2942	31.1665	6.0021	2.6951
Nov	34.7199	9.0752	4.2136	22.0063	6.0354	2.5194	12.6574	4.2928	1.4707
Dec	44.3496	12.5427	6.5042	22.0159	7.4194	3.1851	17.8205	6.5305	2.6188

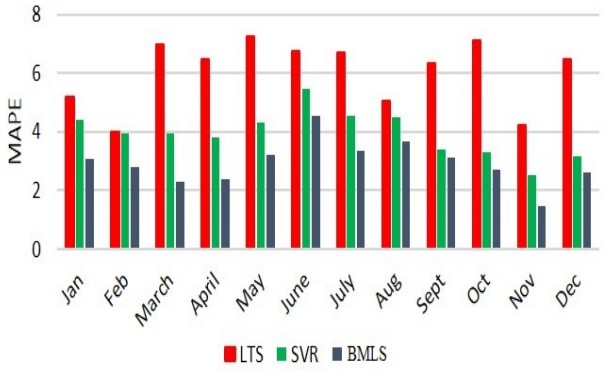

Figure 3.7: Comparison of MAPE of Different Models

features during the process. During the process of generating the basis function, randomly selected features are used instead of all the features. If the selected combination is inappropriate, it may affect the basis function, hence the design matrix and eventually the predicted value. Thus, it is recommended that the feature selection should be given much importance. The comparison of the BMLS model with LTS (Linear Time Series) and SVR (Support Vector Regression) models in terms of MAE, MAPE and Maximum Error using same data inputs is shown in Table 3.6 for each month. Form Table 3.6 it is clear that the performance of BMLS model is better as compared to the LTS and SVR model. Figure 3.7 gave the comparison of LTS, SVR and BMLS model in terms of MAPE. Table 3.7 illustrated the forecasting accuracy of the LTS, SVR and BMLS model and the accuracy of the BMLS model is found better as compared to the other developed model. Thus BMLS model is utilized further in this study for developing load forecasting agent for the proposed multi agent based energy management system

Table 3.7: Model Accuracy

	LTS	**SVR**	**BMLS**
Model Accuracy	93.94871	96.05284	97.05593

3.4 Chapter Summary

Different PV, wind output power generation forecasting and load forecasting models are developed in this chapter . Six combinations of ANFIS based forecasting models have been developed and analyzed the performance with PV and wind historical data. The ANFIS model with fuzzy c means clustering and hybrid optimization algorithm provides better performance as compared to the other developed models. Thus, this work utilized ANFIS model with fuzzy c means clustering and hybrid optimization algorithm to develop agents (PV forecasting agent and wind forecasting agent) for the proposed MAS based microgrid EMS. Also, linear time series, support vector regression and BMLS models have been developed for load forecasting, and the performance of the BMLS model found to better as compared to other developed models. Hence, the BMLS model is used later for developing the load forecasting agent for the proposed MAS EMS.

Chapter 4

Multi Agent based Energy Management System

4.1 Overview

The organization of Chapter 4 is two-fold. Primarily, this chapter proposes forecasting and estimation based multi agent system (MAS) for microgrid energy management as shown in Figure 4.1. In the proposed scheme, the unit commitment agent deployed in the decision making and planning layer collects the information from different agents. The unit commitment agent collected the forecasted load from load forecasting agent and forecasted output power production of photovoltaic, wind from PV agents and wind agents. The current state of charge (SOC) of the battery is very important for planning and unit commitment which is handled by the SOC agent. After receiving real-time information from agents, the unit commitment agent took the unit-commitment decision and passed to DG agents and battery agent for further action. But, this initial model faces some issues and is rectified by incorporating a correction agent in the initial model to give the improved model for MAS based microgrid energy management system (EMS).

4.2 Initial Model of MAS based microgrid EMS

Figure 4.2 represents the schematic diagram of the proposed MAS based EMS for a microgrid (MG). The MG in the proposed model has been developed in

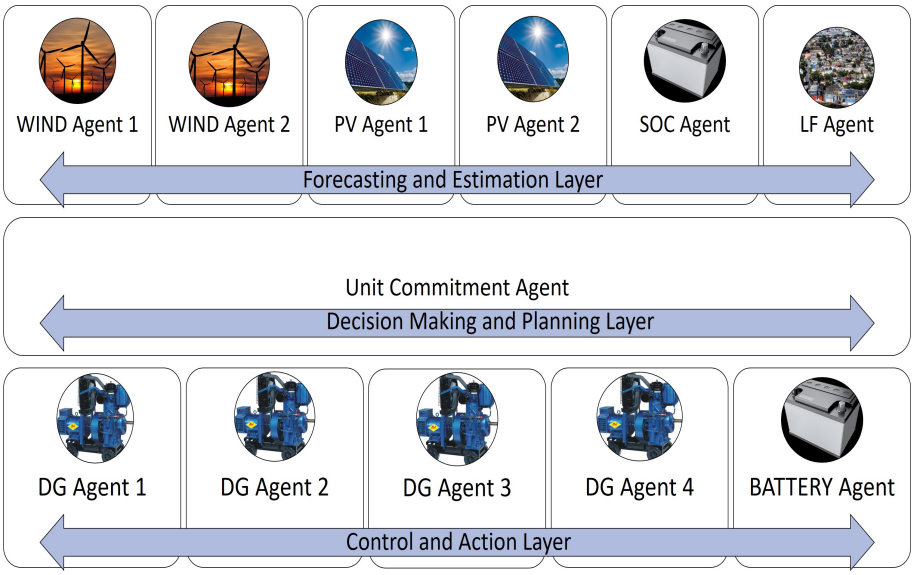

Figure 4.1: Proposed MAS Architecture for microgrid EMS

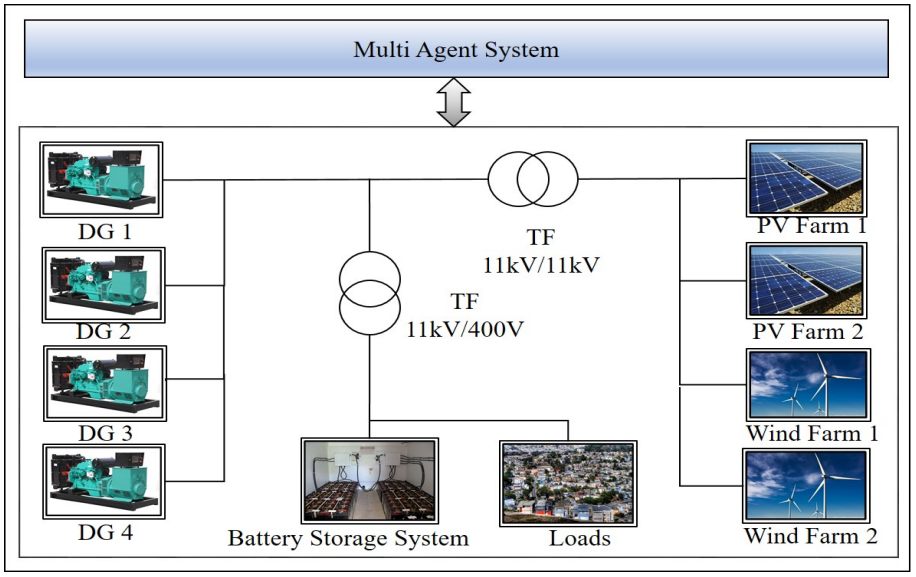

Figure 4.2: Proposed Microgrid MAS-EMS Model

Matlab Simulink with phasor-mode simulation. The detailed modeling and the parameters used for the MG simulation are explained in chapter 2. The agents and their behavior have been modeled using Stateflow by utilizing the concepts of state machines and flowchart etc.

4.2.1 Choice of Agent Platform

An agent platform is an environment where agents live, identical to the universe for human beings. The key purpose of an agent platform is to guarantee commu-

nication that is reliable and deliver multiple communication protocols, languages, and communication media, etc. Different authors have used different platforms namely JADE, ZEUS, PSIM and PSCAD for implementing MAS for MG applications [13]. Some of them are summarized in Table 4.1 where NA represents that the authors of that particular article have not addressed the platform used for the simulation. The advantages/disadvantages and comparison of different platforms can also be found in Table 1.2.

Table 4.1: Different MAS platform used by authors for microgrid simulations

Author	**Platform**
[15, 69, 23, 20] [21] [76] [41] [16] [22] [77] [186][187]	JADE
[17]	PSIM and Simulink
[26]	PSCAD/EMTDC
[39] [102]	ZEUS
[116] [117] [24][25][27][183][184][185]	NA

This thesis adopted a new platform called Stateflow for modeling MAS for the microgrid energy management system . Stateflow is an environment used for modeling and simulating the decision logic and controls in a natural, readable, and understandable form [280] . The Stateflow platform allows to model how a system reacts to particular events, conditions and external factors, etc. moreover, it is tightly coupled with MATLAB and Simulink, providing a competent environment for developing embedded systems that contain control, supervisory, and mode logic. A state machine represents a system that is driven by some events, and can make the transition from one mode to another mode according to the changes in the environment. Also, the state machines are the best known and oldest way of modeling the behavior of any system. The state machine allows designers to imagine the state of any system at the particular point of time and it also describes the behavior of the system based on that state. Moreover, this modeling method is not limited to software system [281]. Mathematically, a finite state machine can be defined as $f(Q, q_0, F, \epsilon, \delta)$[282]:

where,

- ϵ- Finite inputs to the machine.
- Q- Finite set of states
- $q_0 \in Q$ - Initial sates

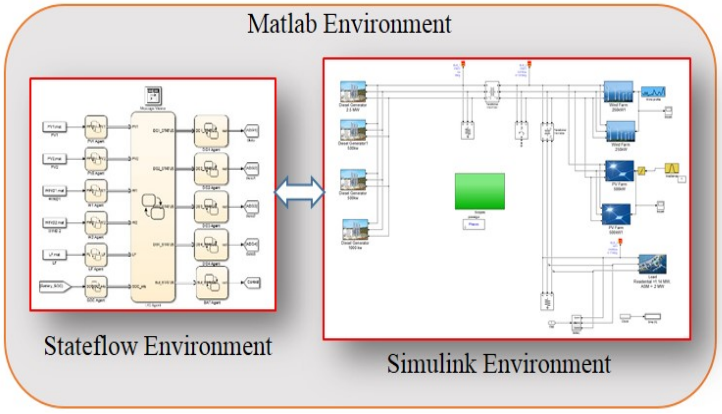

Figure 4.3: Integration of Agents in Stateflow with microgrid in Simulink

- $F \subseteq Q$- Final States
- $\delta : Q \times \epsilon \rightarrow Q$ - Transition function

For modelling a system with finite state machine concept, the system should possess several key characteristics like

- The complete system must be able to be described by a finite set of states.
- A finite set of events/inputs must be in the system to trigger the transition between the states.
- Any event's occurrence or the input and the current state should define the behavior of the system at the particular point of time.
- The system should have specific initial state

The integration of agents developed in Stateflow and the microgrid model developed in Simulink environment of MATLAB and their interaction is shown in Figure 4.3.

4.2.2 Modelling of Proposed MAS

The proposed MAS consists of 12 agents deployed in three layers namely Forecasting and Estimation Layer, Decision Making and Planning Layer and Control, and Action Layer as shown in Figure 4.4. The Algorithm 4.1 show the decision-making process of the agents in the proposed structure for microgrid EMS. Each layer in the proposed system can be described as follows:

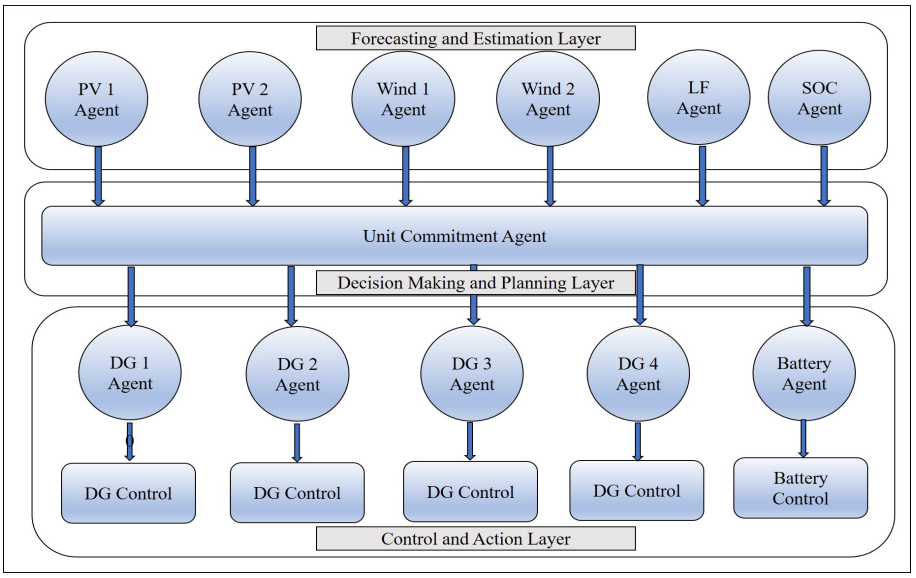

Figure 4.4: Proposed MAS Architecture for microgrid EMS

Algorithm 4.1 Agent Decision Making Process

1: Get historical load data
2: Get historical PV output power data
3: Get historical wind output power data
4: Get SOC information
5: Run load forecasting algorithm
6: Run PV foreasting algorithm
7: Run Wind forecasting algorithm
8: Get Forecasted Load
9: Get PV forecasted output power
10: Get Wind forecasted output power
11: Exchange step 4, step 8, step 9 and step 10 information to UC agent
12: Take unit commitment decision
13: Pass information to DG and battery agents

- **Forecasting and Estimation Layer:** This layer considered as the first layer in the proposed scheme. The first layer consists of six types of agents (2* PV agents, 2* wind agents, load forecasting (LF) agent and SOC agent). The input to this layer is historical data of solar output power, historical data of wind power output, historical load values and current SOC information. The output from this layer is the forecasted power output of PV and wind, forecasted load demand of the microgrid and SOC information of the battery.

- **Decision Making and Planning Layer:** This layer considered as a middle layer in the proposed scheme where the unit commitment agent is deployed. The input to this layer is forecasted values of PV, wind, load demand and

current SOC information of the battery provided by the SOC agent. The output from this layer is the unit commitment decision taken by the unit commitment agent.

- **Control and Action Layer:** This layer is considered as the third layer in the proposed agent architecture. In this layer, diesel generator and battery agents are deployed, and the input to this layer is pieces of information from the middle layer. After receiving the unit commitment decision from the unit commitment agent, the diesel generator and battery agents act accordingly to provide power balance in the system.

The function of individual agents which are deployed in the three layers are as follows:

4.2.2.1 PV Agents

The function of PV agent is to forecast the PV power output from the historical data and pass the information to unit commitment agent for further decision making. Figure 4.5 represents the PV agent developed in Stateflow for the proposed system and its interaction with the unit commitment agent. The PV agent runs intelligent PV power output forecasting algorithm as represented in section 3.2.

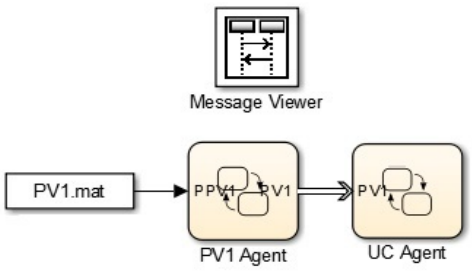

Figure 4.5: PV Agent Model

Figure 4.6 shows the message/information exchanged between PV1 agent during 24 hours of simulation. In Figure 4.6, the forecasted power availability information exchanged by the PV1 agent is shown for each hour, between the PV1 agent and UC agent. For example, the forecasted power availability of PV1, represented by PV1(200.884850), means the power forecasted is 200.884850 kW at the 10 hours as represented in Figure 4.6. The information exchanged between the PV2 agent, and UC agent has not been shown here because the PV arrays used are identical

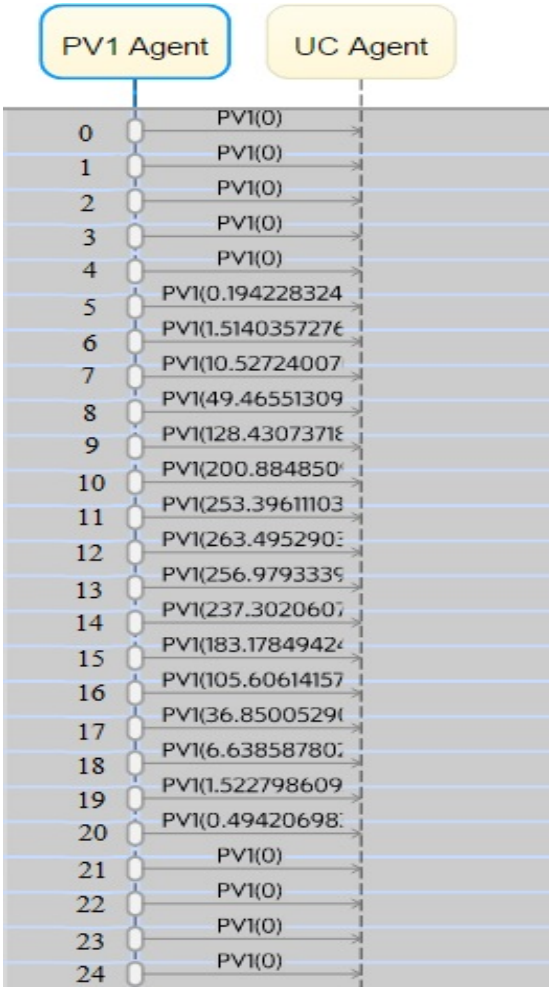

Figure 4.6: Communication of PV Agent with UC Agent

and the irradiance is also same thus it will provide the same power output as that from PV1.

4.2.2.2 Wind Agents

The function of wind agent is to provide the forecasted wind output power availability information to the unit commitment agent for taking the unit commitment decision. Figure 4.7 shows the modeling of wind agent in Stateflow and interaction of wind agent with the unit commitment agent. The wind agent runs an algorithm presented in section 3.2 that forecasts power availability of wind farm at the current time. Figure 4.8 represents the message/information exchanged between wind1 agent during 24 hours of simulation. In Figure 4.8 the forecasted power availability information exchanged by the wind1 agent is shown in each hour for the 24-hour duration, occurring between the wind1 agent and UC agent. The

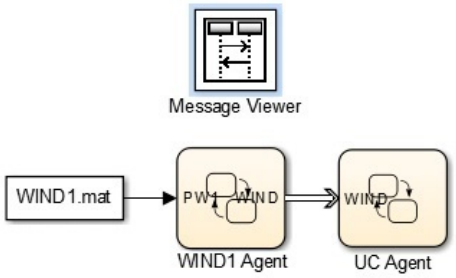

Figure 4.7: Wind Agent Model

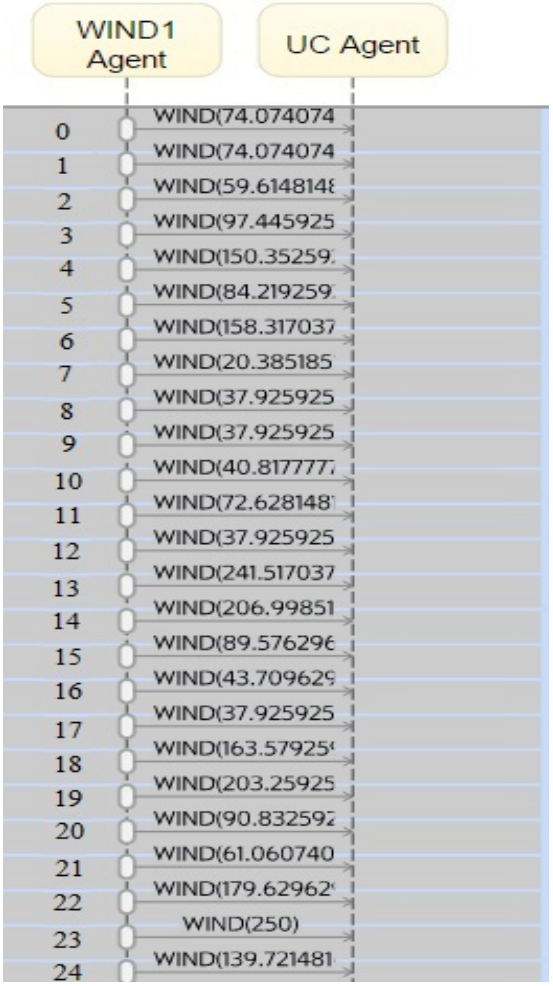

Figure 4.8: Communication of Wind Agent with UC Agent

forecasted power availability of wind1, represented by WIND(72.628148), means the power forecasted is 72.628148 kW at the 11 hours as illustrated in Figure 4.8. The information exchanged between both the wind farms and the UC agent are the same hence the message exchanged by the wind2 agent has not been shown.

4.2.2.3 Load Forecasting (LF) Agent

The function of load forecasting agent is to forecast the load demand of the microgrid and pass the message to the unit commitment agent. The load forecasting agent utilizes the model explained in section 3.3.3. The load forecasting agent modeled in Stateflow has been shown in Figure 4.9. Figure 4.10 gives the message/information exchanged between LF agent and UC agent during the 24-hour simulation with one hour time span. Figure 4.10, LF(1945.0625) represents the forecasted load demand of the MG is 1945.0625 kW at the 9 hours, and the same is exchanged between LF agent and UC agent.

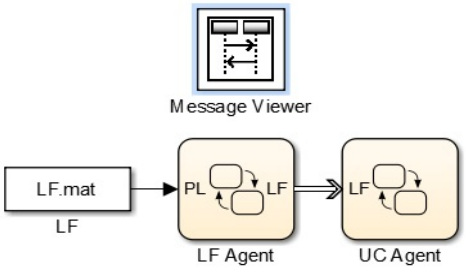

Figure 4.9: Load Forecasting Agent Model

4.2.2.4 SOC Agent

The SOC agent will give the current state of charge of the battery to the unit commitment agent from the MG model. The SOC of the battery is limited between 20 % and 80 % of its ampere-hour capacity for preventing the undercharging and overcharging of the battery storage system respectively. Figure 4.11 gives the model of SOC agent developed in Stateflow and the interaction with the unit commitment agent. The SOC agent senses the current SOC information from the battery. The battery SOC is calculated as in [283] and shown in Eq. (4.1).

$$B_{SOC} = 100[1 - (\frac{1}{Q_B}) \int_0^t i_B(t)dt] \tag{4.1}$$

Where,

B_{SOC}- State of charge of battery in %.

Q_B- Maximum battery capacity in Ampere hour

i_B- Battery current in ampere.

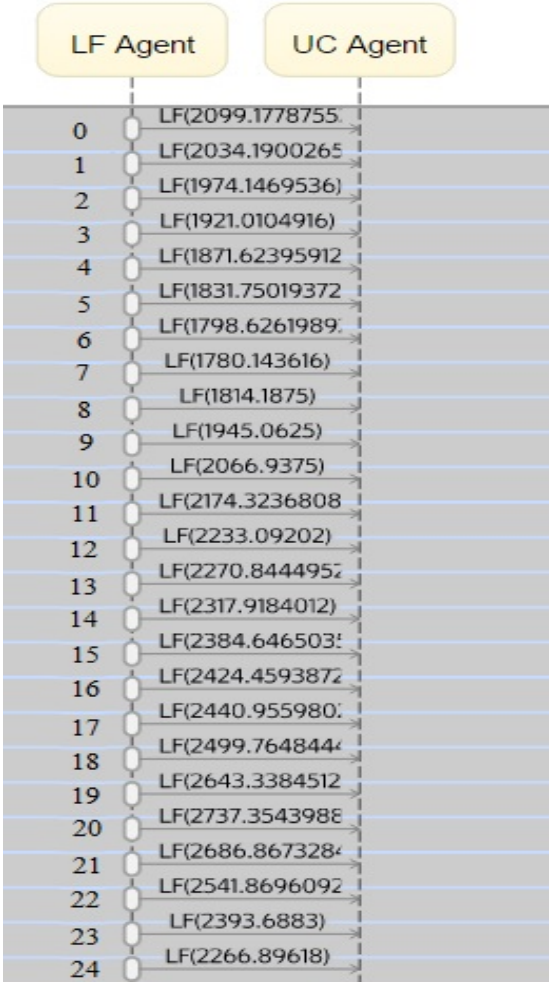

Figure 4.10: Communication of LF Agent with UC Agent

4.2.2.5 Unit Commitment (UC) Agent

The function of unit commitment agent is to provide dispatch strategies for the diesel generators and battery storage system in the proposed model by fully utilising the available output power from the RES to satisfy the load requirement of the microgrid. The UC agent takes the unit commitment decisions after collecting the information from all the agents deployed in the forecasting and estimation layer. The decision taken by the UC agent is sent to the control and action layer where the DG agents and battery agent are deployed for further action. The decision-making process of the unit commitment agent is represented as in Eq. (4.2) and Eq. (4.3).

$$P_{req} = P_{LFA} - (P_{PVA1} + P_{PVA2} + P_{WA1} + P_{WA2}) \tag{4.2}$$

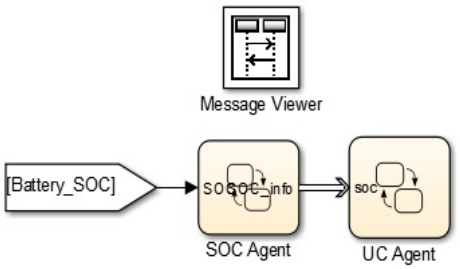

Figure 4.11: SOC Agent Model

where, P_{req} is the required power to fulfill the load in the microgrid after the complete utilization of renewable distributed energy resources. $P_{LFA}, P_{PVA1}, P_{PVA2}, P_{WA1}$ and P_{WA2} respectively represent the forecasted load demand of the microgrid, the forecasted output power of the PV and wind received from the forecasting and estimation layer.

$$UCD = \begin{cases} P_{req} < 0 & ; Fullfill Load + Charge Battery \\ P_{req} > 0 & ; DG_{1on} \\ P_{req} - P_{DG1max} > 0 & ; DG_{1on} + DG_{2on} \\ P_{req} - P_{DG1max} - P_{DG2max} > 0 & ; DG_{1on} + DG_{2on} + DG_{3on} \\ P_{req} - P_{DG1max} - P_{DG2max} - P_{DG3max} > 0 & ; DG_{1on} + DG_{2on} + DG_{3on} + DG_{4on} \end{cases} \tag{4.3}$$

where, P_{DG1max}, P_{DG2max},P_{DG3max} and P_{DG4max} are the maximum power generation capacity of the diesel generators can be found in Table 2.1. The $DG_{1on}, DG_{2on}, DG_{3on}$ and DG_{4on} represent the respective diesel generator which should be activated to fulfill the load requirement of the microgrid.

4.2.2.6 Battery Agent

The battery agents take charging and discharging actions accordingly after receiving the decisions from the unit commitment agent by sending control signals to the battery charging/ discharging controller deployed in the microgrid. The battery charging/ discharging controller is designed in such a way that the battery will charge only from the renewable energy resources when its power output is in excess after satisfying the load requirement of MG and not from the diesel generator. The battery agent can discharge the battery to fulfill the load requirements of the MG when its SOC is greater than 20%.

4.2.2.7 DG Agents

The DG agents take actions accordingly after receiving the decisions from the unit commitment agent. That is when and where, which diesel generator should be activated to meet the load requirement of the MG by completely utilizing the DERs.

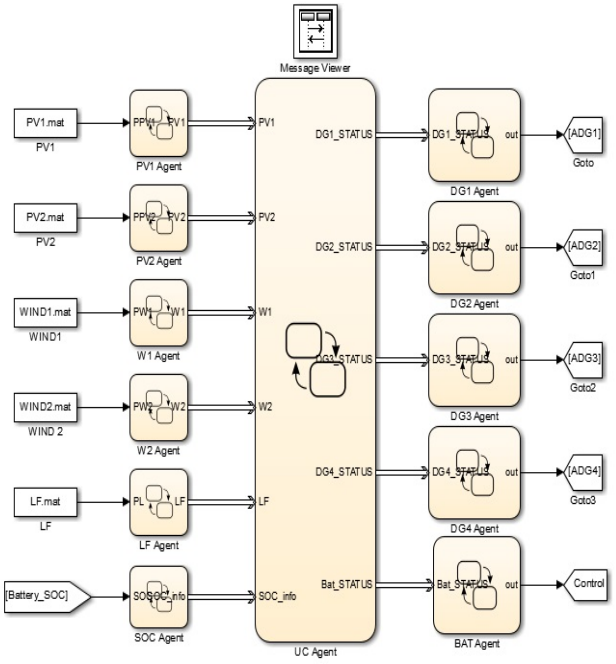

Figure 4.12: Multi Agent System developed for MG EMS in Stateflow

Figure 4.12 represents the MAS developed in Stateflow for the energy management in the microgrid.

4.3 Simulation Results and Analysis

4.3.1 Case Study

The performance of the proposed model is evaluated based on data collected from Tioman Island. The solar irradiation profile, wind speed, residential load and commercial load data used for the simulation study are shown in Figure 2.2(a) and Figure 2.2(b), Figure 2.2(c) and Figure 2.2(d) respectively and also the details can be found in section 2.3. The power output provided by all the diesel generators, wind farms, PV farms and the load requirements are represented in watts. The

SOC of the battery is represented in %. The simulation of the model shown in Figure 4.2 was carried out for 24 hours without the MAS and with the MAS. When considering the case study without the MAS, it has been considered that all the four diesel generators are activated and provide power to the microgrid as shown in Figure 2.7 along with the distributed energy resources. In the case study with MAS, the proposed system activate only the required diesel generators to satisfy the power balance in the system by ensuring the complete utilization of distributed energy resources. For analyzing the performance of the proposed multi agent system for energy management, three different scenarios have been created with some events that generally occur in the system.

4.3.1.1 Scenario 1 (S1)

In scenario 1, the model has been simulated without any disturbances in the system. This scenario is simulated to analyze the performance of the system during normal operations.

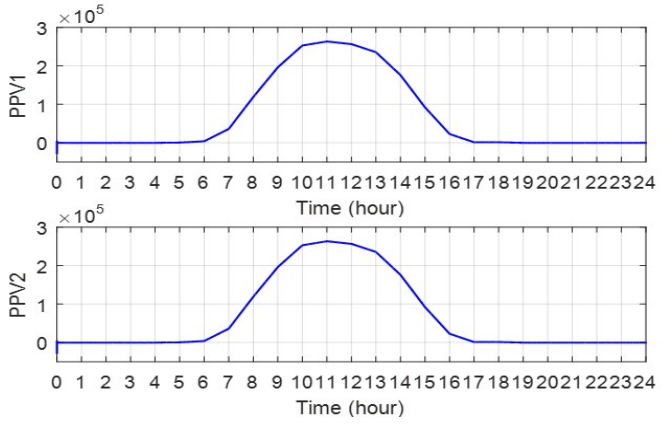

Figure 4.13: Power Output of PV Farm in S1

In Figure 4.13, PPV1 and PPV2 respectively show the output power in watts generated from PV farm1 and PV farm 2 in scenario 1. It is clear from both waveforms that the solar power follows the irradiance pattern represented in Figure 2.2(a). Figure 4.14 display the output power in watts of wind farm 1 (PWIND1) and wind farm 2 (PWIND2) respectively. As the wind power output is proportional to the cube of the wind velocity, it trails the pattern of wind speed represented in Figure 2.2(b). The load demand of the system in watts in scenario 1 is represented in Figure 4.15. Figure 4.16(a) and Figure 4.16(b) shows the output power in watts produced by the diesel generators in absence and presence of proposed agent based

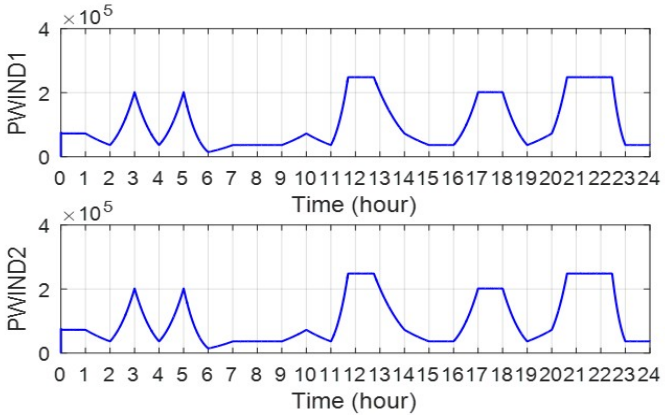

Figure 4.14: Power Output of Wind Farm in S1

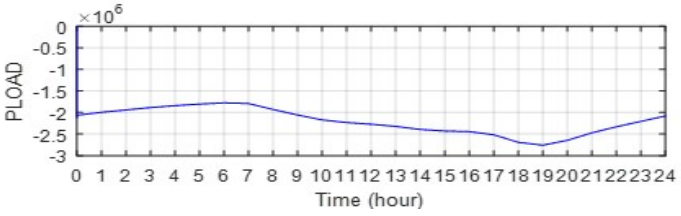

Figure 4.15: Load profile in S1

EMS to meet the load requirement of the MG respectively. The power output produced by the diesel generator 1, diesel generator 2, diesel generator 3 and diesel generator 4 (PDG1-PDG4) have been shown in Figure 4.16(a) and Figure 4.16(b) respectively. In Figure 4.16(a), in the absence of proposed MAS, the diesel generators 1-4 are active for the whole 24-hour duration of the day. On the other hand, in the presence of proposed MAS as in Figure 4.16(b), only diesel generator 1 is active for 24-hour duration and the diesel generator 2 is activated by the DG2 agent only for the short duration, i.e. 16-22 hours for fulfilling the requirement of microgrid after receiving the unit commitment decision from the UC agents. Also, the diesel generator 3 and 4 are deactivated for the complete 24-hour duration by respective DG agents because the DER and remaining diesel generators can satisfy the load demand. Accordingly, it is clear from Figure 4.16(a) and Figure 4.16(b) that the proposed multi agent based solution activated only necessary diesel generators instead of all at the same time and the complete utilization of DERs while ensuring the power balance in the system. The Figure 4.17(a) and Figure 4.17(b) show the state of charge of the battery (in %) in the complete duration of the simulation in absence and presence of proposed MAS. The battery constraint used in the simulation is that the battery will charge only when there is an excess power from the DER (not from diesel generators) and discharge when there is a requirement in the microgrid. In case of absence of MAS, all the diesel generators

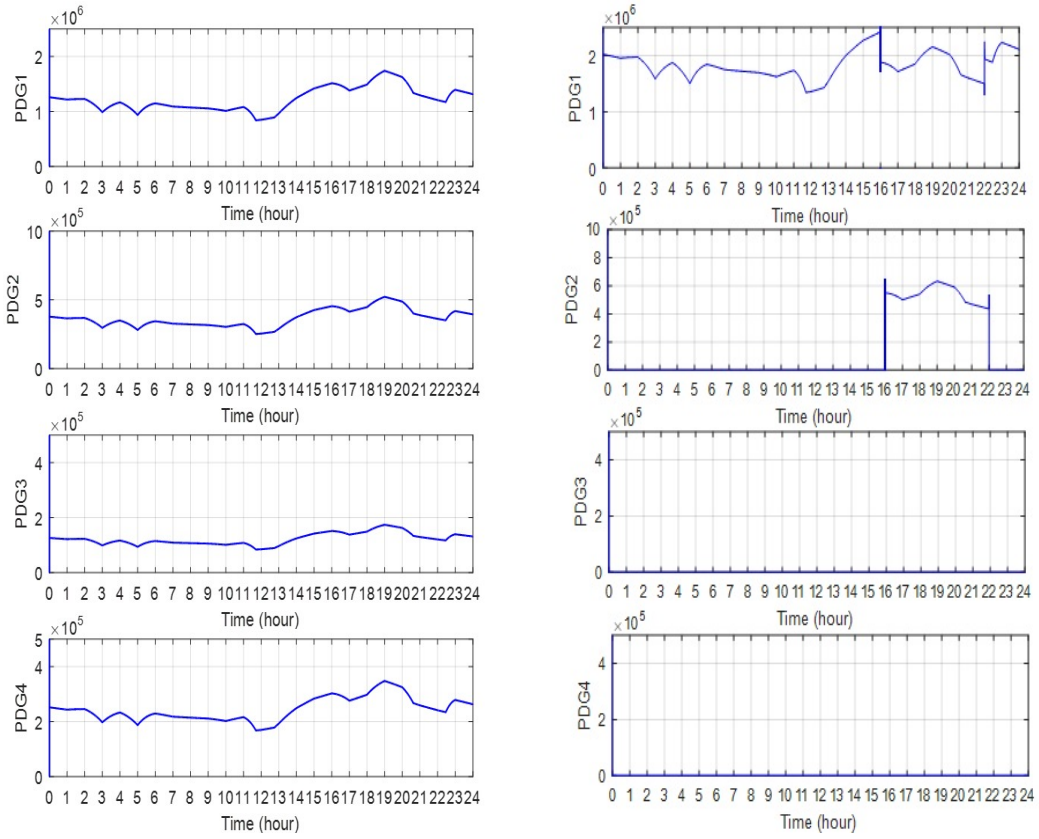

(a) without MAS-EMS

(b) with MAS-EMS

Figure 4.16: Power Output of Diesel Generator in S1

are continuously providing power to the microgrid as in Figure 4.16(a), so there is no excess requirement in the microgrid hence battery is not discharged. Also, the battery is not charged because in the case study the power from the renewable energy resources is not in excess to charge the battery. The same can be found in the Figure 4.17(a) represented as a constant SOC. Figure 4.17(b) the battery is not charged due the same reason explained above. The battery is providing some power to microgrid, whenever there is a requirement in the microgrid as in Figure 4.17(b) as only few diesel generators are activated (Figure 4.16(b)) . Figure 4.18 shows the complete message/information (i.e. forecasted power availability of PV, forecasted power availability of the wind, forecasted load demand, SOC and decisions and control actions to the DG agents, battery agent etc.) exchanged by all the agents in the proposed system during 24 hours of simulation for energy management in the microgrid. The message exchanged between agents for complete 24 hours has not been shown here due to the excessive length of the figure, instead of for some hours it has been shown.

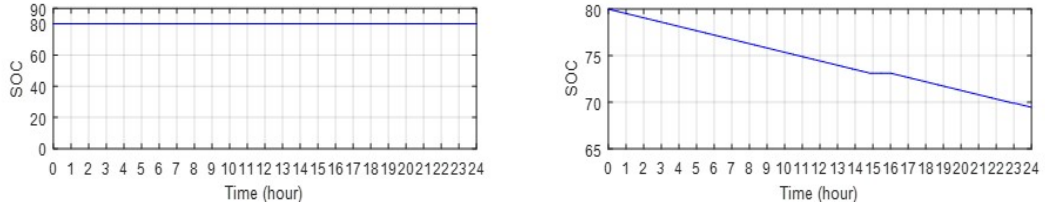

(a) without MAS-EMS (b) with MAS-EMS

Figure 4.17: Battery SOC in S1

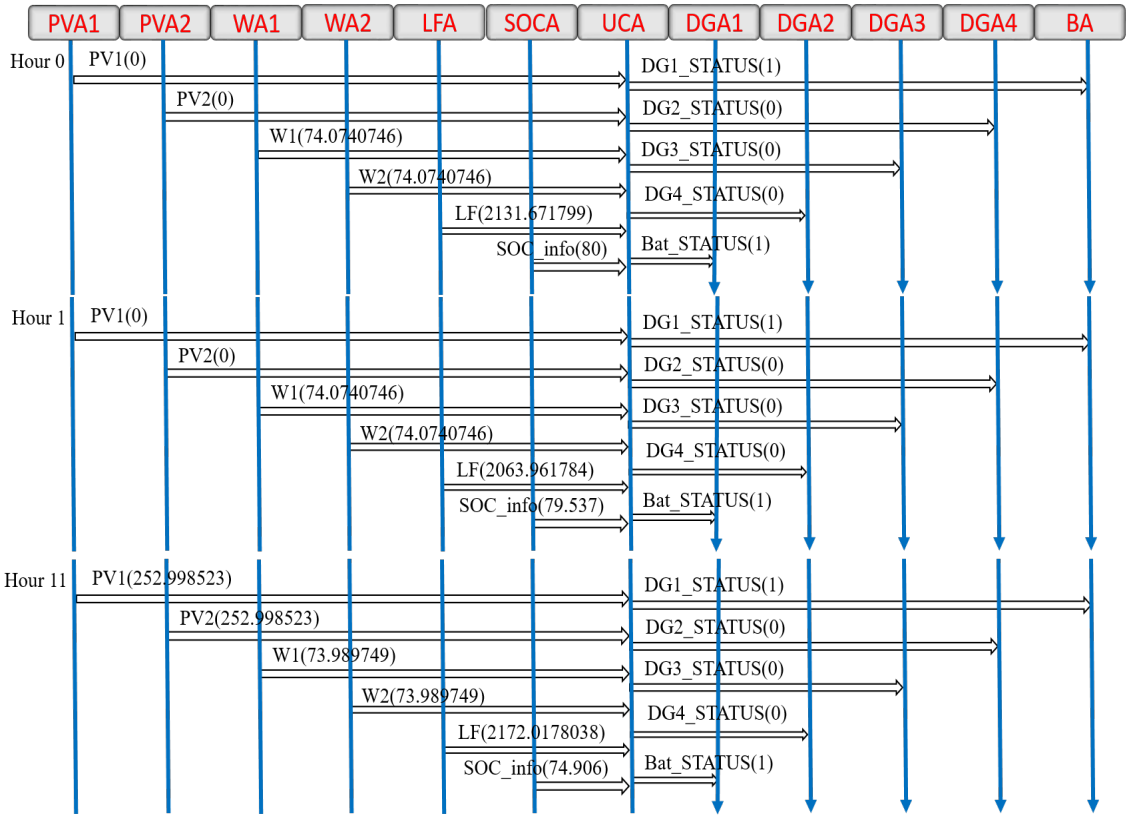

Figure 4.18: Agent Communication in S1

4.3.1.2 Scenario 2 (S2)

In scenario 2, a partial shading effect occurred in the PV system at 10:30 hours for a duration of 1800 seconds and the condition at which the wind speed exceeds the maximal wind speed at 21:00 hours of the simulation has also been considered. This scenario is simulated to study the effect of source side disturbances in the microgrid.

The Figure 4.19 show the output power in watts generated by PV farm 1 (PPV1) and PV farm 2 (PPV2) respectively. A sudden drop in PV output power, found

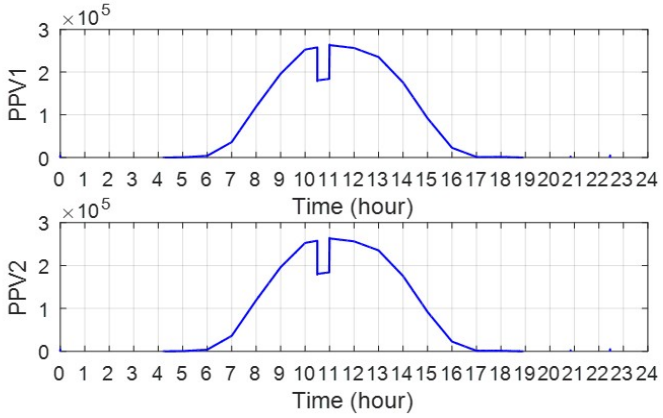

Figure 4.19: Power Output of PV Farm in S2

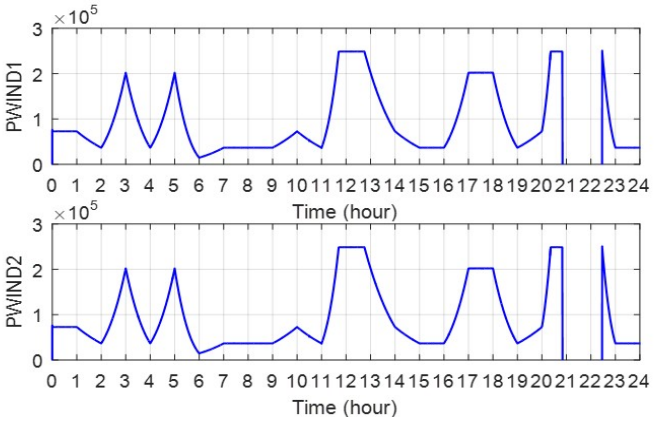

Figure 4.20: Power Output of Wind Farm in S2

at 10:30 hours, for a time span of 30 minutes in Figure 4.19 can be attributed to the effect of the partial shading considered in the study. Power outputs in watts of wind farm 1 (PWIND1) and wind farm 2 (PWIND2) in scenario 2 implemented has shown in Figure 4.20 respectively. In Figure 4.20, the wind power output trails the wind speed (Figure 2.2(b)) since it follows the cube of the wind velocity. However, at 21 hours for some duration, the output wind power is zero because the simulation considers that during this time, the wind speed exceeds the maximum wind speed and the wind turbine is isolated from the microgrid and stays offline until the wind speed returns to its nominal value. The load demand in watts of the system in scenario 2 is represented in Figure 4.21. The output power in watts produced by diesel generators to meet the load demand of the microgrid in presence and in absence of the proposed MAS based energy management system separately is shown in Figure 4.22(a) and Figure 4.22(b). The output powers of the four diesel generators (PDG1-PDG4) are shown by the in Figure 4.22 respectively. In Figure 4.22(b) it can be seen that the diesel generator 1 is active for 24 hours and diesel generator 2 is active only during the 16:00-22:00 hours. Also, the diesel generator 1

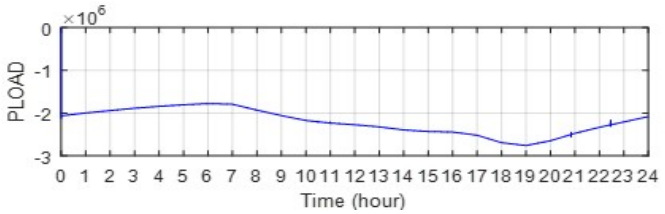

Figure 4.21: Load profile in S2

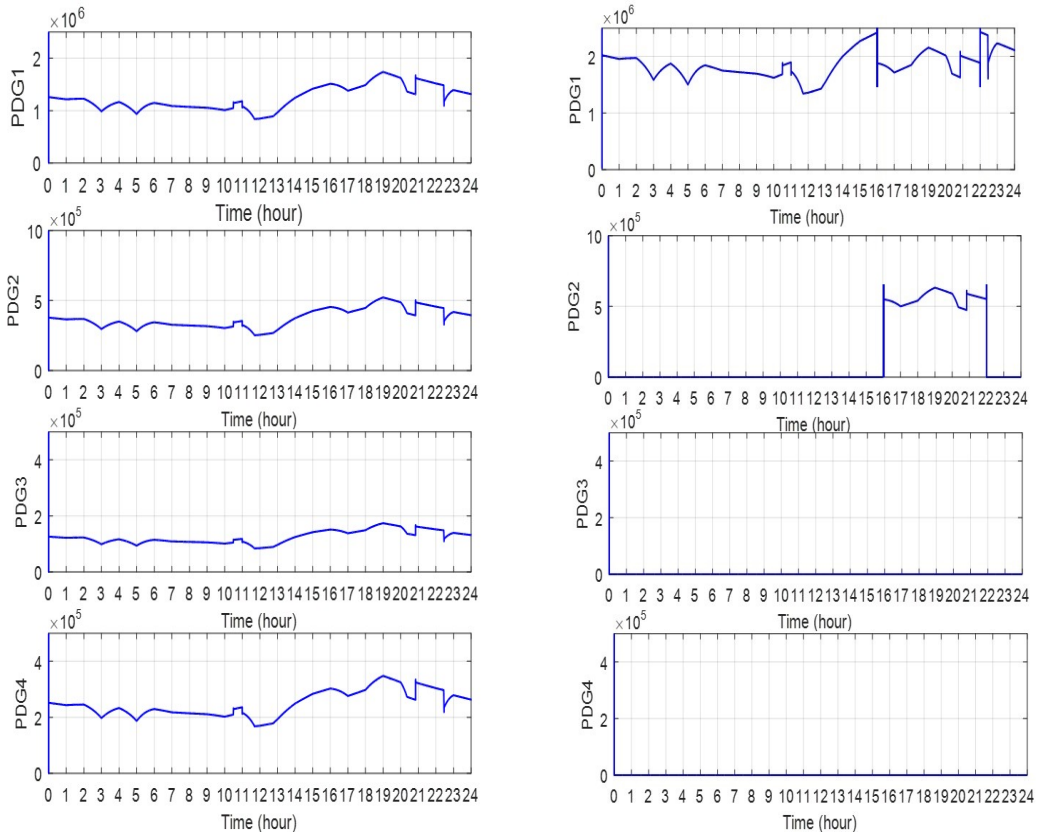

(a) without MAS-EMS

(b) with MAS-EMS

Figure 4.22: Power Output of Diesel Generator in S2

suddenly starts providing more power at 10:30 hours to compensate the reduction in power output of the PV at the same time due to partial shading effect. The diesel generator 3 and diesel generator 4 are not active throughout the simulation. On the other hand, in Figure 4.22(a), in the absence of proposed scheme, all the diesel generators are active for the complete duration of the scenario. Figure 4.23(a) and Figure 4.23(b) show the state of charge of the battery (in %) in both the cases respectively in this scenario. In Figure 4.23(a), the state of charge of the battery is constant. In Figure 4.23(b)) the battery agent can be seen performing the battery control action to supply the load when there is a power shortage in the

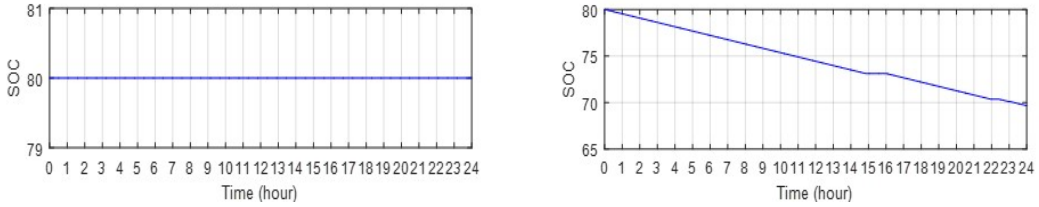

(a) without MAS-EMS (b) with MAS-EMS

Figure 4.23: Battery SOC in S2

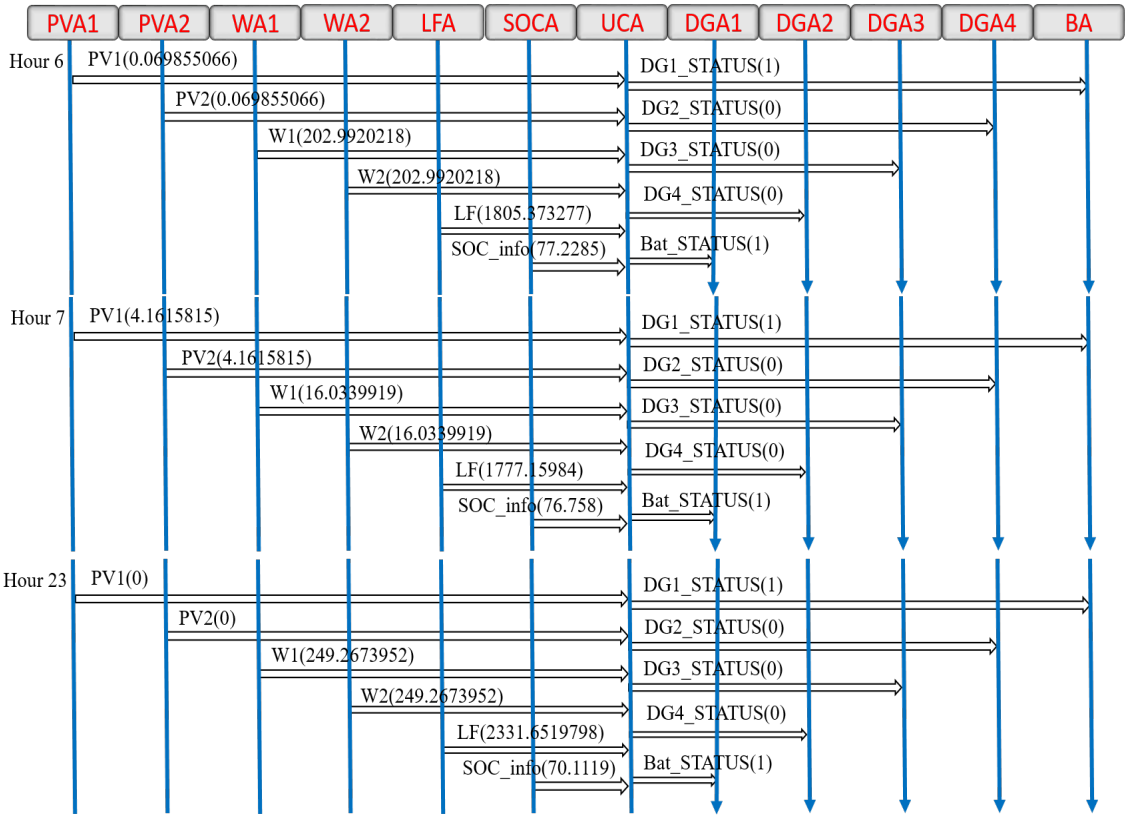

Figure 4.24: Agent Communication in S2

microgrid system. The battery is not charged throughout the simulation because the battery controller is constrained to charge it only when there is an excess power produced by RES. Figure 4.24 gives a snapshot of the messages and information exchanged during the simulation in scenario 2. Due to the excessive length of figure, the information exchanged for 24 hours has not been shown, instead for some hours it is shown.

4.3.1.3 Scenario 3 (S3)

In scenario 3, to show the effect of commercial load in the system, an asynchronous machine having capacity of 0.2 MW was introduced in the system at 20:00 hours of simulation using a circuit breaker. This scenario is created to analyze the performance of microgrid multi agent system during load side disturbance.

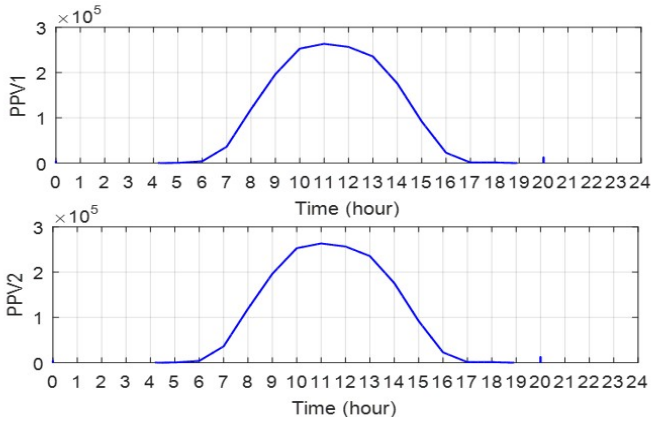

Figure 4.25: Power Output of PV Farm in S3

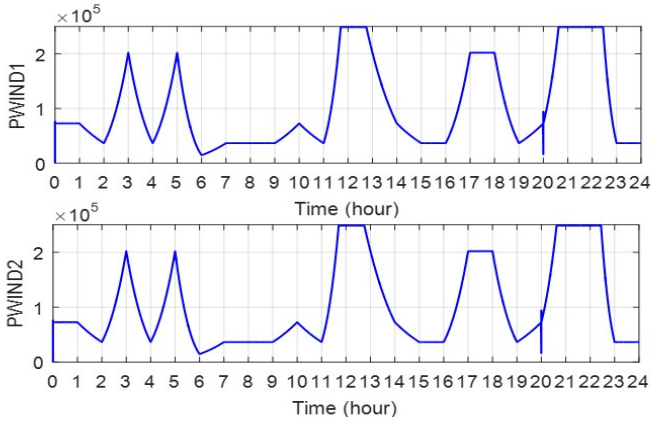

Figure 4.26: Power Output of Wind Farm in S3

Figure 4.25 displays the output power in watts generated from the PV farm1 (PPV1) and PV farm 2 (PPV2) respectively. The Figure 4.26 shows the output power in watts generated by the wind farm 1 (PWIND1) and wind farm 2 (PWIND2) respectively in scenario 3. The load demand in watts of the system in scenario 3 is represented in Figure 4.27. The PLOAD of the Figure 4.27 gives the residential power demand (in watts) and PASM represents the demand of commercial loads (in watts). The output power in watts produced by diesel generators to meet the load demand of the microgrid in presence and absence of proposed

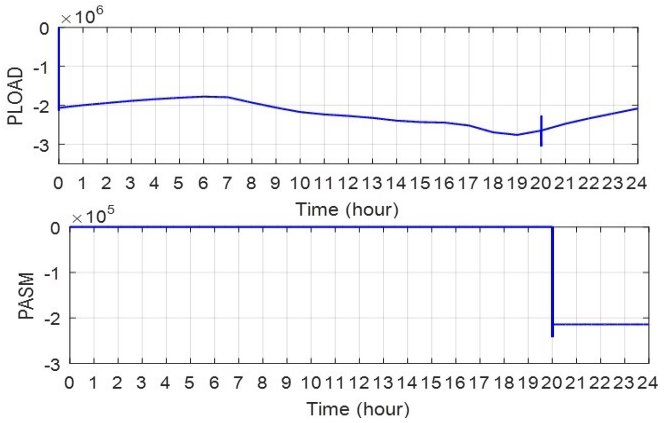

Figure 4.27: Load profile in S3

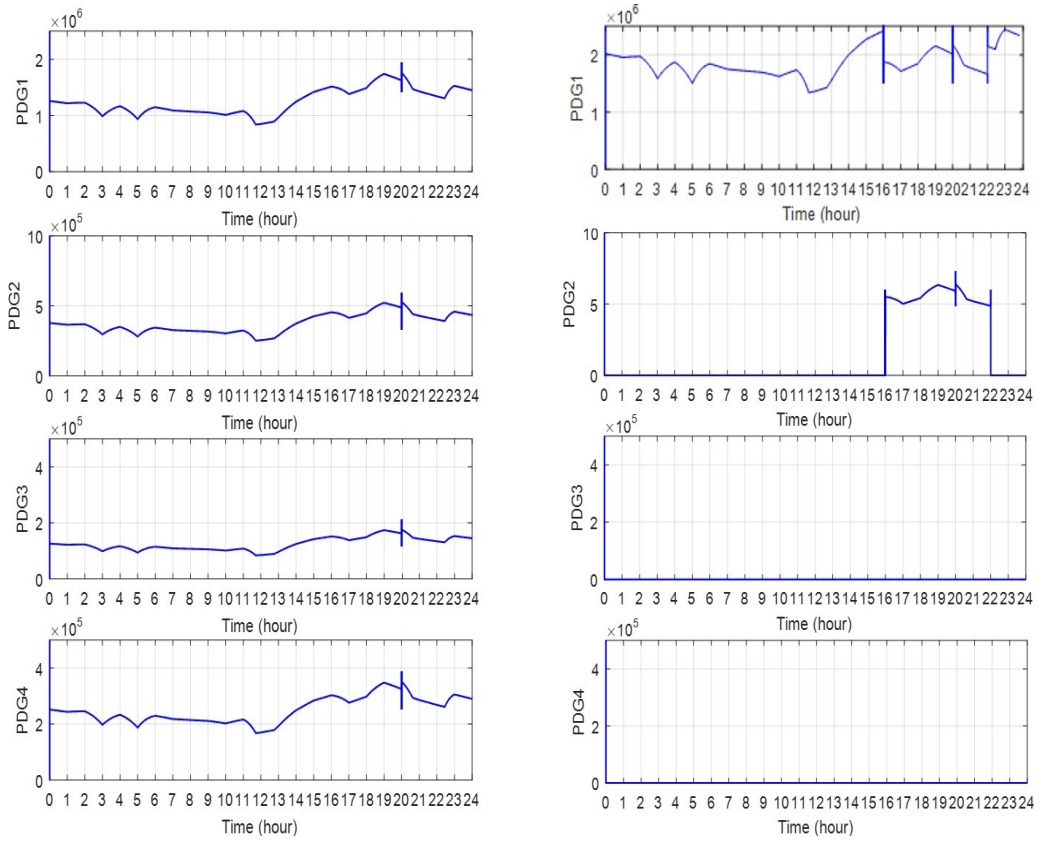

(a) without MAS-EMS

(b) with MAS-EMS

Figure 4.28: Power Output of Diesel Generator in S3

MAS based energy management system separately is shown in Figure 4.28(a) and Figure 4.28(b). In Figure 4.28(b) it can be clearly seen that the DG 3 and DG 4 are completely offline during the complete simulation and DG2 provides power only for some duration. On the other hand in Figure 4.28(a), in the absence of the proposed scheme, all the diesel generators are active for the complete duration of

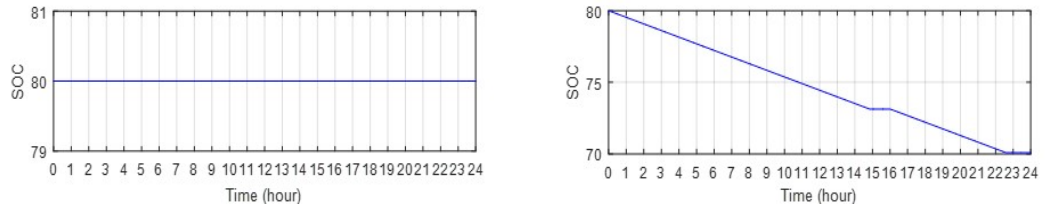

(a) without MAS-EMS (b) with MAS-EMS

Figure 4.29: Battery SOC in S3

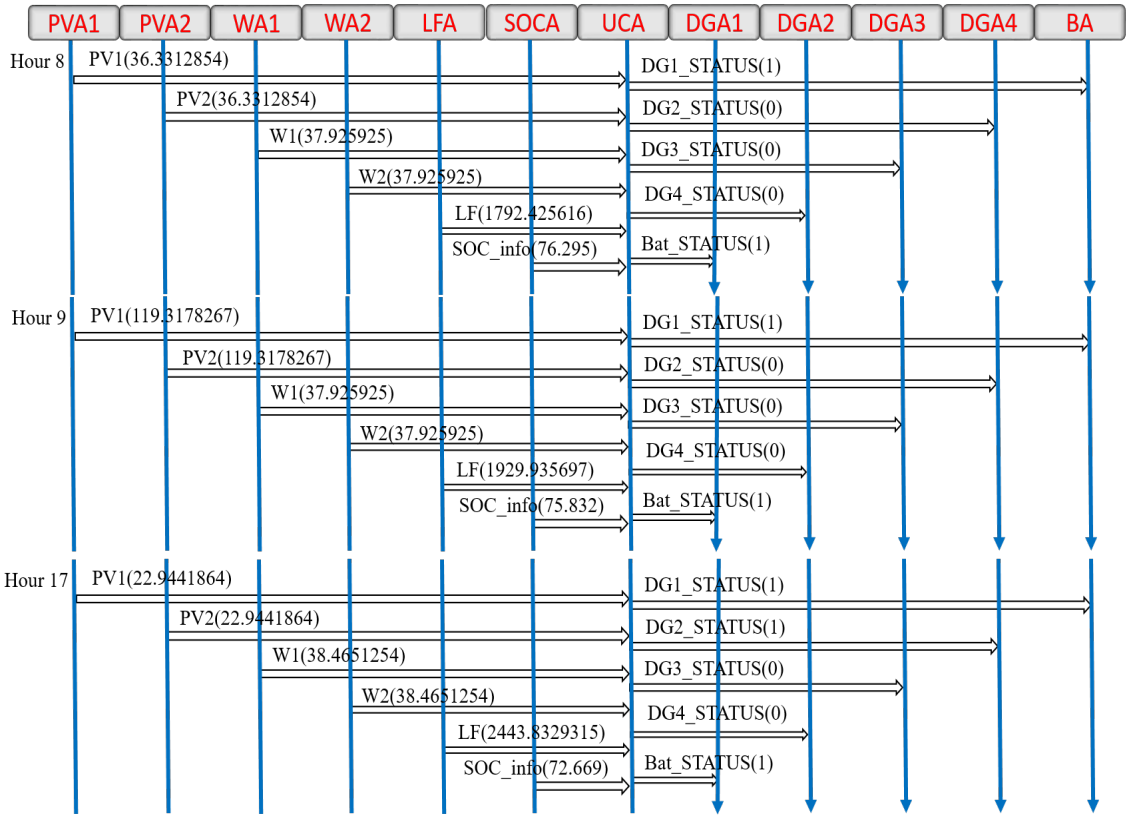

Figure 4.30: Agent Communication in S3

the simulation. Figure 4.29(a) and Figure 4.29(b) illustrate the state of charge of battery (in %) in both the cases respectively in scenario 3. The battery control in this scenario also works as explained in scenario 1 and scenario 2. The Figure 4.30 gives a snapshot of the information exchanged between agents during the simulation in scenario 3. Due to space constraints with the figure, the information exchanged for 24 hour has not been shown, instead for some hours it has been are shown.

4.3.2 Microgrid Performance Evaluation

The efficiency the of proposed microgrid with multi agent system has been calculated based on [253] and has been modified and simplified to suit the case studies. The microgrid efficiency is defined here as the ratio of total demand of the microgrid to the sum of generations of renewable energy sources and diesel generators.The efficiency and percentage power losses of the proposed microgrid with agent based EMS has been calculated based on Eq. (4.4) - Eq. (4.6) . Table 4.2 shows the performance the of proposed agent based EMS in MG that increases efficiency and reduces the power losses in the MG.

$$\eta_{microgrid} = \frac{P_{Load} + i * P_{bat}}{P_{DER} + P_{DG} + j * P_{bat}} \tag{4.4}$$

$$P_{Loss}(\%) = \frac{(P_{DER} + P_{DG} + j * P_{bat}) - (P_{Load} + i * P_{bat})}{P_{DER} + P_{DG} + j * P_{bat}} * 100 \tag{4.5}$$

$$i, j = \begin{cases} i = 1 \; and \; j = 0 & ; when \; battery \; is \; chariging \; (load) \\ i = 0 \; and \; j = 1 & ; when \; battery \; is \; dischariging \; (source) \end{cases} \tag{4.6}$$

Table 4.2: Microgrid Performance Evaluation

	Power Loss in %		**System Efficiency in %**	
Scenario	***Without MAS***	***With MAS***	***Without MAS***	***With MAS***
S1	3.7437	3.7131	96.26	96.29
S2	4.2729	4.1301	95.72	95.85
S3	4.2727	3.9474	95.73	96.05

4.3.3 Conclusion and Limitation

An intelligent multi agent system composed of PV agents, wind agents, load forecasting agent, SOC agent, battery agent, unit commitment agent and diesel generator agents has been developed for energy management in a smart microgrid in the previous section of this chapter. The agents and their behavior have been simulated in Stateflow, and the microgrid has been modeled in Simulink. The proposed model has been simulated to study the effectiveness in presence and absence of agent based EMS. Also, the proposed agent based EMS has the ability to utilize the diesel generators optimally by the combined actions of different agents deployed in the proposed system, and satisfy the load requirement of the

microgrid. But some issues concern to this developed model has been identified, that the control period for the unit commitment decision provided by the unit commitment agent is one hour and if some sudden requirement within this control period may lead to the quick discharging of the battery and fails to satisfy the load requirements. Therefore, to rectify this issue a correction agent is introduced and developed a new architecture named improved model which can solve the above said issue.

4.4 Improved model of MAS based microgrid EMS

4.4.1 Proposed MAS

A three layer multi agent architecture namely Forecasting and Estimation Layer, Control and Action Layer and Real time Monitoring Layer is proposed for the microgrid energy management as illustrated in Figure 4.31.

- **Forecasting and Estimation Layer:** This layer is considered as the top layer in the proposed scheme. The forecasting and estimation layer consists of seven types of agents (2 PV agents, 2 wind agents, LF agent, SOC agent and a unit commitment agent). The input to this layer is historical data of solar power output, historical data of wind power output, historical load values and current estimated SOC information.
- **Control and Action Layer:** This layer is viewed as the middle layer in the proposed agent architecture. In this layer, diesel generator and battery agents are deployed, and the input to this layer is the information from the top layer and bottom layer.
- **Real Time Monitoring Layer** This layer is considered as the bottom layer in the proposed scheme where the correction agent is deployed. The inputs to this layer are real time information from the microgrid.

4.4.1.1 PV Agent

PV Agent forecasts the PV power output of the current hour from the historical data and gives information to unit commitment agent for further decision making.

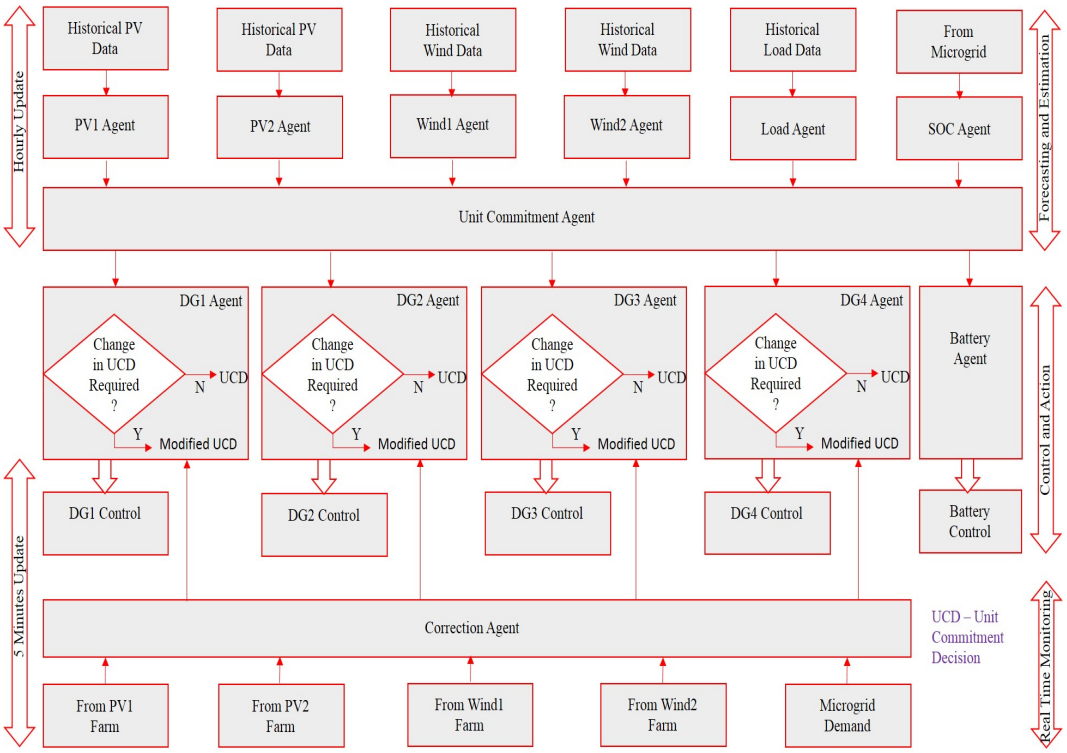

Figure 4.31: Proposed MAS Architecture for microgrid EMS

Detailed modelling is expalined in section 4.2.2.1.

4.4.1.2 Wind Agent

Wind agent gives the forecasted information of wind output power of the present hour to the unit commitment agent as expalined in section 4.2.2.2.

4.4.1.3 Load Forecasting Agent

The load forecasting agent is modeled to give the information of the load forecast for the current hour to the unit commitment agent. Detailed modelling can be found in section 4.2.2.3

4.4.1.4 SOC Agent

The SOC agent will give the current state of charge (SOC) of the battery to the unit commitment agent. More details can be found in section 4.2.2.4.

4.4.1.5 Unit Commitment Agent

The function of the unit commitment (UC) agent is to find the optimum schedule of generating units while satisfying load requirements of the microgrid. The decision making process of unit commitment agent is same as illustrated in section 4.2.2.5.

4.4.1.6 Correction Agent

The requirement of correction agent in the system is mainly because of two reasons. Firstly, the control period is one hour for the unit commitment decision from the unit commitment agent. Secondly, the forecast of the renewable energy sources used (photovoltaic and wind farms) and residential loads are usually very inaccurate due to their high volatility. Based on these issues, it is difficult to assure the power balance in the microgrid. Let us consider, for example, the sudden lack of energy in the microgrid within the control period, when the diesel generators are not activated (the forecast did not indicate the necessity to activate any diesel generator), and the batteries become quickly discharged. How MAS-EMS can react to this situation when it observes the state of the microgrid only once in an hour?. This situation can be avoided in simulation by introducing the correction agent that updates the status of the real microgrid in every 5 minutes. It is also assumed that the battery can supply power to satisfy the load during this 5-minute interval when some sudden requirement of power during this interval.

The function of correction agent in the proposed system is to help DG agents to modify the unit commitment decision from the forecasting and estimation layer when and where required by providing the correction information in every five minutes. The correction agent estimates the current power availability of PV farm 1, PV farm 2, wind farm 1, wind farm 2 and load demand ($P_{pv1}, P_{pv2}, P_{wind1}, P_{wind2}, P_{Load}, P_{Comload}$) respectively as in Eq. (4.9) - Eq. (4.14) and then calculates the required power ΔP_{req} to be generated to fulfill the power balance in system as in Eq. (4.7).

$$\Delta P_{req} = P_{Load} + P_{Comload} - P_{Res} \tag{4.7}$$

$$P_{Res} = P_{pv1} + P_{pv2} + P_{wind1} + P_{wind2} \tag{4.8}$$

$$P_{pv1} = \frac{3}{2} * \|V_{pv1}\| * \|I_{pv1}\| * cos(\angle V_{pv1} - \angle I_{pv1}) \tag{4.9}$$

$$P_{pv2} = \frac{3}{2} * \|V_{pv2}\| * \|I_{pv2}\| * cos(\angle V_{pv2} - \angle I_{pv2}) \tag{4.10}$$

$$P_{wind1} = \frac{3}{2} * \|V_{wind1}\| * \|I_{wind1}\| * cos(\angle V_{wind1} - \angle I_{wind1}) \tag{4.11}$$

$$P_{wind2} = \frac{3}{2} * \|V_{wind2}\| * \|I_{wind2}\| * cos(\angle V_{wind2} - \angle I_{wind2}) \tag{4.12}$$

$$P_{Load} = \frac{3}{2} * \|V_{Load}\| * \|I_{Load}\| * cos(\angle V_{Load} - \angle I_{Load}) \tag{4.13}$$

$$P_{Comload} = \frac{3}{2} * \|V_{Comload}\| * \|I_{Comload}\| * cos(\angle V_{Comload} - \angle I_{Comload}) \tag{4.14}$$

The necessary diesel generators that should be activated to provide the power balance in the system has been calculated using Eq.4.15.

$$P_{DG} \begin{cases} 0; & \Delta P_{req} \leq 0 \\ P_{DG1}; & \Delta P_{req} > 0 \\ P_{DG1} + P_{DG2}; & \Delta P_{req} - P_{DG1(max)} > 0 \\ P_{DG1} + P_{DG2} + P_{DG3}; & \Delta P_{req} - P_{DG1(max)} - P_{DG2(max)} > 0 \\ P_{DG1} + P_{DG2} + P_{DG3} + P_{DG4}; & \Delta P_{req} - P_{DG1(max)} - P_{DG2(max)} - P_{DG3(max)} > 0 \end{cases} \tag{4.15}$$

where, $P_{DG1(max)}, P_{DG2(max)}, P_{DG3(max)}, P_{DG4(max)}$ are the maximum capacities of diesel generator 1, diesel generator 2, diesel generator 3 and diesel generator 4 respectively (Table 2.1).

4.4.1.7 DG Agents

The DG agents receive the unit commitment decision for next one hour from the unit commitment agent and also in every five minutes the status of the generator should be activated to provide power requirement of the system to satisfy the power balance in the system. After receiving this information from unit commitment agent and correction agent, the DG agents identify if there is any requirement to modify the decision from the unit commitment agent. The DG agents sends the control signals to diesel generators (either unit commitment decision or modified unit commitment decisions accordingly).

4.4.1.8 Battery Agent

The battery agents take charging and discharging actions accordingly after receiving the decisions from the unit commitment agent.

4.5 Simulation Results and Analysis

4.5.1 Case Study

The simulation was carried out for 24 hours. For analyzing the performance of the proposed multi agent system for energy management, three different scenarios have been created with some events that generally occur in the system. The solar irradiance, wind speed, residential load and commercial load data used for the simulation are same as explained in section 2.3. The power output of only single PV and wind farms are shown in each scenario because each PV farm and wind farm are identical and produces same power.

4.5.1.1 Scenario 1 (S1)

In scenario 1, the model has been simulated without any disturbances in the system. This scenario is simulated to analyze the performance of the system during normal operating conditions.

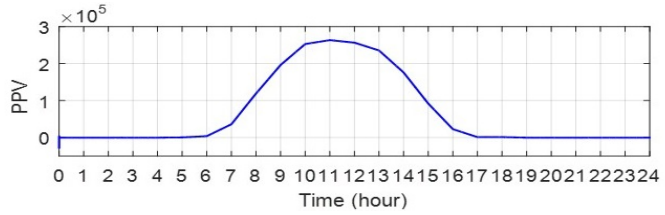

Figure 4.32: Power Output of PV Farm in S1

Figure 4.32 and Figure 4.33 respectively show the output power in watts generated from PV farm and wind farm in scenario 1. It is clear from both waveforms that the solar power follows the irradiance pattern represented in Figure 2.2(a), and since the wind power output is proportional to the cube of the wind velocity, it trails the pattern of wind speed represented in Figure 2.2(b). The load demand of

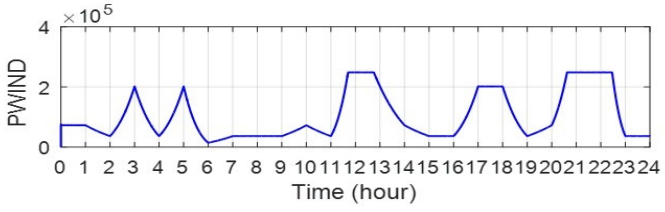

Figure 4.33: Power Output of Wind Farm in S1

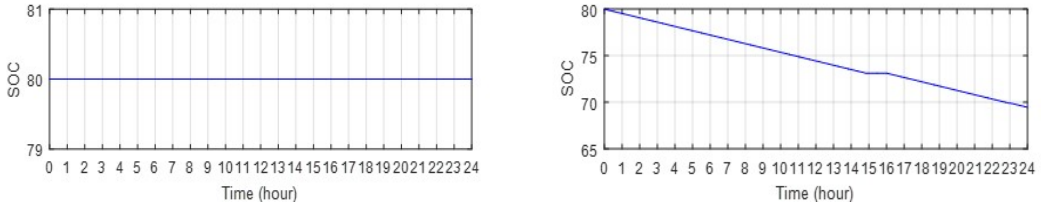

(a) without MAS-EMS (b) with MAS-EMS

Figure 4.34: Battery SOC in S1

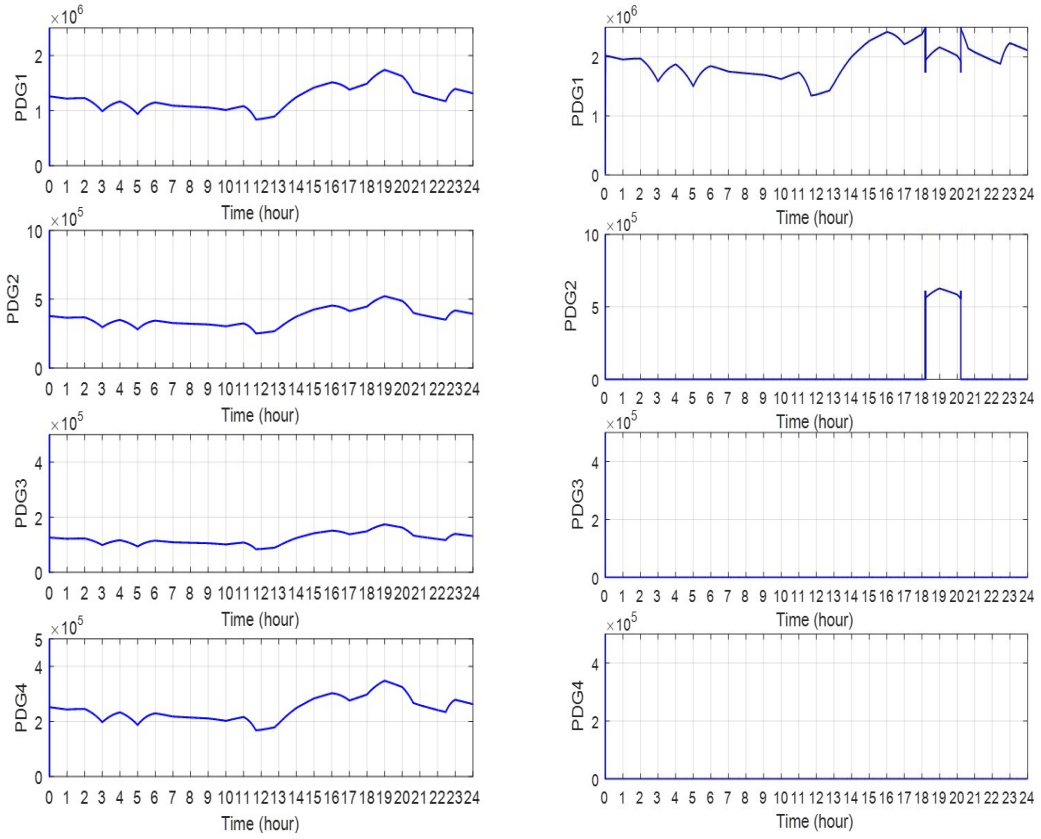

(a) without MAS-EMS (b) with MAS-EMS

Figure 4.35: Power Output of Diesel Generator in S1

the system in scenario 1 is represented in Figure 2.2(c). Figure 4.34 shows the state of charge of the battery (in %) during scenario 1 without and with MAS. In Figure 4.34(b), the battery agent is performing the battery control action to supply the load when there is a shortage of power in the microgrid system. The battery is not charged throughout the simulation because the battery controller is constrained to that the battery will charge whenever there is an excess power produced by renewable distributed energy resources. Figure 4.34(a) shows a constant SOC

because in this case the all the diesel generators are active and hence no shortage of power. The output power in watts produced by diesel generators to meet the load demand of the microgrid in the absence and presence of the proposed MAS based energy management system separately is shown in Figure 4.35(a) and Figure 4.35(b) respectively. Figure 4.35 show the power produced by the diesel generator 1, diesel generator 2, diesel generator 3 and diesel generator 4 (PDG1-PDG4) respectively. In Figure 4.35(b) it can be seen that the diesel generator 1 is active for 24 hours and diesel generator 2 is active only during the period 18:00-20:00 hours. The diesel generator 3 and diesel generator 4 are not active throughout the simulation. On the other hand in Figure 4.35(a) , in the absence of proposed scheme, all the diesel generators are active for the complete duration of the scenario.

4.5.1.2 Scenario 2 (S2)

In scenario 2, a partial shading effect occurred in the PV system at 10:30 hours for a duration of 1800 seconds and the condition at which the wind speed exceeds the maximal wind speed at 21:00 hour of the simulation have been considered. This scenario is simulated to study how the proposed system will react to the power output variations of distributed energy resources in the microgrid.

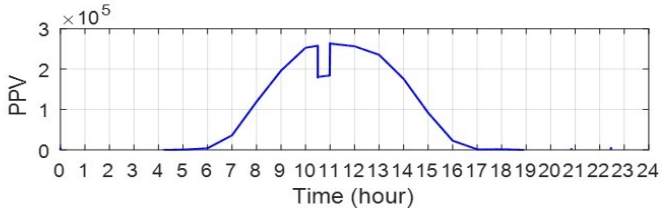

Figure 4.36: Power Output of PV Farm in S2

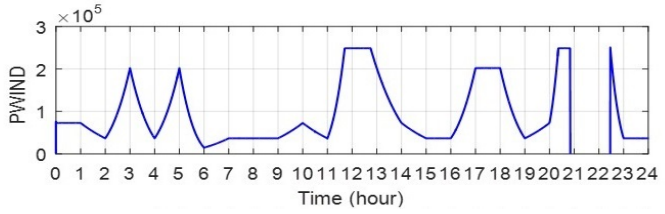

Figure 4.37: Power Output of Wind Farm in S2

The Figure 4.36 shows the output power generated by PV farm in scenario 2. A sudden drop in PV output power found at 10:30 hours, for a time span of

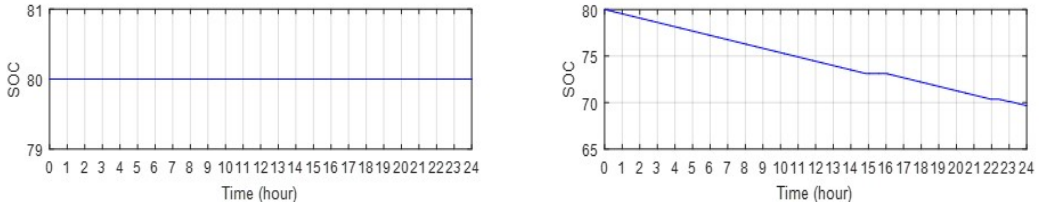

(a) without MAS-EMS (b) with MAS-EMS

Figure 4.38: Battery SOC in S2

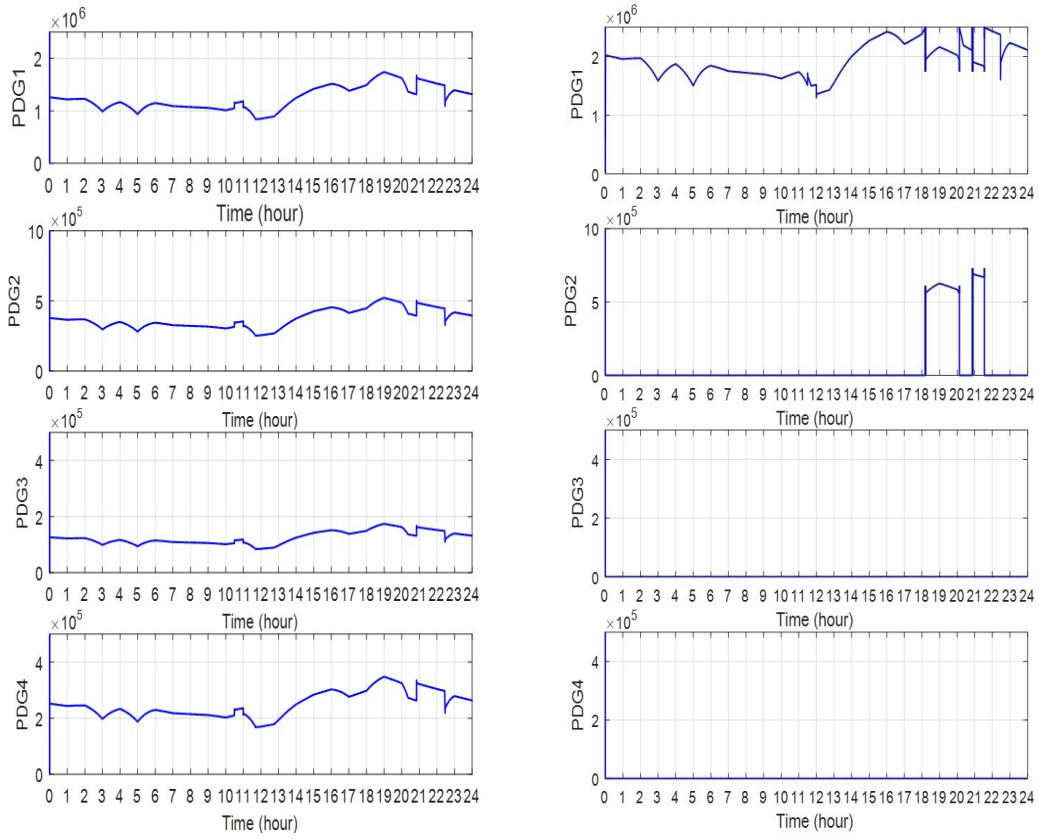

(a) without MAS-EMS (b) with MAS-EMS

Figure 4.39: Power Output of Diesel Generator in S2

30 minutes in Figure 4.36 can be attributed to the effect of the partial shading considered in the study. The power output in watts of wind farm during scenario 2 can be found in Figure 4.37. In Figure 4.37, the wind power output trails the wind speed since it follows the cube of the wind velocity. However, at 21:00 hours for some duration, the wind output power is zero because the simulation considers that during this time, the wind speed exceeds the maximum wind speed and the wind turbine is isolated from the microgrid and stays offline until the wind speed returns

to its nominal value. The load demand in watts of the system used in scenario 2 was represented in Figure 2.2(c). Figure 4.38 shows the state of charge of the battery (in %) in this scenario for the complete 24-hour duration. In Figure 4.38(b) the battery agent can be seen performing the battery control action to supply the load when there is a power shortage in the microgrid system. The battery is not charged throughout the simulation and in Figure 4.38(a) battery SOC is constant because of the same reason as explained in scenario 1. The output power in watts produced by diesel generators to meet the load demand of the microgrid in the presence and in the absence of the proposed MAS based energy management system separately is shown in Figure 4.39(a) and Figure 4.39(b). The output powers of the four diesel generators (PDG1-PDG4) are shown in Figure 4.39 respectively. In Figure 4.39(b), it can be seen that the diesel generator 1 is active for 24 hours and diesel generator 2 is active only during the 18:00-20:00 hours as in scenario 1. In addition from 21:00 hours for some duration due to the effect the wind speed exceeds the maximum wind speed as considered in the scenario 2 the diesel generator 2 is remain activated by the proposed multi agent system to fulfill the requirement of microgrid during the same time. As soon as the diesel generator 1 and the other distributed energy resources can manage the requirements of microgrid the diesel generator 2 is deactivated even during the absence of wind farm. It supports the fact that the proposed system can be able to detect the output power variations in the distributed energy resources and manage the power balance in the system by activating the necessary diesel generators if required. Also, during 10:30 hour the diesel generator 2 is not activated because during that time the diesel generator 1 and all other renewable energy resources can together provide power to nullify the effect of partial shading effect and manage the power balance in the system. Also, the diesel generator 1 suddenly starts providing more power at 10:30 hours to compensate the reduction in power output of the PV farm at the same time due to partial shading effect respectively within its capacity. The diesel generator 3 and diesel generator 4 are not active throughout the simulation, showing that the proposed system can support the effective utilization of diesel generator. On the other hand, in Figure 4.39(a), in the absence of proposed scheme, all the diesel generators are active for the complete duration of the scenario.

4.5.1.3 Scenario 3 (S3)

In scenario 3, to show the effect of commercial load in the system, an asynchronous machine having a capacity of 0.2 MW was introduced in the system at 20:00 hours

of simulation using a circuit breaker. This scenario is created to analyze the performance of microgrid multi agent system during sudden variation in load.

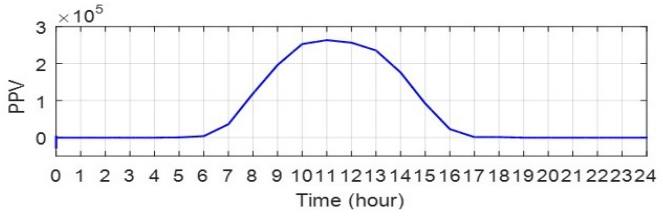

Figure 4.40: Power Output of PV Farm in S3

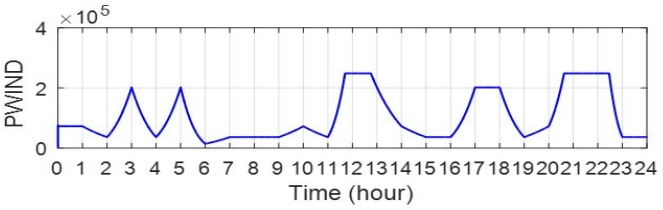

Figure 4.41: Power Output of Wind Farm in S3

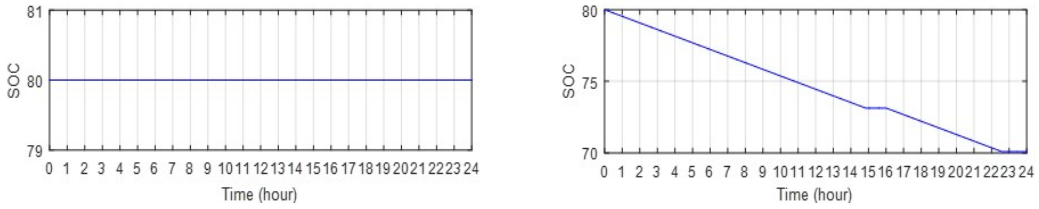

(a) without MAS-EMS (b) with MAS-EMS

Figure 4.42: Battery SOC in S3

Figure 4.40 and Figure 4.41 display the output power in watts generated from the PV farm and the output power in watts generated by the wind farm respectively in scenario 3. The load profile illustrated in Figure 2.2(c)(residential power demand) and Figure 2.2(d)(demand of commercial loads) together have been considered in the simulation for scenario 3. Figure 4.42 shows the state of charge (in %) of the battery during 24-hour simulation in scenario 3. The battery control in this scenario also works as explained in scenario 1 and scenario 2. The output power in watts produced by diesel generators to meet the load demand of the microgrid in presence and absence of proposed MAS based energy management system separately is shown in Figure 4.43(a) and Figure 4.43(b). In Figure 4.43(b) it can be clearly seen that the diesel generator 1 is active during the complete duration

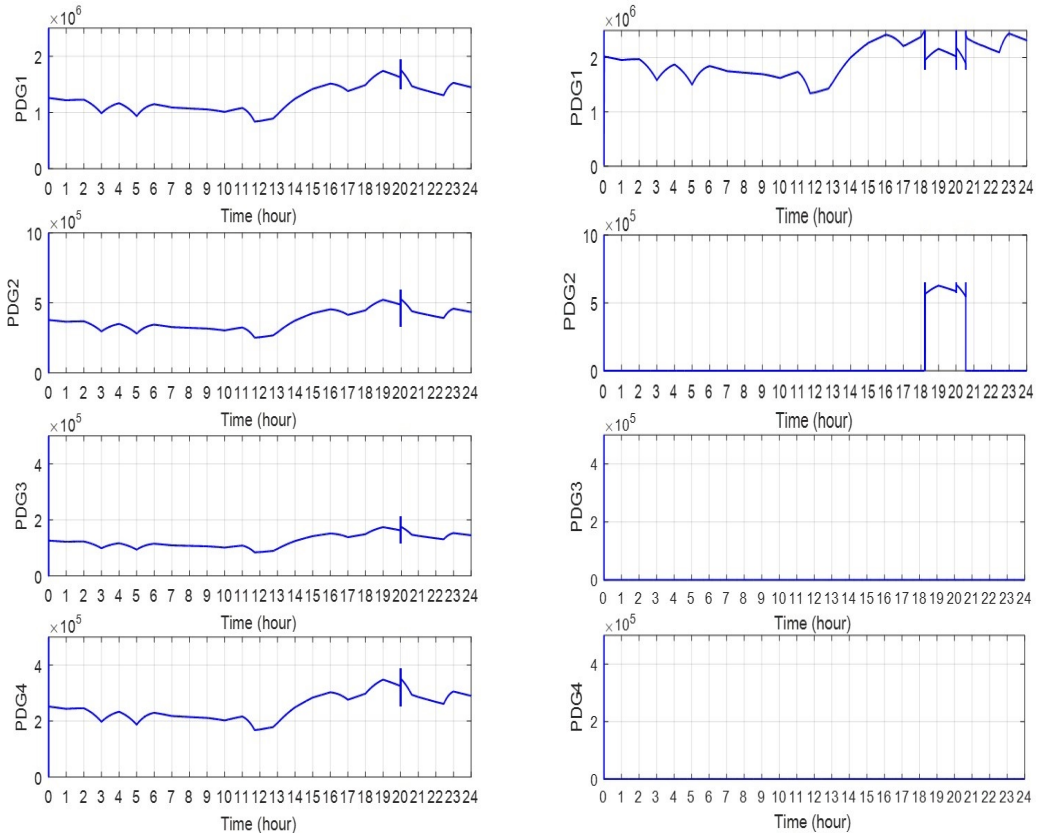

(a) without MAS-EMS

(b) with MAS-EMS

Figure 4.43: Power Output of Diesel Generator in S3

of the simulation. The diesel generator 2 is activated for 18:00 hours as in the normal condition shown in the scenario 1 but deactivated not at 20:00 hours. But it is online for the greater duration in this scenario because of the commercial load introduced in the scenario at 20 hours, which increases the total load requirement of the microgrid as compared to scenario 1. So, here the proposed multi agent system identifies the variation in load and acts accordingly to provide the power balance in the system by activating the diesel generator 2. In this scenario, also the DG 3 and DG 4 are completely offline during the entire simulation, and DG2 provides power only for some duration. This result indicates that the proposed multi agent scheme can effectively act to the load changes in the system and utilize the diesel generator effectively. Whereas, Figure 4.43(a) shows all the diesel generators are providing power for the complete duration of the simulation.

4.5.2 Microgrid Performance Evaluation

The efficiency and percentage power losses of the proposed microgrid with agent based EMS has been calculated based on Eq. (4.4) - Eq. (4.6). Table 4.3 represents the performance of microgrid concerning power loss and system efficiency. Figure 4.44 displays the communication of different agents during the simulation. Where, PVA1, PVA2, WA1, WA2, LFA, SOCA, UCA, DGA1, DGA2, DGA3, DGA2, BA and CA respectively represents PV 1 agent, PV 2 agent, wind 1 agent, wind 2 agent, load forecasting agent, SOC agent, unit commitment agent, DG1 agent, DG2 agent, DG3 agent, DG4 agent, battery agent and Correction agent.

Table 4.3: Microgrid Performance Evaluation

	Power Loss in %		**System Efficiency in %**	
Scenario	***Without MAS***	***With MAS***	***Without MAS***	***With MAS***
S1	3.7437	3.6971	96.26	96.30
S2	4.2729	4.0512	95.72	95.95
S3	4.2727	3.7093	95.73	96.29

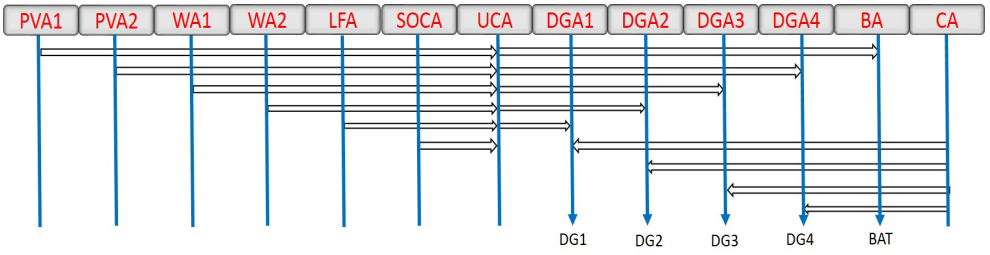

Figure 4.44: Agent Communication Diagram

4.6 Chapter Summary

An intelligent multi agent system for microgrid energy management system was developed in this chapter in two phases (i.e Initial model and improved model). Different agents namely PV agents, wind agents, load forecasting agents, SOC agent, unit commitment agents, diesel generator agents, battery agent and real time correction agent have been developed and deployed in the simulation which represented each component of the microgrid EMS. The simulation was carried out by considering the fluctuations in renewable energy resources and load variations. The effectiveness of the proposed multi agent based energy management system was tested by comparing the power losses and microgrid system efficiency in different scenarios. The simulation results indicate that the proposed MAS based

EMS has better performance as compared to the conventional EMS. Also, the proposed EMS has the capability to use the diesel generators optimally to satisfy the load requirement of the microgrid. The final model developed in this chapter has been utilized in chapter 5 to develop a microgrid energy management system with self-healing capabilities.

Chapter 5

MAS based Microgrid EMS with Self-Healing Capabilities

5.1 Overview

This chapter focuses on improving the dynamic performance of a microgrid by developing a multi agent energy management system with self-healing capabilities by employing a four-layer multi agent concept. The first layer of the proposed system is a forecasting and estimation layer and is responsible for providing the real-time forecasts for RES output power, load and battery state of charge (SOC). The second layer is a control and action layer, assigned with the duties of taking the control decisions and actions accordingly by collecting information from different agents deployed in the system. The third layer is a real-time monitoring and control layer that provides the real-time information of the microgrid to the second layer. The fourth layer is fault detection and action layer that facilitates the self-healing capability in the proposed microgrid. The performance and the applicability of the proposed model represented in Figure 5.1 are tested by simulating the faults at different locations in the system.

5.2 Proposed Multi Agent System(MAS)

A four layer multi agent architecture consisting of different layers namely Forecasting and Estimation Layer (FEL), Control and Action Layer (CAL), Real Time Monitoring Layer (RTML) and Fault Detection and Action Layer (FDAL) has been

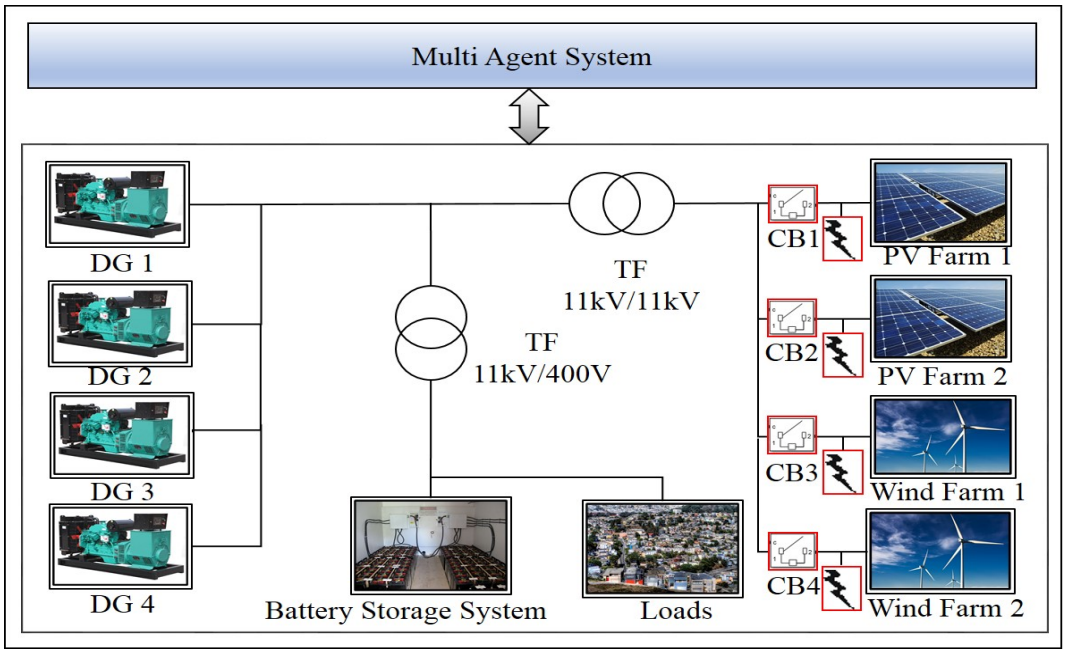

Figure 5.1: Proposed Microgrid EMS with Self-healing Capabilities

proposed for the MG EMS with self-healing capabilities during faults as illustrated in Figure 5.2.

FEL: The FEL consists of seven types of agents (2 PV agents, 2 wind agents, Load Forecasting (LF) agent, SOC agent and a unit commitment agent). The input to this layer is historical data of solar output power, historical data of wind power output, historical load values and current estimated SOC information.

CAL: In this layer, battery agent and diesel generator agents (DGA) are deployed, and the input to this layer is the information from the FEL along with that from RTML.

RTML: The inputs to this layer are real-time information from the microgrid and the information from the FDAL. This layer is formed by a correction agent which provides the correction information to the CAL.

FDAL: This layer collects the real-time information form the microgrid and identifies whether any fault or outage has occurred in the system and transfer the information to the RTML. It also sends control signals to circuit breakers (CBs) either to isolate or to restore.

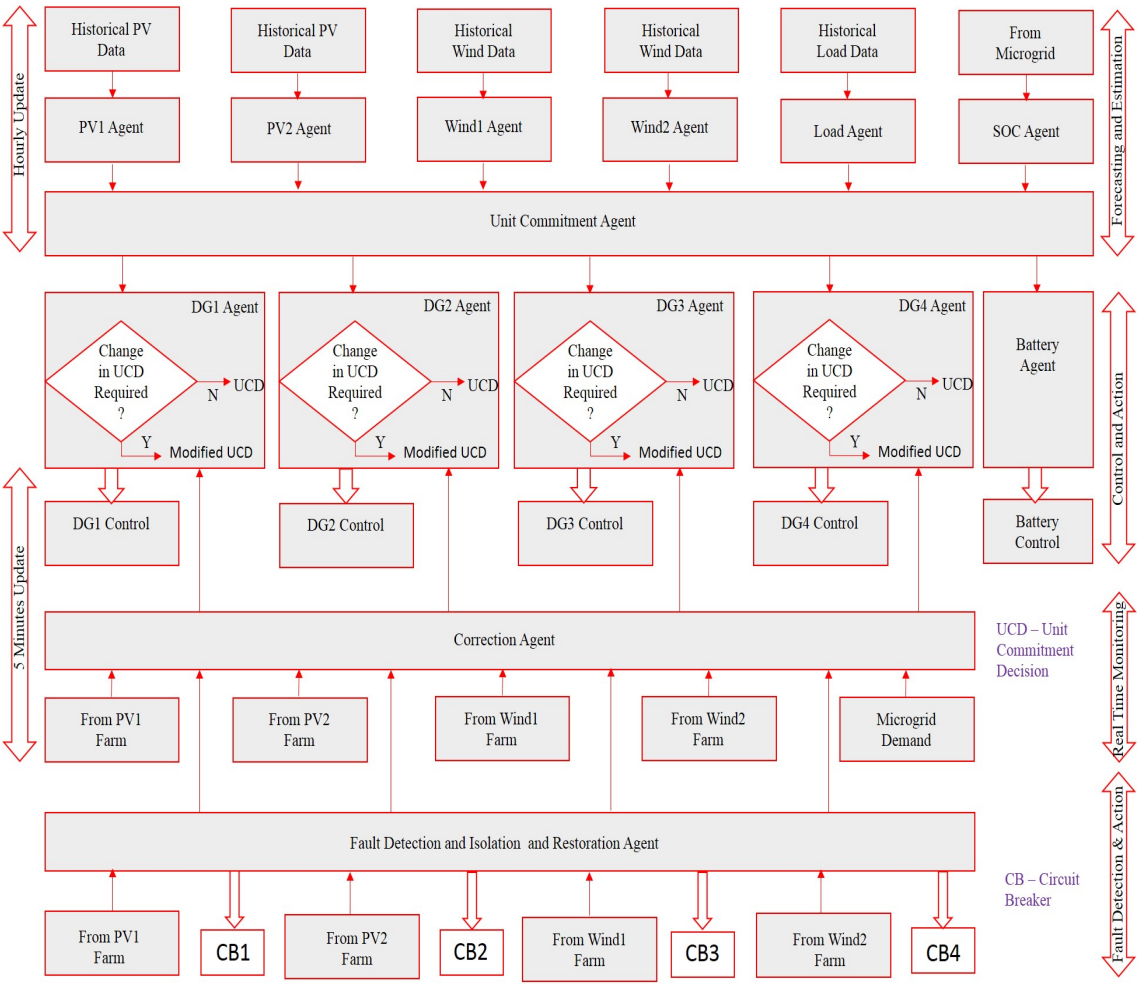

Figure 5.2: Proposed MAS

5.2.1 PV Agent (PVA)

The PVA provides the forecasted output power of PV as expalined in section 4.2.2.1

5.2.2 Wind Agent (WA)

WA gives the forecasted information of wind output power as detailed in section 4.2.2.2

5.2.3 Load Forecasting Agent (LFA)

The LFA is modeled to give the information of the load forecast as illustarted in section 4.2.2.3

5.2.4 SOC Agent (SOCA)

The SOCA will provide the present state of charge (SOC) of the battery to the UCA. More details can be found in section 4.2.2.4.

5.2.5 Unit Commitment Agent (UCA)

The function of unit commitment agent is same as explained in section 4.2.2.5.

5.2.6 Correction Agent (CA)

The function of CA in the proposed system is to help DGAs to modify the unit commitment decision from the forecasting and estimation layer when and where required by providing the correction information in every five minutes. The CA estimates the total power availability of renewable energy sources (RES) and the current power availability of PV farm 1, PV farm 2, wind farm 1, wind farm 2 and load demand (P_{Res} and $P_{pv1}, P_{pv2}, P_{wind1}, P_{wind2}, P_{Load}$) respectively as given by Eqns. (5.2 - 5.7) and then calculates the required power ΔP_{req} to be generated to fulfill the power balance in system as in Eq. (5.1).

$$\Delta P_{req} = P_{Load} - P_{Res} \tag{5.1}$$

$$P_{Res} = P_{pv1} + P_{pv2} + P_{wind1} + P_{wind2} \tag{5.2}$$

$$P_{pv1} = \frac{3}{2} * \|V_{pv1}\| * \|I_{pv1}\| * cos(\angle V_{pv1} - \angle I_{pv1}) \tag{5.3}$$

$$P_{pv2} = \frac{3}{2} * \|V_{pv2}\| * \|I_{pv2}\| * cos(\angle V_{pv2} - \angle I_{pv2}) \tag{5.4}$$

$$P_{wind1} = \frac{3}{2} * \|V_{wind1}\| * \|I_{wind1}\| * cos(\angle V_{wind1} - \angle I_{wind1}) \tag{5.5}$$

$$P_{wind2} = \frac{3}{2} * \|V_{wind2}\| * \|I_{wind2}\| * cos(\angle V_{wind2} - \angle I_{wind2}) \tag{5.6}$$

$$P_{Load} = \frac{3}{2} * \|V_{Load}\| * \|I_{Load}\| * cos(\angle V_{Load} - \angle I_{Load}) \tag{5.7}$$

The necessary diesel generators (DGs) that should be activated to provide the power balance in the system are identified by performing the calculations using Eq. (5.8).

$$P_{DG} = \begin{cases} 0; & \Delta P_{req} \leq 0 \\ P_{DG1}; & \Delta P_{req} > 0 \\ P_{DG1} + P_{DG2}; & \Delta P_{req} - P_{DG1(max)} > 0 \\ P_{DG1} + P_{DG2} + P_{DG3}; & \Delta P_{req} - P_{DG1(max)} - P_{DG2(max)} > 0 \\ P_{DG1} + P_{DG2} + P_{DG3} + P_{DG4}; & \Delta P_{req} - P_{DG1(max)} - P_{DG2(max)} - P_{DG3(max)} > 0 \end{cases} \tag{5.8}$$

where, $P_{DG1(max)}, P_{DG2(max)}, P_{DG3(max)}, P_{DG4(max)}$ are the maximum capacities of DG1, DG2, DG3 and DG4 respectively (Table 2.1). If any fault or outage is detected the fault detection and isolation and restoration agent helps the CA to update the situation during and maintain the power balance.

5.2.7 DG Agents (DGAs)

The DGAs receive the unit commitment decision for next one hour from the UCA and also in every five minutes the status of the generator should be activated to provide power requirement of the system to satisfy the power balance in the system from CA. After receiving this information from UCA and CA, the DGAs identify if there is any requirement to modify the decision from the UCA. The DGAs send the control signals to DGs (either unit commitment decision or modified unit commitment decisions accordingly).

5.2.8 Battery Agent (BA)

The BA takes charging and discharging actions accordingly after receiving the decisions from the UCA.

5.2.9 Fault Detection and Isolation and Restoration Agent (FDIRA)

The function of FDIRA is to detect the fault by comparing the magnitude of current during the simulation with a reference value. Also, this agent sends the control signals to the respective circuit breakers (CBs) to isolate faulty portion and restore after clearing the fault.

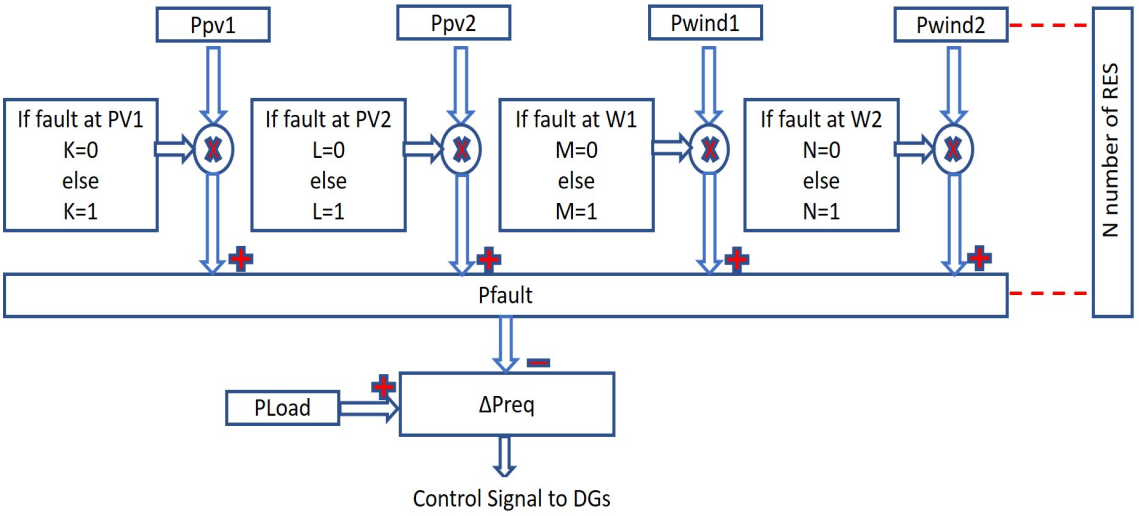

Figure 5.3: Online updation process of FDIRA

- Fault Detection Process

  $\|I_{pv1}\| > \|I_{pv1ref}\| \Rightarrow$ A fault at PV1

  $\|I_{pv2}\| > \|I_{pv2ref}\| \Rightarrow$ A fault at PV2

  $\|I_{wind1}\| > \|I_{wind1ref}\| \Rightarrow$ A fault at wind farm 1

  $\|I_{wind2}\| > \|I_{wind2ref}\| \Rightarrow$ A fault at wind farm 2

  where, $I_{pv1ref}, I_{pv2ref}, I_{wind1ref}, I_{wind2ref}$ respectively represents the reference value of currents at PV1, PV2, wind farm 1 and wind farm 2 identified by running the simulation during normal condition and fault condition.

  The generalized schematic of the online updation process of FDIRA for the MG consist of N number of RES is shown in Figure. 5.3. In Figure. 5.3 Ppv1, Ppv2, Pwind1, Pwind2....., up to N RES respectively represents the power from different RES. The Pfault in Figure. 5.3 represents the total power availability of the RES, which is calculated by the sum of the product of individual RES power with the respective decision variables (K, L, M, N...etc) value depending upon the status of fault. The ΔPreq is the required power to be generated to fulfill the load requirement of the MG after the complete utilization of the RES, which is calculated by subtracting the Pfault from the total load requirement (PLoad). The online updation process of the FDIRA for the case study considered in this work as shown in Figure. 5.1 during the different type of faults are as follows.

- When fault is detected at PV1, the FDIRA sends a control signal '0' to CB1 and updates CA by modifying the Eq. (5.2) and Eq. (5.1) as represented in

Eq. (5.9) and Eq. (5.10) respectively.

$$P_{Respv1fault} = P_{pv2} + P_{wind1} + P_{wind2} \tag{5.9}$$

$$\Delta P_{req} = P_{Load} - P_{Respv1fault} \tag{5.10}$$

where, $P_{Respv1fault}$ is the total power availability of RES during fault at PV1.

- When fault is detected at PV2, the FDIRA sends a control signal '0' to CB2 and updates CA by modifying the Eq. (5.2) and Eq. (5.1) as represented in Eq. (5.11) and Eq. (5.12) respectively.

$$P_{Respv2fault} = P_{pv1} + P_{wind1} + P_{wind2} \tag{5.11}$$

$$\Delta P_{req} = P_{Load} - P_{Respv2fault} \tag{5.12}$$

where, $P_{Respv2fault}$ is the total power availability of RES during fault at PV2.

- When fault is detected at wind farm 1, the FDIRA sends a control signal '0' to CB3 and updates CA by modifying the Eq. (5.2) and Eq. (5.1) as represented in Eq. (5.13) and Eq. (5.14) respectively.

$$P_{Reswind1fault} = P_{pv1} + P_{pv2} + P_{wind2} \tag{5.13}$$

$$\Delta P_{req} = P_{Load} - P_{Reswind1fault} \tag{5.14}$$

where, $P_{Reswind1fault}$ is the total power availability of RES during fault at wind farm 1.

- When fault is detected at wind farm 2, the FDIRA sends a control signal '0' to CB4 and updates CA by modifying the Eq. (5.2) and Eq. (5.1) as represented in Eq. (5.15) and Eq. (5.16) respectively.

$$P_{Reswind2fault} = P_{pv1} + P_{pv2} + P_{wind1} \tag{5.15}$$

$$\Delta P_{req} = P_{Load} - P_{Reswind2fault} \tag{5.16}$$

where, $P_{Reswind2fault}$ is the total power availability of RES during fault at wind farm 2

- When fault is detected at both PV1 and wind farm 1, the FDIRA sends a control signal '0' to both CB1 and CB3 and updates CA by modifying the Eq. (5.2) and Eq. (5.1) as represented in Eq. (5.17) and Eq. (5.18)

respectively.

$$P_{Respv1wind1fault} = P_{pv2} + P_{wind2} \tag{5.17}$$

$$\Delta P_{req} = P_{Load} - P_{Respv1wind1fault} \tag{5.18}$$

where, $P_{Respv1wind1fault}$ is the total power availability of RES during fault at PV1 and wind farm 1.

- When fault is detected at both PV2 and wind farm 2, the FDIRA sends a control signal '0' to both CB2 and CB4 and updates CA by modifying the Eq. (5.2) and Eq. (5.1) as represented in Eq. (5.19) and Eq. (5.20) respectively.

$$P_{Respv2wind2fault} = P_{pv1} + P_{wind1} \tag{5.19}$$

$$\Delta P_{req} = P_{Load} - P_{Respv2wind2fault} \tag{5.20}$$

where, $P_{Respv2wind2fault}$ is the total power availability of RES during fault at PV2 and wind farm 2.

- When fault is detected at both PV1 and wind farm 2, the FDIRA sends a control signal '0' to both CB1 and CB4 and updates CA by modifying the Eq. (5.2) and Eq. (5.1) as represented in Eq. (5.21) and Eq. (5.22) respectively.

$$P_{Respv1wind2fault} = P_{pv2} + P_{wind1} \tag{5.21}$$

$$\Delta P_{req} = P_{Load} - P_{Respv1wind2fault} \tag{5.22}$$

where, $P_{Respv1wind2fault}$ is the total power availability of RES during fault at PV1 and wind farm 2.

- When fault is detected at both PV2 and wind farm 1, the FDIRA sends a control signal '0' to both CB2 and CB3 and updates CA by modifying the Eq. (5.2) and Eq. (5.1) as represented in Eq. (5.23) and Eq. (5.24) respectively.

$$P_{Respv2wind1fault} = P_{pv1} + P_{wind2} \tag{5.23}$$

$$\Delta P_{req} = P_{Load} - P_{Respv2wind1fault} \tag{5.24}$$

where, $P_{Respv2wind1fault}$ is the total power availability of RES during fault at PV2 and wind farm 1.

- When fault is detected at PV1, PV2 and wind farm 1, the FDIRA sends a control signal '0' to CB1, CB2 and CB3 respectively and updates CA by modifying the Eq. (5.2) and Eq. (5.1) as represented in Eq. (5.25) and Eq. (5.26) respectively.

$$P_{Respv1pv2wind1fault} = P_{wind2} \tag{5.25}$$

$$\Delta P_{req} = P_{Load} - P_{Respv1pv2wind1fault} \tag{5.26}$$

where, $P_{Respv1pv2wind1fault}$ is the total power availability of RES during fault at PV1, PV2 and wind farm 1.

- When fault is detected at PV2, wind farm 1 and wind farm 2, the FDIRA sends a control signal '0' to CB2, CB3 and CB4 respectively and updates CA by modifying the Eq. (5.2) and Eq. (5.1) as represented in Eq. (5.27) and Eq. (5.28) respectively.

$$P_{Respv2wind1wind2fault} = P_{pv1} \tag{5.27}$$

$$\Delta P_{req} = P_{Load} - P_{Respv2wind1wind2fault} \tag{5.28}$$

where, $P_{Respv2wind1wind2fault}$ is the total power availability of RES during fault at PV2, wind farm 1 and wind farm 2.

- When fault is detected at PV1, wind farm 1 and wind farm 2, the FDIRA sends a control signal '0' to CB1, CB3 and CB4 respectively and updates CA by modifying the Eq. (5.2) and Eq. (5.1) as represented in Eq. (5.29) and Eq. (5.30) respectively.

$$P_{Respv1wind1wind2fault} = P_{pv2} \tag{5.29}$$

$$\Delta P_{req} = P_{Load} - P_{Respv1wind1wind2fault} \tag{5.30}$$

where, $P_{Respv1wind1wind2fault}$ is the total power availability of RES during fault at PV1, wind farm 1 and wind farm 2.

- When fault is detected at PV1, PV2 and wind farm 2, the FDIRA sends a control signal '0' to CB1, CB2 and CB4 respectively and updates CA by modifying the Eq. (5.2) and Eq. (5.1) as represented in Eq. (5.31) and Eq. (5.32) respectively.

$$P_{Respv1pv2wind2fault} = P_{wind1} \tag{5.31}$$

$$\Delta P_{req} = P_{Load} - P_{Respv1pv2wind2fault} \tag{5.32}$$

where, $P_{Respv1pv2wind2fault}$ is the total power availability of RES during fault at PV1, PV2 and wind farm 2.

- When fault is detected at PV1, PV2, wind farm 1 and wind farm 2, the FDIRA sends a control signal '0' to CB1, CB2, CB3 and CB4 respectively and updates CA by modifying the Eq. (5.2) and Eq. (5.1) as represented in Eq. (5.33) and Eq. (5.34) respectively.

$$P_{Respv1pv2wind1wind2fault} = 0 \tag{5.33}$$

$$\Delta P_{req} = P_{Load} - P_{Respv1pv2wind1wind2fault} \tag{5.34}$$

where, $P_{Respv1pv2wind1wind2fault}$ is the total power availability of RES during fault at PV1, PV2, wind farm 1 and wind farm 2.

During the normal conditions all the RES are available and hence the CA follows the Eq. (5.2) and Eq. (5.1) and sends a control signal '1' to all the CBs to remain closed.

5.3 Results and Discussion

The faults (line to ground) at different locations in the MG have been simulated as represented in Figure 5.1 to analyze the performance of EMS of MG with self healing capabilities during the outage of different RES.

5.3.1 Normal

In normal condition, the MG in Figure 5.1 is simulated without considering any fault in the system. Figure. 5.4 shows the load requirements of the microgrid in watts for the 24 hours duration. Figure. 5.5 shows the output power provided by DGs 1 and 2 (PDG1 and PDG2) respectively in watts for 24 hours to satisfy the load requirements of the microgrid during normal condition. The output power produced by the DGs 3 and 4 are not shown because they are not activated during the entire simulation as PDG1 and PDG2 are sufficient to provide the load requirements of MG along with the RES.

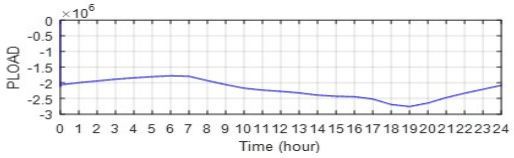

Figure 5.4: Microgrid Load Requirement

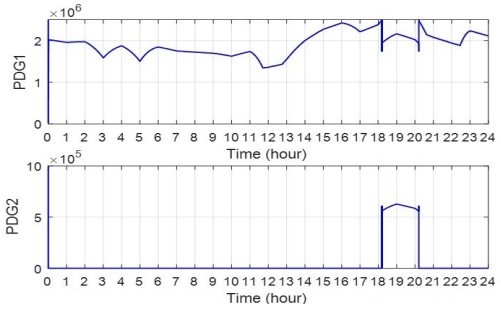

Figure 5.5: Power output of Diesel Generator in Normal Condition

5.3.2 Fault 1

During this condition, a fault at wind farm 1 as in Figure 5.1 occurring at 17-18 hour has been considered. This time of 17-18 hour has been considered as the load is maximum, and all the sources are crucial during this interval.

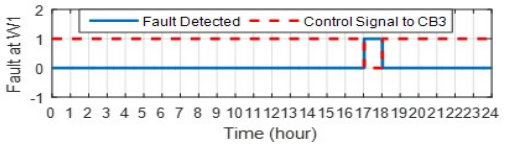

Figure 5.6: Fault 1 detected by FDIRA & Self-healing action

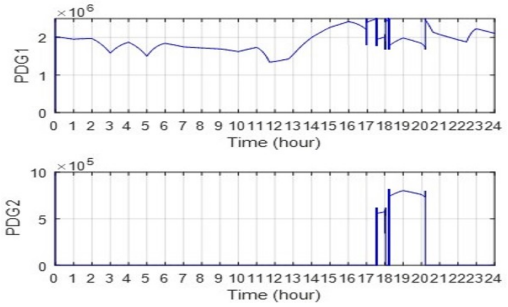

Figure 5.7: Power output of Diesel Generator during fault 1

Figure. 5.6 shows fault detected by the FDIR agent and self-healing action performed. As soon as the fault is detected by the FDIR agent, it sends a '0' signal to the CB3 and isolates the faulty portion (wind farm 1) as represented in Figure. 5.6. Also at the same time, it provides the information to the CA that the wind

farm 1 is isolated and unable to supply any power to the MG. The CA update accordingly as shown in Eq. (5.13) and Eq. (5.14) respectively. So, the DG should provide more power to maintain the power balance in the system. Figure. 5.7 displays the output power provided by DGs 1 and 2 (PDG1 and PDG2) in watts for 24 hours to satisfy the load requirements of the MG during fault 1. From this, it is clear that during 17-18 hour both DGs are providing more power as compared to the normal condition in Figure. 5.5. The DG 2 is not even active during 17-18 hour during the normal condition but in this case, the DGs 2 is active and providing power because of the successful performance of the agents which are deployed in the system with the knowledge of wind farm 1 that is isolated. At 18 hour once the fault is cleared the FDIR agent send a '1' to CB3 to restore the wind farm 1 as shown in Figure. 5.6 and also provides the same information to the correction agent. After receiving the information CA follows the Eq. (9) and Eq. (8) respectively. Hence, a reduction in power production is observed at 18 hours in PDG1 and PDG2.

5.3.3 Fault 2

During fault 2 condition, a fault at PV1 as in Figure 5.1 has been considered at 11-12 hour. The fault is considered at 11-12 hour as the maximum power production from PV farm is at this time. Figure. 5.8 represents the fault detected by the

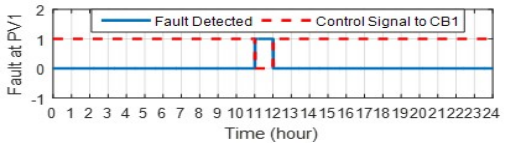

Figure 5.8: Fault 2 detected by FDIRA & Self-healing action

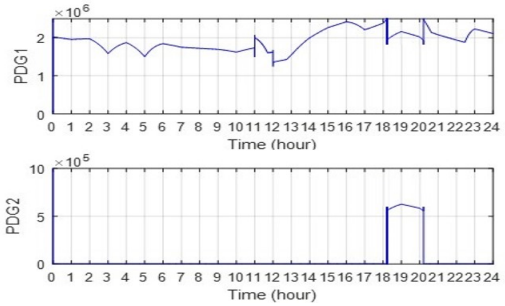

Figure 5.9: Power output of Diesel Generator during fault 2

FDIR agent and signal send to perform self-healing action in the proposed system.

After detecting a fault at 11 hours, the FDIR agent sends a control signal '0' to CB1 to isolate the PV farm 1 as indicated in Figure. 5.8. Also, it provides the same information (i.e., unavailability of PV farm 1 to provide power to MG) to CA. The CA considers this information and transfers the updates as explained in section 5.2.9 to the control and action layer. The control and action layer act accordingly to satisfy the load requirement of MG during this interval. From the Figure. 5.9, it is clear that the output power provided by the DG 1 during 11-12 hour is more as compared to the normal condition (Figure. 5.5) to manage the power balance in the system in the absence of the PV farm 1. Whereas, the DGs (DG2, DG3, and DG4) are not activated during this interval because the DG1 itself can fulfill the load requirement. After clearing the fault at 12 hours, the FDIR agent sends a control signal '1' to CB1 and restored the PV farm 1 to the MG as shown in Figure. 5.8 . As soon as, the PV farm 1 present in the MG, the power produced by the DG1 is reduced at 12 hours.

5.3.4 Fault 3

During this condition, a fault at both PV farms has been considered at 11-12 hour. The reason being selecting 11-12 hour duration is same as explained section 5.3.3.

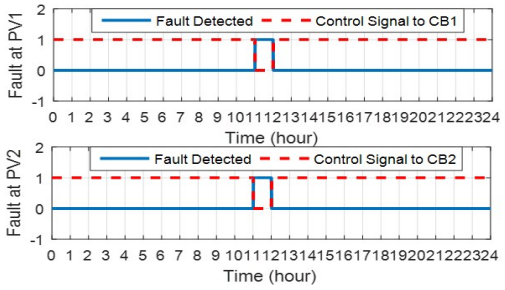

Figure 5.10: Fault 3 detected by FDIRA & Self-healing action

Figure. 5.10 shows the fault detected by the FDIR agent at 11-12 hour on both PV farms and self-healing action performed. As soon as fault detected, FDIR agent sends control signal '0' to both CB1 and CB2 and isolated both PV farms respectively as represented in Figure. 5.10. In this case, also DG1 provided more power as in Figure. 5.11 at 11-12 hour as compared to Figure. 5.9. Where only PV farm 1 was isolated. Here, both PV farms are isolated and hence required more power to meet the load requirements. In this case, the DG2, DG3 and DG 4 are also not activated during the 11-12 hour due to the same reason as explained

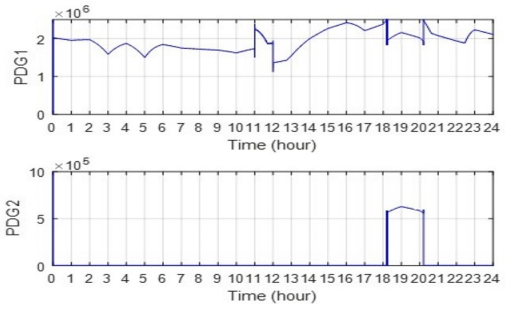

Figure 5.11: Power output of Diesel Generator during fault 3

in section 5.3.3. At 12 hour the fault is cleared and restored both the PV farms by FDIR agent as illustrated in Figure. 5.10. This effect reflected by the reduction in power production of DG1 as in Figure. 5.11 at 12 hours.

5.3.5 Fault 4

During fault 4, a fault at both wind farms has been considered at 17-18 hours. The reason being considering fault at 17-18 hour is same as explained in section 5.3.2.

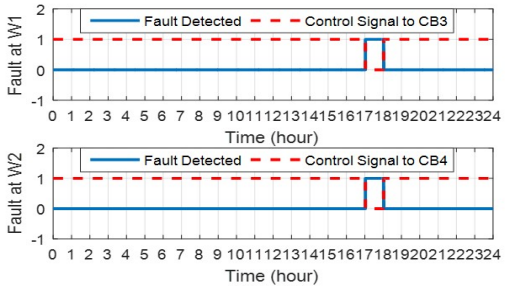

Figure 5.12: Fault 4 detected by FDIRA & Self-healing action

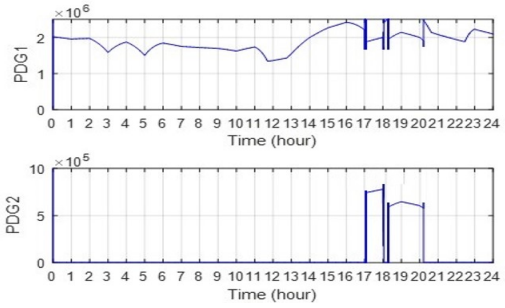

Figure 5.13: Power output of Diesel Generator during fault 4

Figure. 5.12 shows the fault identified by FDIR agent at both wind farms at 17-18 hours and self-healing actions preformed. In this case, FDIR agent sends control

signal '0' to CB3 and CB4 to isolate both wind farms as represented in Figure. 5.12. Also at the same time, FDIR agent passes the information to the CA. After receiving the information, the CA is updated accordingly as explained in section 5.2.9. Hence the shortage of requirement in power due to the isolation of both wind farms should be managed by the DGs. The load requirement of the MG is unable to be met by the DG1 alone. Thus, at the 17 hours, DG2 is also activated by the proposed MAS and the same can be seen in Figure. 5.13. The DG2 in Figure. 5.13 is activated early as compared to the Figure. 5.7 due to the increased power requirement of MG because of the isolation of both wind farms as compared to section 5.3.2. After clearing the fault at 18-hour FDIR agent restore both wind farms as shown in Figure. 5.12 and the same effect is reflected in Figure. 5.13.

5.3.6 Fault 5

During this condition, a fault at PV farm 1 at 11-12 hour and a fault at wind farm 1 at 11.30- 12.30 hour have been considered.

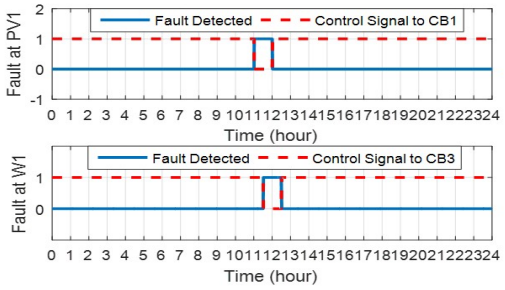

Figure 5.14: Fault 5 detected by FDIRA & Self-healing action

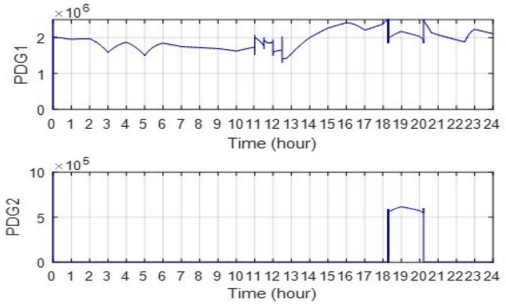

Figure 5.15: Power output of Diesel Generator during fault 5

Figure. 5.14 represents the fault detected by the FDIR agent at 11-12 and 11.30-12.30 hour at PV farm 1 and wind farm 1 respectively and the self-healing action performed . After detecting the fault, the FDIR agent sends a control signal '0' to CB1 and CB3 to isolate respective PV and wind farm as represented in Figure.

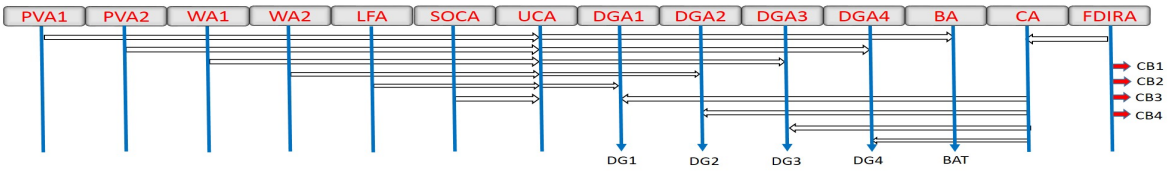

Figure 5.16: Agent Communication Diagram

5.14. Also, the FDIRA passes this information to CA, and the CA act accordingly as explained in section 5.2.9. Figure. 5.15 shows the power supplied by the DG during fault 5. The PDG1 of the Figure. 5.15 shows a sudden variation in power production during 11-11.30 hours, 11.30-12 hours and 12-12.30 hours. During 11-11.30 hour PV farm 1 is isolated, so some increment in PDG1 as compared to normal condition is found. At 11.30- 12 hour the variation is occurred due to the isolation of wind farm 1. The variation at 12-12.30 hour is that the PV farm 1 is restored by FDIR agent (Figure. 5.14) at 12 hour and only wind farm 1 is now isolated. At 12.30 hours the reduction in power production can be found due to the restoration of wind farm 1 at 12 hours by FDIR agent (Figure. 5.14). Figure. 5.16 represents the communication of all the agents deployed in the proposed MG EMS architecture.

5.4 Chapter Summary

A four-layer multi agent architecture for energy management in an MG with self-healing capabilities is proposed in this chapter. In the proposed architecture, different type of agents namely PV agent, wind agent, SOC agent, unit commitment agent, correction agent, and fault detection and isolation and restoration agent, battery agent, DG agents, have been deployed in different layers with particular responsibilities. The performance of the proposed model is analyzed by simulating faults at different locations in the MG. The simulation results reflected the capability of proposed MAS to self-heal the outages occurred in the system and the potential for energy management to meet the load requirements of the system.

Chapter 6

Conclusion

This chapter provides the concluding remarks of the work carried out through the entire thesis work. The summary of significant findings of this study are highlighted in section 6.1 while the next section lists the future scope for research.

6.1 Summary of Significant Findings

The summary of significant findings of this study can be highlighted as follows:

1. A microgrid test system is modeled for implementing the proposed multi agent based microgrid energy management architecture.
2. Different agents and the responsibilities of each agent are identified and implemented for MAS based microgrid energy management.
3. A load forecasting agent is developed by utilizing Bayesian Multivariate Linear Spline (BMLS) model for the proposed multi agent based microgrid energy management architecture.
4. The PV and wind forecasting agents are developed by using an adaptive neuro-fuzzy inference system (ANFIS) based forecasting model for the proposed multi agent based microgrid energy management architecture.
5. An intelligent multi agent system for microgrid energy management system is proposed. The different agents, namely PV agents, wind agents, load forecasting agents, SOC agent, unit commitment agents, diesel generator

agents, battery agent and real time correction agent is developed and deployed in the simulation which represented each component of the microgrid EMS. The effectiveness of the proposed multi agent based energy management system has been tested by comparing the power losses and microgrid system efficiency in different scenarios. The simulation results indicate that the proposed MAS based EMS has better performance as compared to the conventional EMS. Also, the proposed EMS can use the diesel generators optimally to satisfy the load requirement of the microgrid.

6. A four-layer multi agent architecture for energy management in an MG with self-healing capabilities is also proposed. In the proposed architecture, different type of agents namely PV agent, wind agent, SOC agent, unit commitment agent, correction agent, and fault detection and isolation and restoration agent, battery agent, DG agents, have been deployed in different layers with particular responsibilities. The performance of the proposed model is analyzed by simulating faults at different locations in the MG. The simulation results reflected the capability of proposed MAS to self-heal the outages occurred in the system and the potential for energy management to meet the load requirements of the system.

7. A new multi agent platform (Stateflow) is explored in this work to simulate and study the performance of the proposed multi agent based microgrid energy management architecture.

6.2 Future Scope for Research

Research is a continuous process, and always there is a scope. A multi agent based energy management architecture with self-healing capabilities in a microgrid is presented in this research work. As a path forward, some of the identified areas and research directions are given as follows.

1. More capabilities or functionalities to the proposed system can be incorporated by introducing particular agents including responsibilities with the interactions between existing agents in the proposed architecture.

2. In future, more accurate load forecasting models can be developed and implemented as load forecasting agent in the proposed system for better performance.

3. More accurate models for PV and wind forecasting can be developed and implemented as RES forecasting agent in the proposed system for better performance.

4. The proposed model can be extended to the energy management for multiple microgrids in future.

5. The electric vehicles can be incorporated into the existing microgrid model with the vehicle to grid (V2G), and grid to vehicle (G2V) functionalities and can be studied the performance of the multi agent based energy management by the addition of suitable agents to the system.

6. In this study, the diesel generators are allowed to operate up to the maximum capacity to fulfill the load requirement of the microgrid. In future, methods to find the optimum operating point for each diesel generator to provide maximum environmental benefits can be incorporated.

Appendix A

List of Publications

Journal Publications

1. Sujil A, Rajesh Kumar and R C Bansal "Multi Agent based Autonomous Energy Management System with Self-Healing Capabilities for a Microgrid", IEEE Transactions on Industrial Informatics [Online].

2. Sujil A, Jatin Verma and Rajesh Kumar, "Multi agent system: concepts, platforms and applications in power systems", Artificial Intelligence Review, Volume 49, Feb 2018, pp. 153–182, Springer.

3. Sujil A, Rajesh Kumar and R C Bansal "FCM Clustering Based Adaptive Neuro Fuzzy Inference System based PV and Wind Generation Forecasting Agent for Energy Management in a Smart Microgrid.", IET The Journal of Engineering, [Accepted].

4. Sujil A, S K Agarwal and Rajesh Kumar, "Feasibility Study of Centralized Multi-agent Self-healing Power System with Superconducting Fault Current Limiter", Technology and Economics of Smart Grids and Sustainable Energy, Volume 1, Feb 2016, pp. 1–12, Springer.

5. Sujil A, Rajesh Kumar and R C Bansal "An Intelligent Multi Agent based Approach for Autonomous Energy Management in a Microgrid", Sustainable Energy, Grids and Networks, Elsevier [Under Review].

6. Sujil A, Rajesh Kumar and R C Bansal, "Stateflow based Modeling of Multi Agent System for Smart Microgrid Energy Management", Automation Technol-

ogy: Methods and Applications of Control, Regulation, and Information Technology, De Gruyter [Under Review].

International Conference Publications

1. Sujil A, Sreenu Sreekumar, Jatin Verma and Rajesh Kumar, "Matrix based Univariate and Multivariate Short Term Load Forecasting for Power System", Proceedings of the Second IEEE International Conference on Electrical, Computer and Communication Technologies (IEEE ICECCT 2017), Coimbatore, 22-24 February 2017

2. Sujil A and Rajesh Kumar, "Multi Agent based Energy Management System for Smart Microgrid", Proceedings of the 2nd International Conference on Recent Developments in Control, Automation & Power Engineering (RDCAPE-2017), Noida, India,26-27th October 2017

3. Sujil A and Rajesh Kumar, "Smart Micro Grid Test System for Agent based Energy Management System",Proceedings of 7th IEEE India International Conference on Power Electronics (IICPE),Patiala, India,17 Nov - 19 Nov 2016

4. Sujil A, Simran Choudhary, Jatin Verma and Rajesh Kumar, "Agent Based Intelligent Fault Detection, Isolation and Restoration in Smart Power System", Proceedings of the IEEE Students' Conference on Electrical, Electronics and Computer Science, Bhopal, 5-6 March 2016

5. Sujil A, Rajesh Kumar and R C Bansal "Markov Chain Monte Carlo Sampling Based Bayesian Multivariate Linear Spline Load Forecasting Agent for Smart Microgrid Energy Management System", IET Renewable Power Generation Conference 2019 [Submitted].

Bibliography

[1] Y. Zoka, H. Sasaki, N. Yorino, K. Kawahara, and C. Liu, "An interaction problem of distributed generators installed in a microgrid," in *Proceedings of the IEEE International Conference on Electric Utility Deregulation, Restructuring and Power Technologies,(DRPT 2004)*, vol. 2, pp. 795–799, IEEE, 2004.

[2] B. Zhao, X. Zhang, P. Li, K. Wang, M. Xue, and C. Wang, "Optimal sizing, operating strategy and operational experience of a stand-alone microgrid on dongfushan island," *Applied Energy*, vol. 113, pp. 1656–1666, 2014.

[3] A. Baziar and A. Kavousi-Fard, "Considering uncertainty in the optimal energy management of renewable micro-grids including storage devices," *Renewable Energy*, vol. 59, pp. 158–166, 2013.

[4] B. Kroposki, R. Lasseter, T. Ise, S. Morozumi, S. Papathanassiou, and N. Hatziargyriou, "Making microgrids work," *IEEE Power and Energy Magazine*, vol. 6, no. 3, pp. 40–53, 2008.

[5] R. H. Lasseter, "Microgrids," in *Power Engineering Society Winter Meeting*, vol. 1, pp. 305–308, IEEE, 2002.

[6] J. Zhao, C. Wang, B. Zhao, F. Lin, Q. Zhou, and Y. Wang, "A review of active management for distribution networks: current status and future development trends," *Electric Power Components and Systems*, vol. 42, no. 3-4, pp. 280–293, 2014.

[7] S. Mohammadi, S. Soleymani, and B. Mozafari, "Scenario-based stochastic operation management of microgrid including wind, photovoltaic, microturbine, fuel cell and energy storage devices," *International Journal of Electrical Power & Energy Systems*, vol. 54, pp. 525–535, 2014.

[8] K. Tan, P. So, Y. Chu, and M. Chen, "Coordinated control and energy management of distributed generation inverters in a microgrid," *IEEE transactions on power delivery*, vol. 28, no. 2, pp. 704–713, 2013.

[9] M. Castañeda, A. Cano, F. Jurado, H. Sánchez, and L. M. Fernández, "Sizing optimization, dynamic modeling and energy management strategies of a stand-alone pv/hydrogen/battery-based hybrid system," *International journal of hydrogen energy*, vol. 38, no. 10, pp. 3830–3845, 2013.

[10] C.-S. Karavas, G. Kyriakarakos, K. G. Arvanitis, and G. Papadakis, "A multi-agent decentralized energy management system based on distributed intelligence for the design and control of autonomous polygeneration microgrids," *Energy Conversion and Management*, vol. 103, pp. 166–179, 2015.

[11] C.-x. Dou, W.-q. Wang, D.-W. Hao, and X.-b. Li, "Mas-based solution to energy management strategy of distributed generation system," *International Journal of Electrical Power & Energy Systems*, vol. 69, pp. 354–366, 2015.

[12] Z. Jun, L. Junfeng, W. Jie, and H. Ngan, "A multi-agent solution to energy management in hybrid renewable energy generation system," *Renewable Energy*, vol. 36, no. 5, pp. 1352–1363, 2011.

[13] A. Sujil, J. Verma, and R. Kumar, "Multi agent system: concepts, platforms and applications in power systems," *Artificial Intelligence Review*, pp. 1–30, 2016.

[14] S. D. McArthur, E. M. Davidson, V. M. Catterson, A. L. Dimeas, N. D. Hatziargyriou, F. Ponci, and T. Funabashi, "Multi-agent systems for power engineering applicationsPart I: Concepts, approaches, and technical challenges," *IEEE Transactions on Power Systems*, vol. 22, no. 4, pp. 1743–1752, 2007.

[15] H. N. Aung, A. Khambadkone, D. Srinivasan, and T. Logenthiran, "Agent-based intelligent control for real-time operation of a microgrid," in *Joint International Conference on Power Electronics, Drives and Energy Systems (PEDES) & 2010 Power India, 2010*, pp. 1–6, IEEE, 2010.

[16] T. Logenthiran, D. Srinivasan, A. Khambadkone, and H. Aung, "Scalable Multi-Agent System (MAS) for operation of a microgrid in islanded mode," in *Joint International Conference on Power Electronics, Drives and Energy Systems (PEDES) & 2010 Power India*, pp. 1–6, IEEE, 2010.

[17] J. Rocabert, G. Azevedo, A. Luna, J. M. Guerrero, J. I. Candela, and P. Rodriguez, "Intelligent connection agent for three-phase grid-connected microgrids," *IEEE Transactions on Power Electronics*, vol. 26, no. 10, pp. 2993–3005, 2011.

[18] C. Dou, D. Yue, X. Li, and Y. Xue, "Mas-based management and control strategies for integrated hybrid energy system," *IEEE Transactions on Industrial Informatics*, vol. 12, no. 4, pp. 1332–1349, 2016.

[19] F. Luo, Y. Chen, Z. Xu, G. Liang, Y. Zheng, and J. Qiu, "Multiagent-based cooperative control framework for microgrids energy imbalance," *IEEE Transactions on Industrial Informatics*, vol. 13, no. 3, pp. 1046–1056, 2017.

[20] F. Eddy, H. B. Gooi, and S. X. Chen, "Multi-agent system for distributed management of microgrids," *IEEE Transactions on Power Systems*, vol. 30, no. 1, pp. 24–34, 2015.

[21] M. K. Kouluri and R. K. Pandey, "Intelligent agent based micro grid control," in *2nd International Conference on Intelligent Agent and Multi-Agent Systems (IAMA)*, pp. 62–66, IEEE, 2011.

[22] T. Logenthiran, D. Srinivasan, A. M. Khambadkone, and H. N. Aung, "Multiagent system for real-time operation of a microgrid in real-time digital simulator," *IEEE Transactions on Smart Grid*, vol. 3, no. 2, pp. 925–933, 2012.

[23] C.-X. Dou and B. Liu, "Multi-agent based hierarchical hybrid control for smart microgrid," *IEEE Transactions on Smart Grid*, vol. 4, no. 2, pp. 771–778, 2013.

[24] C. Dou, M. Lv, T. Zhao, Y. Ji, and H. Li, "Decentralised coordinated control of microgrid based on multi-agent system," *Generation, Transmission & Distribution, IET*, vol. 9, no. 16, pp. 2474–2484, 2015.

[25] Q. Li, F. Chen, M. Chen, J. M. Guerrero, and D. Abbott, "Agent-based decentralized control method for islanded microgrids," *IEEE Transactions on Smart Grid*, vol. 7, no. 2, pp. 637–649, 2016.

[26] W. Liu, W. Gu, W. Sheng, X. Meng, S. Xue, and M. Chen, "Pinning-based distributed cooperative control for autonomous microgrids under uncertain communication topologies," *IEEE Transactions on Power Systems*, vol. 31, no. 2, pp. 1320–1329, 2016.

[27] T. Morstyn, B. Hredzak, and V. G. Agelidis, "Distributed cooperative control of microgrid storage," *IEEE Transactions on Power Systems*, vol. 30, pp. 2780–2789, Sept 2015.

[28] B. Zhao, M. Xue, X. Zhang, C. Wang, and J. Zhao, "An mas based energy management system for a stand-alone microgrid at high altitude," *Applied Energy*, vol. 143, pp. 251–261, 2015.

[29] L. Raju, R. S. Milton, and S. Mahadevan, "Application of multi agent systems in automation of distributed energy management in micro-grid using macsimjx," *Intelligent Automation & Soft Computing*, vol. 0, no. 0, pp. 1–9, 2017.

[30] Z. Wang, L. Wang, A. I. Dounis, and R. Yang, "Multi-agent control system with information fusion based comfort model for smart buildings," *Applied Energy*, vol. 99, pp. 247–254, 2012.

[31] P. H. Shaikh, N. B. M. Nor, P. Nallagownden, I. Elamvazuthi, and T. Ibrahim, "Intelligent multi-objective control and management for smart energy efficient buildings," *International Journal of Electrical Power & Energy Systems*, vol. 74, pp. 403–409, 2016.

[32] C.-X. Dou, D.-W. Hao, B. Jin, W.-Q. Wang, and N. An, "Multi-agent-system-based decentralized coordinated control for large power systems," *International Journal of Electrical Power & Energy Systems*, vol. 58, pp. 130–139, 2014.

[33] G. Kyriakarakos, D. D. Piromalis, A. I. Dounis, K. G. Arvanitis, and G. Papadakis, "Intelligent demand side energy management system for autonomous polygeneration microgrids," *Applied Energy*, vol. 103, pp. 39–51, 2013.

[34] E. Kuznetsova, Y.-F. Li, C. Ruiz, and E. Zio, "An integrated framework of agent-based modelling and robust optimization for microgrid energy management," *Applied Energy*, vol. 129, pp. 70–88, 2014.

[35] A. Vaccaro, V. Loia, G. Formato, P. Wall, and V. Terzija, "A self-organizing architecture for decentralized smart microgrids synchronization, control, and monitoring," *IEEE transactions on Industrial Informatics*, vol. 11, no. 1, pp. 289–298, 2015.

[36] R. de Azevedo, M. H. Cintuglu, T. Ma, and O. A. Mohammed, "Multiagent-based optimal microgrid control using fully distributed diffusion strategy," *IEEE Transactions on Smart Grid*, vol. 8, no. 4, pp. 1997–2008, 2017.

[37] W. Zhang, Y. Xu, W. Liu, C. Zang, and H. Yu, "Distributed online optimal energy management for smart grids," *IEEE Transactions on Industrial Informatics*, vol. 11, no. 3, pp. 717–727, 2015.

[38] H. K. Nunna and S. Doolla, "Multiagent-based distributed-energy-resource management for intelligent microgrids," *IEEE Transactions on Industrial Electronics*, vol. 60, no. 4, pp. 1678–1687, 2013.

[39] M. Pipattanasomporn, H. Feroze, and S. Rahman, "Multi-agent systems in a distributed smart grid: Design and implementation," in *Power Systems Conference and Exposition. PSCE'09. IEEE/PES*, pp. 1–8, IEEE, 2009.

[40] J. Lagorse, D. Paire, and A. Miraoui, "A multi-agent system for energy management of distributed power sources," *Renewable energy*, vol. 35, no. 1, pp. 174–182, 2010.

[41] T. Logenthiran, D. Srinivasan, and D. Wong, "Multi-agent coordination for DER in MicroGrid," in *IEEE International Conference on Sustainable Energy Technologies, ICSET*, pp. 77–82, IEEE, 2008.

[42] E. M. Davidson, S. D. McArthur, J. R. McDonald, T. Cumming, and I. Watt, "Applying multi-agent system technology in practice: automated management and analysis of scada and digital fault recorder data," *IEEE Transactions on Power Systems*, vol. 21, no. 2, p. 559, 2006.

[43] M. Wooldridge, *An introduction to multiagent systems*. John Wiley & Sons, 2009.

[44] S. Franklin and A. Graesser, "Is it an Agent, or just a Program?: A Taxonomy for Autonomous Agents," in *Intelligent agents III agent theories, architectures, and languages*, pp. 21–35, Springer, 1997.

[45] B. Hayes-Roth, K. Pfleger, P. Lalanda, P. Morignot, and M. Balabanovic, "A domain-specific software architecture for adaptive intelligent systems," *IEEE Transactions on Software Engineering*, vol. 21, no. 4, pp. 288–301, 1995.

[46] F. M. T. Brazier, B. M. Dunin-Keplicz, N. R. Jennings, and J. Treur, "Desire: Modelling multi-agent systems in a compositional formal framework," *Int. Journal of Cooperative Information Systems*, vol. 6, no. 1, pp. 67–94, 1997.

[47] C. A. Iglesias, M. Garijo, J. C. González, and J. R. Velasco, "Analysis and design of multiagent systems using MAS-commonKADS," in *Intelligent Agents IV Agent Theories, Architectures, and Languages*, pp. 313–327, Springer, 1998.

[48] N. Lidula and A. Rajapakse, "Microgrids research: A review of experimental microgrids and test systems," *Renewable and Sustainable Energy Reviews*, vol. 15, no. 1, pp. 186–202, 2011.

[49] M. Dastani, J. Hulstijn, F. Dignum, and J.-J. C. Meyer, "Issues in multiagent system development," in *Proceedings of the Third International Joint Conference on Autonomous Agents and Multiagent Systems, vol.2*, pp. 922–929, IEEE Computer Society, 2004.

[50] F. Zambonelli, N. R. Jennings, and M. Wooldridge, "Organisational abstractions for the analysis and design of multi-agent systems," in *Agent-oriented software engineering*, pp. 235–251, Springer, 2001.

[51] D. Kinny, M. Georgeff, and A. Rao, "A methodology and modelling technique for systems of bdi agents," in *Agents breaking away*, pp. 56–71, Springer, 1996.

[52] A. Omicini, "Soda: Societies and infrastructures in the analysis and design of agent-based systems," in *Agent-oriented software engineering*, pp. 185–193, Springer, 2001.

[53] J. Castro, M. Kolp, and J. Mylopoulos, "Towards requirements-driven information systems engineering: the tropos project," *Information systems*, vol. 27, no. 6, pp. 365–389, 2002.

[54] R. H. Bordini, M. Dastani, and M. Winikoff, "Current issues in multi-agent systems development," in *Engineering Societies in the Agents World VII*, pp. 38–61, Springer, 2006.

[55] J. Ghorbani, Y. P. Fallah, M. A. Choudhry, and A. Feliachi, "Investigation of communication media requirements for self healing power distribution systems," in *Energytech, 2013 IEEE*, pp. 1–7, IEEE, 2013.

[56] A. Sujil, S. K. Agarwal, and R. Kumar, "Centralized multi-agent implementation for securing critical loads in pv based microgrid," *Journal of Modern Power Systems and Clean Energy*, vol. 2, no. 1, pp. 77–86, 2014.

[57] R. Simmons, T. Smith, M. B. Dias, D. Goldberg, D. Hershberger, A. Stentz, and R. Zlot, "A layered architecture for coordination of mobile robots," in *Multi-robot systems: from swarms to intelligent automata*, pp. 103–112, Springer, 2002.

[58] A. Tews and G. F. Wyeth, "Multi-robot coordination in the robot soccer environment," in *Proceedings of the Australian Conference on Robotics and Automation (ACRA'99), March*, pp. 90–95, Citeseer, 1999.

[59] A. Tews and G. Wyeth, "Maps: A system for multi-agent coordination," *Advanced Robotics*, vol. 14, no. 1, pp. 37–50, 2000.

[60] C. Wang, T. Zhang, and F. Ma, "A multi-agent based hierarchical control system for ders management in islanded micro-grid," in *Chinese Automation Congress (CAC)*, pp. 1371–1376, IEEE, 2015.

[61] M. Ding, K. Ma, R. Bi, M. Mao, and L. Chang, "A hierarchical control scheme based on multi-agent system for islanded multi-microgrids," in *4th IEEE International Symposium on Power Electronics for Distributed Generation Systems (PEDG)*, pp. 1–5, IEEE, 2013.

[62] L. Jianfang, S. Xiaohui, and M. Xiaoli, "Hierarchical control model of smart distribution network based on self-organizing multi-agent system," in *International Conference on Renewable Power Generation (RPG 2015)*, pp. 1–6, IET, 2015.

[63] C. H. Brooks, E. H. Durfee, and A. Armstrong, "An introduction to congregating in multi-agent systems," in *Proceedings. Fourth International Conference on MultiAgent Systems*, pp. 79–86, IEEE, 2000.

[64] D. C. Parker, S. M. Manson, M. A. Janssen, M. J. Hoffmann, and P. Deadman, "Multi-agent systems for the simulation of land-use and land-cover change: a review," *Annals of the association of American Geographers*, vol. 93, no. 2, pp. 314–337, 2003.

[65] S. R. Islam, D. Sutanto, and K. M. Muttaqi, "A distributed multi-agent based emergency control approach following catastrophic disturbances in interconnected power systems," *IEEE Transactions on Power Systems*, vol. 31, pp. 2764–2775, July 2016.

[66] G. Weiss, *Multiagent systems: a modern approach to distributed artificial intelligence*. MIT press, 1999.

[67] A. Sujil, S. K. Agrwal, and R. Kumar, "Centralized multi-agent self-healing power system with super conducting fault current limiter," in *IEEE Conference on Information & Communication Technologies (ICT)*, pp. 622–627, IEEE, 2013.

[68] B. Hu, W. Guo, and Z. Jing, "Electric vehicles operation simulation system based on multi-agent system," in *Transportation Electrification Asia-Pacific (ITEC Asia-Pacific), IEEE Conference and Expo*, pp. 1–5, IEEE, 2014.

[69] C. M. Colson and M. H. Nehrir, "Comprehensive real-time microgrid power management and control with distributed agents," *IEEE Transactions on Smart Grid*, vol. 4, no. 1, pp. 617–627, 2013.

[70] C. Colson, M. Nehrir, and R. Gunderson, "Distributed multi-agent microgrids: a decentralized approach to resilient power system self-healing," in *4th International Symposium on Resilient Control Systems (ISRCS), 2011*, pp. 83–88, IEEE, 2011.

[71] A. L. Dimeas and N. D. Hatziargyriou, "Operation of a multiagent system for microgrid control," *IEEE Transactions on Power Systems*, vol. 20, no. 3, pp. 1447–1455, 2005.

[72] S. B. Ghosn, P. Ranganathan, S. Salem, J. Tang, D. Loegering, and K. E. Nygard, "Agent-oriented designs for a self healing smart grid," in *First IEEE International Conference on Smart Grid Communications (SmartGridComm)*, pp. 461–466, IEEE, 2010.

[73] K. Huang, S. K. Srivastava, D. Cartes, M. Sloderbeck, *et al.*, "Intelligent agents applied to reconfiguration of mesh structured power systems," in *International Conference on Intelligent Systems Applications to Power Systems,(ISAP)*, pp. 1–7, IEEE, 2007a.

[74] K. Huang, S. K. Srivastava, D. A. Cartes, and L.-H. Sun, "Market-based multiagent system for reconfiguration of shipboard power systems," *Electric Power Systems Research*, vol. 79, no. 4, pp. 550–556, 2009.

[75] T. Logenthiran and D. Srinivasan, "Multi-agent system for managing a power distribution system with plug-in hybrid electrical vehicles in smart grid," in *Innovative Smart Grid Technologies-India (ISGT India), 2011 IEEE PES*, pp. 346–351, IEEE, 2011.

[76] U. Leeton and T. Kulworawanichpong, "Multi-agent based optimal power flow solution," in *Asia-Pacific Power and Energy Engineering Conference (APPEEC)*, pp. 1–4, IEEE, 2012.

[77] P. H. Nguyen, W. L. Kling, and P. F. Ribeiro, "A game theory strategy to integrate distributed agent-based functions in smart grids," *IEEE Transactions on Smart Grid*, vol. 4, no. 1, pp. 568–576, 2013.

[78] M. M. Nordman and M. Lehtonen, "Distributed agent-based state estimation for electrical distribution networks," *IEEE Transactions on Power Systems*, vol. 20, no. 2, pp. 652–658, 2005.

[79] K. Nareshkumar, M. Choudhry, J. Lai, and A. Feliachi, "Application of multi-agents for fault detection and reconfiguration of power distribution systems," in *Power & Energy Society General Meeting, PES'09*, pp. 1–8, IEEE, 2009.

[80] M. Nasri, H. Farhangi, A. Palizban, and M. Moallem, "Multi-agent control system for real-time adaptive VVO/CVR in smart substation," in *Electrical Power and Energy Conference (EPEC)*, pp. 1–7, IEEE, 2012.

[81] J. Oyarzabal, J. Jimeno, J. Ruela, A. Engler, and C. Hardt, "Agent based micro grid management system," in *International Conference on Future Power Systems*, p. 6, IEEE, 2005.

[82] P. Papadopoulos, N. Jenkins, L. M. Cipcigan, I. Grau, and E. Zabala, "Coordination of the charging of electric vehicles using a multi-agent system," *IEEE Transactions on Smart Grid*, vol. 4, no. 4, pp. 1802–1809, 2013.

[83] H. Pezeshki, P. J. Wolfs, and M. Johnson, "Multi-agent systems for modeling high penetration photovoltaic system impacts in distribution networks," in *Innovative Smart Grid Technologies Asia (ISGT), IEEE PES*, pp. 1–8, IEEE, 2011.

[84] R. Roche, L. Idoumghar, B. Blunier, and A. Miraoui, "Optimized fuel cell array energy management using multi-agent systems," in *Industry Applications Society Annual Meeting (IAS)*, pp. 1–8, IEEE, 2011.

[85] S. Rivera, A. M. Farid, and K. Youcef-Toumi, "A multi-agent system transient stability platform for resilient self-healing operation of multiple microgrids," in *Innovative Smart Grid Technologies Conference (ISGT), IEEE PES*, pp. 1–5, IEEE, 2014.

[86] S. Mocci, N. Natale, S. Ruggeri, and F. Pilo, "Multi-agent control system for increasing hosting capacity in active distribution networks with EV," in *IEEE International Energy Conference (ENERGYCON)*, pp. 1409–1416, IEEE, 2014.

[87] T. Sweda and D. Klabjan, "An agent-based decision support system for electric vehicle charging infrastructure deployment," in *Vehicle Power and Propulsion Conference (VPPC)*, pp. 1–5, IEEE, 2011.

[88] H. Wan, K. Li, and K. Wong, "Multi-agent application of substation protection coordination with distributed generators," in *International Conference on Future Power Systems*, p. 6, IEEE, 2005.

[89] J. Zeng, J. Liu, H. Ngan, and J. Wu, "A multi-agent solution to energy management of distributed hybrid renewable energy generated system," *,8th International Conference on Advances in Power System Control, Operation and Management (APSCOM 2009)*, p. 112, 2009.

[90] Z. Wang and R. Paranjape, "An evaluation of electric vehicle penetration under demand response in a multi-agent based simulation," in *Electrical Power and Energy Conference (EPEC), IEEE*, pp. 220–225, IEEE, 2014.

[91] Z. He, Z. Zhang, X. Yin, Z. Li, X. Kong, and Y. Wang, "Multi-agent based wide area backup protection for series compensated lines," in *Power and Energy Engineering Conference (APPEEC), 2011 Asia-Pacific*, pp. 1–4, IEEE, 2011.

[92] F. Ren, M. Zhang, and D. Sutanto, "A multi-agent solution to distribution system management by considering distributed generators," *IEEE Transactions on Power Systems*, vol. 28, no. 2, pp. 1442–1451, 2013.

[93] G. G. Karady, M. Mohamed, *et al.*, "Improving transient stability using fast valving based on tracking rotor-angle and active power," in *Power Engineering Society Summer Meeting*, vol. 3, pp. 1576–1581, IEEE, 2002.

[94] G. G. Karady, A. Daoud, M. Mohamed, *et al.*, "On-line transient stability enhancement using multi-agent technique," in *Power Engineering Society Winter Meeting*, vol. 2, pp. 893–899, IEEE, 2002.

[95] J. Lagorse, M. G. Simões, and A. Miraoui, "A multiagent fuzzy-logic-based energy management of hybrid systems," *IEEE Transactions on Industry Applications*, vol. 45, no. 6, pp. 2123–2129, 2009.

[96] D. Coury, J. Thorp, K. Hopkinson, and K. Birman, "Improving the protection of EHV teed feeders using local agents," in *Seventh International Conference on (IEE) Developments in Power System Protection*, pp. 527–530, IET, 2001.

[97] D. V. Coury, J. S. Thorp, K. M. Hopkinson, and K. P. Birman, "An agent-based current differential relay for use with a utility intranet," *IEEE Transactions on Power Delivery*, vol. 17, no. 1, pp. 47–53, 2002.

[98] S. Sheng, K. Li, W. Chan, X. Zeng, and D. Xianzhong, "Agent-based wide area current differential protection system," in *Industry Applications Conference, 2005. Fourtieth IAS Annual Meeting. Conference Record of the 2005*, vol. 1, pp. 453–458, IEEE, 2005.

[99] I. Lim, S. Lee, M. Choi, and P. Crossley, "Multi-agent system-based protection coordination of distribution feeders," in *International Conference on Intelligent Systems Applications to Power Systems (ISAP)*, pp. 1–6, IEEE, 2007.

[100] M. Meiqin, D. Wei, and L. Chang, "Design of a novel simulation platform for the EMS-MG based on MAS," in *Energy Conversion Congress and Exposition (ECCE), IEEE*, pp. 2670–2675, IEEE, 2011.

[101] M. Mao, P. Jin, N. D. Hatziargyriou, and L. Chang, "Multiagent-based hybrid energy management system for microgrids," *IEEE Transactions on Sustainable Energy*, vol. 5, no. 3, pp. 938–946, 2014.

[102] T. Li, Z. Xiao, M. Huang, J. Yu, and J. Hu, "Control system simulation of microgrid based on IP and Multi-Agent," in *International Conference on Information Networking and Automation (ICINA)*, vol. 1, pp. 235–239, IEEE, 2010.

[103] C. Dou, C. Mao, Z. Bo, and X. Zhang, "A multi-agent model based decentralized coordinated control for large power system transient stability improvement," in *45th International Universities Power Engineering Conference (UPEC), 2010*, pp. 1–5, IEEE, 2010.

[104] R. Giovanini, K. Hopkinson, D. V. Coury, and J. S. Thorp, "A primary and backup cooperative protection system based on wide area agents," *IEEE Transactions on Power Delivery*, vol. 21, no. 3, pp. 1222–1230, 2006.

[105] J. Yen, Y. Yan, B. Wang, P. Sin, and F. F. Wu, "Multi-agent coalition formation in power transmission planning," in *Proceedings of the Thirty-First Hawaii International Conference on System Sciences*, vol. 4, pp. 433–443, IEEE, 1998.

[106] C. P. Nguyen and A. J. Flueck, "Agent based restoration with distributed energy storage support in smart grids," *IEEE Transactions on Smart Grid*, vol. 3, no. 2, pp. 1029–1038, 2012.

[107] Z. Xiangjun, K. Li, W. Chan, and S. Sheng, "Multi-agents based protection for distributed generation systems," *Proceedings of the IEEE International Conference on Electric Utility Deregulation, Restructuring and Power Technologies, (DRPT)*, vol. 1, pp. 393–397, 2004.

[108] C. Gao, C. Dong, and F. Xue, "Design and implementation of simulation software for electric vehicle charging behavior based on multi-agent system," *Proceedings of the CSEE*, vol. 31, p. 008, 2012.

[109] M. Shafie-khah and J. P. Catalão, "A stochastic multi-layer agent-based model to study electricity market participants behavior," *IEEE Transactions on Power Systems*, vol. 30, no. 2, pp. 867–881, 2015.

[110] Y. Tomita, C. Fukui, H. Kudo, J. Koda, and K. Yabe, "A cooperative protection system with an agent model," *IEEE Transactions on Power Delivery*, vol. 13, no. 4, pp. 1060–1066, 1998.

[111] X. Tong, X. Wang, R. Wang, F. Huang, X. Dong, K. M. Hopkinson, and G. Song, "The study of a regional decentralized peer-to-peer negotiation-based wide-area backup protection multi-agent system," *IEEE Transactions on Smart Grid*, vol. 4, no. 2, pp. 1197–1206, 2013.

[112] S. Vandael, N. Boucké, T. Holvoet, and G. Deconinck, "Decentralized demand side management of plug-in hybrid vehicles in a smart grid," in *Proceedings of the First International Workshop on Agent Technologies for Energy Systems (ATES 2010)*, pp. 67–74, 2010.

[113] S. Weckx, R. D'hulst, B. Claessens, and J. Driesensam, "Multiagent charging of electric vehicles respecting distribution transformer loading and voltage limits," *IEEE Transactions on Smart Grid*, vol. 5, no. 6, pp. 2857–2867, 2014.

[114] S. Wong and A. Kalam, "Development of a power protection system using an agent based architecture," in *Proceedings of International Conference on Energy Management and Power Delivery, EMPD'95*, vol. 1, pp. 433–438, IEEE, 1995.

[115] Z. Jian, A. Qian, J. Chuanwen, W. Xingang, Z. Zhanghua, and G. Chenghong, "The application of multi agent system in microgrid coordination control," in *International Conference on Sustainable Power Generation and Supply, SUPERGEN'09*, pp. 1–6, IEEE, 2009.

[116] W. Zhang, W. Liu, X. Wang, L. Liu, and F. Ferrese, "Distributed multiple agent system based online optimal reactive power control for smart grids," *IEEE Transactions on Smart Grid*, vol. 5, no. 5, pp. 2421–2431, 2014.

[117] B. Zhao, C. Guo, and Y. Cao, "A multiagent-based particle swarm optimization approach for optimal reactive power dispatch," *IEEE Transactions on Power Systems*, vol. 20, no. 2, pp. 1070–1078, 2005.

[118] E. L. Karfopoulos, P. Papadopoulos, S. Skarvelis-Kazakos, I. Grau, L. M. Cipcigan, N. Hatziargyriou, and N. Jenkins, "Introducing electric vehicles in the microgrids concept," in *16th International Conference on Intelligent System Application to Power Systems (ISAP)*, pp. 1–6, IEEE, 2011.

[119] E. L. Karfopoulos and N. D. Hatziargyriou, "A multi-agent system for controlled charging of a large population of electric vehicles," *IEEE Transactions on Power Systems*, vol. 28, no. 2, pp. 1196–1204, 2013.

[120] J. K. Kok, C. J. Warmer, and I. Kamphuis, "Powermatcher: multiagent control in the electricity infrastructure," in *Proceedings of the fourth international joint conference on Autonomous agents and multiagent systems*, pp. 75–82, ACM, 2005.

[121] I. S. Baxevanos and D. P. Labridis, "Implementing multiagent systems technology for power distribution network control and protection management," *IEEE Transactions on Power Delivery*, vol. 22, no. 1, pp. 433–443, 2007.

[122] L. Wehinger, G. Hug-Glanzmann, M. D. Galus, G. Andersson, *et al.*, "Modeling electricity wholesale markets with model predictive and profit maximizing agents," *IEEE Transactions on Power Systems*, vol. 28, no. 2, pp. 868–876, 2013.

[123] K. Mets, R. D'hulst, and C. Develder, "Comparison of intelligent charging algorithms for electric vehicles to reduce peak load and demand variability in a distribution grid," *Journal of Communications and Networks*, vol. 14, no. 6, pp. 672–681, 2012.

[124] H. E. Farag and E. El-Saadany, "Voltage regulation in distribution feeders with high DG penetration: From traditional to smart," in *Power and Energy Society General Meeting*, pp. 1–8, IEEE, 2011.

[125] R. Fazal, J. Solanki, and S. K. Solanki, "Demand response using multi-agent system," in *North American Power Symposium (NAPS), 2012*, pp. 1–6, IEEE, 2012.

[126] K. Huang, S. K. Srivastava, D. Cartes, L. Liu, *et al.*, "Agent solutions for navy shipboard power systems," in *IEEE International Conference on System of Systems Engineering, SoSE'07*, pp. 1–6, IEEE, 2007b.

[127] T. Nagata, R. Hatano, and H. Saiki, "A multi-agent based distributed reactive power control method," in *Power & Energy Society General Meeting, 2009. PES'09. IEEE*, pp. 1–7, IEEE, 2009.

[128] E. Cortese, F. Quarta, G. Vitaglione, and P. Vrba, "Scalability and performance of jade message transport system," in *AAMAS Workshop on AgentCities, Bologna*, vol. 16, p. 28, 2002.

[129] S. F. Railsback, S. L. Lytinen, and S. K. Jackson, "Agent-based simulation platforms: Review and development recommendations," *Simulation*, vol. 82, no. 9, pp. 609–623, 2006.

[130] H. S. Nwana, D. T. Ndumu, L. C. Lee, and J. C. Collis, "Zeus: a toolkit and approach for building distributed multi-agent systems," in *Proceedings of the third annual conference on Autonomous Agents*, pp. 360–361, ACM, 1999.

[131] H. Manitoba, "Research centre," *PSCAD/EMTDC: Electromagnetic transients program including dc systems*, 1994.

[132] K. Hopkinson, X. Wang, R. Giovanini, J. Thorp, K. Birman, and D. Coury, "Epochs: a platform for agent-based electric power and communication simulation built from commercial off-the-shelf components," *IEEE Transactions on Power Systems*, vol. 21, no. 2, pp. 548–558, 2006.

[133] T. Ackermann, G. Andersson, and L. Söder, "Distributed generation: a definition," *Electric power systems research*, vol. 57, no. 3, pp. 195–204, 2001.

[134] P. P. Barker and R. W. De Mello, "Determining the impact of distributed generation on power systems. I. Radial distribution systems," in *Power Engineering Society Summer Meeting*, vol. 3, pp. 1645–1656, IEEE, 2000.

[135] M. T. Doyle, "Reviewing the impacts of distributed generation on distribution system protection," in *Power Engineering Society Summer Meeting*, vol. 1, pp. 103–105, IEEE, 2002.

[136] M. A. Abido, "Environmental/economic power dispatch using multiobjective evolutionary algorithms," *IEEE Transactions on Power Systems*, vol. 18, no. 4, pp. 1529–1537, 2003.

[137] F. L. Bellifemine, G. Caire, and D. Greenwood, *Developing multi-agent systems with JADE*, vol. 7. John Wiley & Sons, 2007.

[138] A. Elmitwally, M. Elsaid, M. Elgamal, and Z. Chen, "A fuzzy-multiagent self-healing scheme for a distribution system with distributed generations," *IEEE Transactions on Power Systems*, vol. 30, no. 5, pp. 2612–2622, 2014.

[139] A. Elmitwally, M. Elsaid, M. Elgamal, and Z. Chen, "A fuzzy-multiagent servce restoration scheme for distribution system with distributed generation," *IEEE Transactions on Sustainable Energy*, vol. 6, no. 3, pp. 810–821, 2015.

[140] A. Pahwa, S. A. DeLoach, B. Natarajan, S. Das, A. R. Malekpour, S. Shafiul Alam, and D. M. Case, "Goal-based holonic multiagent system for operation of power distribution systems," *IEEE Transactions on Smart Grid*, vol. 6, no. 5, pp. 2510–2518, 2015.

[141] K. Manickavasagam, "Intelligent energy control center for distributed generators using multi-agent system," *IEEE Transactions on Power Systems*, vol. 30, no. 5, pp. 2442–2449, 2015.

[142] A. Sharma, D. Srinivasan, and A. Trivedi, "A decentralized multiagent system approach for service restoration using dg islanding," *IEEE Transactions on Smart Grid*, vol. 6, no. 6, pp. 2784–2793, 2015.

[143] Q. Sun, R. Han, H. Zhang, J. Zhou, and J. M. Guerrero, "A multiagent-based consensus algorithm for distributed coordinated control of distributed

generators in the energy internet," *IEEE Transactions on Smart Grid*, vol. 6, no. 6, pp. 3006–3019, 2015.

[144] J. Lopes, F. J. Soares, and P. R. Almeida, "Identifying management procedures to deal with connection of electric vehicles in the grid," in *Powertech, IEEE Bucharest*, pp. 1–8, IEEE, 2009.

[145] Q. Gong, S. Midlam-Mohler, V. Marano, and G. Rizzoni, "Study of PEV charging on residential distribution transformer life," *IEEE Transactions on Smart Grid*, vol. 1, no. 3, pp. 404–412, 2012.

[146] A. G. Anastasiadis, E. Voreadi, and N. D. Hatziargyriou, "Probabilistic Load Flow methods with high integration of Renewable Energy Sources and Electric Vehicles-case study of Greece," in *PowerTech, 2011 IEEE Trondheim*, pp. 1–8, IEEE, 2011.

[147] K. Clement-Nyns, E. Haesen, and J. Driesen, "The impact of charging plug-in hybrid electric vehicles on a residential distribution grid," *IEEE Transactions on Power Systems*, vol. 25, no. 1, pp. 371–380, 2010.

[148] A. Karnama, F. Resende, J. Lopes, *et al.*, "Optimal management of battery charging of electric vehicles: A new microgrid feature," in *PowerTech, 2011 IEEE Trondheim*, pp. 1–8, IEEE, 2011.

[149] A. S. Masoum, S. Deilami, P. S. Moses, M. Masoum, A. Abu-Siada, *et al.*, "Smart load management of plug-in electric vehicles in distribution and residential networks with charging stations for peak shaving and loss minimisation considering voltage regulation," *Generation, Transmission & Distribution, IET*, vol. 5, no. 8, pp. 877–888, 2011.

[150] S. Deilami, A. S. Masoum, P. S. Moses, and M. A. Masoum, "Real-time coordination of plug-in electric vehicle charging in smart grids to minimize power losses and improve voltage profile," *IEEE Transactions on Smart Grid*, vol. 2, no. 3, pp. 456–467, 2011.

[151] E. Sortomme, M. M. Hindi, S. J. MacPherson, and S. Venkata, "Coordinated charging of plug-in hybrid electric vehicles to minimize distribution system losses," *IEEE Transactions on Smart Grid*, vol. 2, no. 1, pp. 198–205, 2011.

[152] E. L. Karfopoulos and N. D. Hatziargyriou, "Distributed coordination of electric vehicles providing v2g services," *IEEE Transactions on Power Systems*, vol. 31, no. 1, pp. 329–338, 2016.

[153] Y. Xu, "Optimal distributed charging rate control of plug-in electric vehicles for demand management," *IEEE Transactions on Power Systems*, vol. 30, no. 3, pp. 1536–1545, 2015.

[154] A. Ford and W. Harm, "Market based adequacy: reliability and CBM/ATC calculations. An independent system operator's perspective," in *Power Engineering Society Winter Meeting*, vol. 1, pp. 18–23, IEEE, 2002.

[155] T. Mount, W. Schulze, and R. E. Schuler, "Markets for reliability and financial options in electricity: Theory to support the practice," in *Proceedings of the 36th Annual Hawaii International Conference on System Sciences*, pp. 10–pp, IEEE, 2003.

[156] S. J. Rassenti, V. L. Smith, and B. J. Wilson, "Structural features that contribute to market power in electric power networks: Some preliminary results," in *Proceedings of the 33rd Annual Hawaii International Conference on System Sciences*, pp. 6–pp, IEEE, 2000.

[157] F. L. Alvarado, "Is system control entirely by price feasible?," in *Proceedings of the 36th Annual Hawaii International Conference on System Sciences*, pp. 53–58, IEEE, 2003.

[158] M. H. Cintuglu, H. Martin, and O. A. Mohammed, "Real-time implementation of multiagent-based game theory reverse auction model for microgrid market operation," *IEEE Transactions on Smart Grid*, vol. 6, no. 2, pp. 1064–1072, 2015.

[159] Y. Dusonchet and A. El-Abiad, "Transmission planning using discrete dynamic optimizing," *IEEE Transactions on Power Apparatus and Systems*, no. 4, pp. 1358–1371, 1973.

[160] R. Bennon, J. Juves, and A. Meliopoulos, "Use of sensitivity analysis in automated transmission planning," *IEEE Transactions on Power Apparatus and Systems*, no. 1, pp. 53–59, 1982.

[161] S. T. Lee, K. L. Hicks, and E. Hnyilicza, "Transmission expansion by branch-and-bound integer programming with optimal cost-capacity curves," *IEEE Transactions on Power Apparatus and Systems*, no. 5, pp. 1390–1400, 1974.

[162] D. Gately, "Sharing the gains from regional cooperation: A game theoretic application to planning investment in electric power," *International Economic Review*, pp. 195–208, 1974.

[163] M. Ortega-Vazquez, D. S. Kirschen, *et al.*, "Assessment of generation expansion mechanisms using multi-agent systems," in *Power and Energy Society General Meeting-Conversion and Delivery of Electrical Energy in the 21st Century*, pp. 1–7, IEEE, 2008.

[164] H. Cai, Z. Qu, D. Gan, and J. Dorsey, "A comparison and simulation study of nonlinearly designed robust controllers for power system transient stability," *International Journal of Electrical Power & Energy Systems*, vol. 22, no. 1, pp. 15–28, 2000.

[165] L. Alberto and N. Bretas, "Required damping to assure multiswing transient stability: the SMIB case," *International Journal of Electrical Power & Energy Systems*, vol. 22, no. 3, pp. 179–185, 2000.

[166] M. Luck, P. McBurney, and C. Preist, "Agent Technology: Enabling Next Generation Computing," January 2003.

[167] X. Wang, P. Zhang, Z. Wang, V. Dinavahi, G.-k. Chang, J. Martinez, A. Davoudi, A. Mehrizi-Sani, and S. Abhyankar, "Interfacing issues in multi-agent simulation for smart grid applications," *IEEE Transactions on Power Delivery*, vol. 28, no. 3, pp. 1918–1927, 2013.

[168] X. Zhang, A. J. Flueck, and C. P. Nguyen, "Agent-based distributed volt/var control with distributed power flow solver in smart grid," *IEEE Transactions on Smart Grid*, 2015.

[169] M. Mao, M. Ding, L. Zhang, J. Su, and M. Sun, "Testbed and information integration of EMS for a microgrid with multi-energy generation systems," *Automation of Electric Power Systems*, vol. 1, pp. 106–111, 2010.

[170] D. E. Olivares, C. Cañizares, M. Kazerani, *et al.*, "A centralized optimal energy management system for microgrids," in *Power and Energy Society General Meeting*, pp. 1–6, IEEE, 2011.

[171] N. Hatziargyriou, A. Dimeas, and A. Tsikalakis, "Centralized and decentralized control of microgrids," *International Journal of Distributed Energy Resources*, vol. 1, no. 3, pp. 197–212, 2005.

[172] M. A. A. Pedrasa, T. D. Spooner, and I. F. MacGill, "Coordinated scheduling of residential distributed energy resources to optimize smart home energy services," *IEEE Transactions on Smart Grid*, vol. 1, no. 2, pp. 134–143, 2010.

[173] A. G. Tsikalakis and N. D. Hatziargyriou, "Centralized control for optimizing microgrids operation," in *Power and Energy Society General Meeting*, pp. 1–8, IEEE, 2011.

[174] H. Kanchev, D. Lu, F. Colas, V. Lazarov, and B. Francois, "Energy management and operational planning of a microgrid with a PV-based active generator for smart grid applications," *IEEE Transactions on Industrial Electronics*, vol. 58, no. 10, pp. 4583–4592, 2011.

[175] C. Chen, S. Duan, T. Cai, B. Liu, and G. Hu, "Smart energy management system for optimal microgrid economic operation," *IET renewable power generation*, vol. 5, no. 3, pp. 258–267, 2011.

[176] S. Conti, R. Nicolosi, S. Rizzo, and H. Zeineldin, "Optimal dispatching of distributed generators and storage systems for MV islanded microgrids," *IEEE Transactions on Power Delivery*, vol. 27, no. 3, pp. 1243–1251, 2012.

[177] S. Chakraborty, M. D. Weiss, and M. G. Simoes, "Distributed intelligent energy management system for a single-phase high-frequency AC microgrid," *IEEE Transactions on Industrial Electronics*, vol. 54, no. 1, pp. 97–109, 2007.

[178] A. H. Etemadi, E. J. Davison, and R. Iravani, "A decentralized robust control strategy for multi-DER microgridsPart I: Fundamental concepts," *IEEE Transactions on Power Delivery*, vol. 27, no. 4, pp. 1843–1853, 2012.

[179] A. H. Etemadi, E. J. Davison, and R. Iravani, "A decentralized robust control strategy for multi-DER microgrids–Part II: Performance evaluation," *IEEE Transactions on Power Delivery*, vol. 27, no. 4, pp. 1854–1861, 2012.

[180] K. Tan, X. Peng, P. L. So, Y. C. Chu, and M. Chen, "Centralized control for parallel operation of distributed generation inverters in microgrids," *IEEE Transactions on Smart Grid*, vol. 3, no. 4, pp. 1977–1987, 2012.

[181] Y.-K. Chen, Y.-C. Wu, C.-C. Song, and Y.-S. Chen, "Design and implementation of energy management system with fuzzy control for DC microgrid systems," *IEEE Transactions on Power Electronics*, vol. 28, no. 4, pp. 1563–1570, 2013.

[182] F. Katiraei and M. R. Iravani, "Power management strategies for a microgrid with multiple distributed generation units," *IEEE Transactions on Power Systems*, vol. 21, no. 4, pp. 1821–1831, 2006.

[183] T. Morstyn, B. Hredzak, and V. G. Agelidis, "Cooperative multi-agent control of heterogeneous storage devices distributed in a dc microgrid," *IEEE Transactions on Power Systems*, vol. 31, pp. 2974–2986, July 2016.

[184] T. Morstyn, B. Hredzak, G. D. Demetriades, and V. G. Agelidis, "Unified distributed control for dc microgrid operating modes," *IEEE Transactions on Power Systems*, vol. 31, no. 1, pp. 802–812, 2016.

[185] J. Ni and Q. Ai, "Economic power transaction using coalitional game strategy in micro-grids," *IET Generation, Transmission & Distribution*, vol. 10, no. 1, pp. 10–18, 2016.

[186] H. Shirzeh, F. Naghdy, P. Ciufo, and M. Ros, "Balancing energy in the smart grid using distributed value function (dvf)," *IEEE Transactions on Smart Grid*, vol. 6, no. 2, pp. 808–818, 2015.

[187] J. Ansari, A. Gholami, and A. Kazemi, "Holonic structure: a state-of-the-art control architecture based on multi-agent systems for optimal reactive power dispatch in smart grids," *IET Generation, Transmission Distribution*, vol. 9, no. 14, pp. 1922–1934, 2015.

[188] N. R. Jennings, E. Mamdani, J. M. Corera, I. Laresgoiti, F. Perriolat, P. Skarek, and L. Z. Varga, "Using archon to develop real-world dai applications. 1," *IEEE expert*, vol. 11, no. 6, pp. 64–70, 1996.

[189] T. Wittig, N. R. Jennings, and E. Mamdani, "Archon: framework for intelligent cooperation," *Intelligent Systems Engineering*, vol. 3, no. 3, pp. 168–179, 1994.

[190] J. A. Hossack, J. Menal, S. D. McArthur, and J. R. McDonald, "A multi-agent architecture for protection engineering diagnostic assistance," *IEEE Transactions on Power Systems*, vol. 18, no. 2, pp. 639–647, 2003.

[191] S. D. McArthur, S. M. Strachan, and G. Jahn, "The design of a multi-agent transformer condition monitoring system," *IEEE Transactions on Power Systems*, vol. 19, no. 4, pp. 1845–1852, 2004.

[192] A. Brown, V. Catterson, M. Fox, D. Long, and S. McArthur, "Learning models of plant behavior for anomaly detection and condition monitoring," in *International Conference on Intelligent Systems Applications to Power Systems, 2007. ISAP 2007*, pp. 1–6, IEEE, 2007.

[193] V. Catterson, S. Rudd, S. McArthur, and G. Moss, "On-line transformer condition monitoring through diagnostics and anomaly detection," in *15th International Conference on Intelligent System Applications to Power Systems, 2009. ISAP'09*, pp. 1–6, IEEE, 2009.

[194] V. M. Catterson, S. D. McArthur, M. D. Judd, and A. S. Zaher, "Managing remote online partial discharge data," *IEEE Transactions on Power Delivery*, vol. 23, no. 4, pp. 1754–1762, 2008.

[195] P. Baker, V. Catterson, and S. McArthur, "Integrating an agent-based wireless sensor network within an existing multi-agent condition monitoring system," in *15th International Conference on Intelligent System Applications to Power Systems, 2009. ISAP'09*, pp. 1–6, IEEE, 2009.

[196] B. C.-C. Liu, J. Jung, G. T. Heydt, V. Vittal, and A. G. Phadke, "The strategic power infrastructure defense (spid) system. a conceptual design," *Control Systems, IEEE*, vol. 20, no. 4, pp. 40–52, 2000.

[197] H. Li, G. W. Rosenwald, J. Jung, and C.-C. Liu, "Strategic power infrastructure defense," *Proceedings of the IEEE*, vol. 93, no. 5, pp. 918–933, 2005.

[198] D. M. Staszesky, D. Craig, and C. Befus, "Advanced feeder automation is here," *Power and Energy Magazine, IEEE*, vol. 3, no. 5, pp. 56–63, 2005.

[199] D. Macleman, W. Bik, and A. Jones, "Evaluation of a self healing distribution automation scheme on the isle of wight," in *Electricity Distribution-Part 1, CIRED 2009. 20th International Conference and Exhibition on*, pp. 1–4, IET, 2009.

[200] K. Kok, "Multi-agent coordination in the electricity grid, from concept towards market introduction," in *Proceedings of the 9th International Conference on Autonomous Agents and Multiagent Systems: Industry track*, pp. 1681–1688, International Foundation for Autonomous Agents and Multiagent Systems, 2010.

[201] E. Davidson, M. Dolan, G. Ault, and S. McArthur, "Aura-nms: An autonomous regional active network management system for edf energy and sp energy networks," in *Power and Energy Society General Meeting*, pp. 1–6, IEEE, 2010.

[202] E. M. Davidson, S. D. McArthur, C. Yuen, and M. Larsson, "Aura-nms: Towards the delivery of smarter distribution networks through the application

of multi-agent systems technology," in *Power and Energy Society General Meeting-Conversion and Delivery of Electrical Energy in the 21st Century*, pp. 1–6, IEEE, 2008.

[203] N. Hadjsaid, L. Le-Thanh, R. Caire, B. Raison, F. Blache, B. Ståhl, and R. Gustavss, "Integrated ict framework for distribution network with decentralized energy resources: Prototype, design and development," in *Power and Energy Society General Meeting*, pp. 1–4, IEEE, 2010.

[204] G. Peppink, R. Kamphuis, K. Kok, A. Dimeas, E. Karfopoulos, N. Hatziargyriou, N. Hadjsaid, R. Caire, R. Gustavsson, J. M. Salas, *et al.*, "Integral: Ict-platform based distributed control in electricity grids with a large share of distributed energy resources and renewable energy sources," in *Energy-Efficient Computing and Networking*, pp. 215–224, Springer, 2010.

[205] E. Lorenz, T. Scheidsteger, J. Hurka, D. Heinemann, and C. Kurz, "Regional pv power prediction for improved grid integration," *Progress in Photovoltaics: Research and Applications*, vol. 19, no. 7, pp. 757–771, 2011.

[206] J. P. d. S. Catalão, H. M. I. Pousinho, and V. M. F. Mendes, "Short-term wind power forecasting in portugal by neural networks and wavelet transform," *Renewable energy*, vol. 36, no. 4, pp. 1245–1251, 2011.

[207] A. Mellit, M. Benghanem, and S. A. Kalogirou, "An adaptive wavelet-network model for forecasting daily total solar-radiation," *Applied Energy*, vol. 83, no. 7, pp. 705–722, 2006.

[208] L. Karthikeyan and D. N. Kumar, "Predictability of nonstationary time series using wavelet and emd based arma models," *Journal of hydrology*, vol. 502, pp. 103–119, 2013.

[209] I. G. Damousis, M. C. Alexiadis, J. B. Theocharis, and P. S. Dokopoulos, "A fuzzy model for wind speed prediction and power generation in wind parks using spatial correlation," *IEEE Transactions on Energy Conversion*, vol. 19, no. 2, pp. 352–361, 2004.

[210] M. Monfared, H. Rastegar, and H. M. Kojabadi, "A new strategy for wind speed forecasting using artificial intelligent methods," *Renewable energy*, vol. 34, no. 3, pp. 845–848, 2009.

[211] G.-f. Fan, W.-s. Wang, C. Liu, and H.-z. DAI, "Wind power prediction based on artificial neural network," *Proceedings of the CSEE*, vol. 34, pp. 118–123, 2008.

[212] M. A. Mohandes, T. O. Halawani, S. Rehman, and A. A. Hussain, "Support vector machines for wind speed prediction," *Renewable Energy*, vol. 29, no. 6, pp. 939–947, 2004.

[213] S. Salcedo-Sanz, E. G. Ortiz-Garcı, Á. M. Pérez-Bellido, A. Portilla-Figueras, L. Prieto, *et al.*, "Short term wind speed prediction based on evolutionary support vector regression algorithms," *Expert Systems with Applications*, vol. 38, no. 4, pp. 4052–4057, 2011.

[214] X. Cheng and P. Guo, "Short-term wind speed prediction based on support vector machine of fuzzy information granulation," in *25th Chinese Control and Decision Conference (CCDC)*, pp. 1918–1923, IEEE, 2013.

[215] D. Liu, D. Niu, H. Wang, and L. Fan, "Short-term wind speed forecasting using wavelet transform and support vector machines optimized by genetic algorithm," *Renewable Energy*, vol. 62, pp. 592–597, 2014.

[216] H. Ying, Y. Ding, S. Li, and S. Shao, "Comparison of necessary conditions for typical takagi-sugeno and mamdani fuzzy systems as universal approximators," *IEEE Transactions on Systems, Man, and Cybernetics-Part A: Systems and Humans*, vol. 29, no. 5, pp. 508–514, 1999.

[217] K. Liu, S. Subbarayan, R. Shoults, M. Manry, C. Kwan, F. Lewis, and J. Naccarino, "Comparison of very short-term load forecasting techniques," *IEEE Transactions on power systems*, vol. 11, no. 2, pp. 877–882, 1996.

[218] A. Khotanzad, R. Afkhami-Rohani, and D. Maratukulam, "Annstlf-artificial neural network short-term load forecaster-generation three," *IEEE Transactions on Power Systems*, vol. 13, no. 4, pp. 1413–1422, 1998.

[219] H. S. Hippert, C. E. Pedreira, and R. C. Souza, "Neural networks for short-term load forecasting: A review and evaluation," *IEEE Transactions on power systems*, vol. 16, no. 1, pp. 44–55, 2001.

[220] M. Adya, F. Collopy, J. S. Armstrong, and M. Kennedy, "Automatic identification of time series features for rule-based forecasting," *International Journal of Forecasting*, vol. 17, no. 2, pp. 143–157, 2001.

[221] E. Cadenas and W. Rivera, "Short term wind speed forecasting in la venta, oaxaca, méxico, using artificial neural networks," *Renewable Energy*, vol. 34, no. 1, pp. 274–278, 2009.

[222] N. Amjady, F. Keynia, and H. Zareipour, "A new hybrid iterative method for short-term wind speed forecasting," *International Transactions on Electrical Energy Systems*, vol. 21, no. 1, pp. 581–595, 2011.

[223] D. C. Park, M. El-Sharkawi, R. Marks, L. Atlas, M. Damborg, *et al.*, "Electric load forecasting using an artificial neural network," *IEEE Transactions on Power Systems*, vol. 6, no. 2, pp. 442–449, 1991.

[224] K. Metaxiotis, A. Kagiannas, D. Askounis, and J. Psarras, "Artificial intelligence in short term electric load forecasting: a state-of-the-art survey for the researcher," *Energy Conversion and Management*, vol. 44, no. 9, pp. 1525–1534, 2003.

[225] O. A. Carpinteiro, R. C. Leme, A. C. Z. de Souza, C. A. Pinheiro, and E. M. Moreira, "Long-term load forecasting via a hierarchical neural model with time integrators," *Electric Power Systems Research*, vol. 77, no. 3, pp. 371–378, 2007.

[226] T. Yalcinoz and U. Eminoglu, "Short term and medium term power distribution load forecasting by neural networks," *Energy Conversion and Management*, vol. 46, no. 9, pp. 1393–1405, 2005.

[227] K. Liu, S. Subbarayan, R. Shoults, M. Manry, C. Kwan, F. Lewis, and J. Naccarino, "Comparison of very short-term load forecasting techniques," *IEEE Transactions on Power Systems*, vol. 11, no. 2, pp. 877–882, 1996.

[228] E. A. Feinberg and D. Genethliou, "Load forecasting," in *Applied mathematics for restructured electric power systems*, pp. 269–285, Springer, 2005.

[229] S. Sreekumar, J. Verma, A. Sujil, and R. Kumar, "One day forth forecasting of hourly electrical load using genetically tuned support vector regression for smart grid frame work," in *2015 2nd International Conference on Recent Advances in Engineering & Computational Sciences (RAECS)*, pp. 1–6, IEEE, 2015.

[230] M. Shahidehpour, H. Yamin, and Z. Li, "Short-term load forecasting," *Market Operations in Electric Power Systems: Forecasting, Scheduling, and Risk Management*, pp. 21–56, 2002.

[231] H. Al-Hamadi and S. Soliman, "Long-term/mid-term electric load forecasting based on short-term correlation and annual growth," *Electric power systems research*, vol. 74, no. 3, pp. 353–361, 2005.

[232] D. Niu, H. Shi, J. Li, and Y. Wei, "Research on short-term power load time series forecasting model based on bp neural network," in *2nd International Conference on Advanced Computer Control (ICACC)*, vol. 4, pp. 509–512, IEEE, 2010.

[233] M. Mirhosseini, M. Marzband, and M. Oloomi, "Short term load forecasting by using neural network structure," in *6th International Conference on Electrical Engineering/Electronics, Computer, Telecommunications and Information Technology-ECTI-CON 2009*, vol. 1, pp. 240–243, IEEE, 2009.

[234] G.-D. Li, C.-H. Wang, S. Masuda, and M. Nagai, "A research on short term load forecasting problem applying improved grey dynamic model," *International Journal of Electrical Power & Energy Systems*, vol. 33, no. 4, pp. 809–816, 2011.

[235] E. Kayacan, B. Ulutas, and O. Kaynak, "Grey system theory-based models in time series prediction," *Expert systems with applications*, vol. 37, no. 2, pp. 1784–1789, 2010.

[236] Y.-S. Lee and L.-I. Tong, "Forecasting energy consumption using a grey model improved by incorporating genetic programming," *Energy Conversion and Management*, vol. 52, no. 1, pp. 147–152, 2011.

[237] A. Karsaz, H. R. Mashhadi, and M. M. Mirsalehi, "Market clearing price and load forecasting using cooperative co-evolutionary approach," *International Journal of Electrical Power & Energy Systems*, vol. 32, no. 5, pp. 408–415, 2010.

[238] Á. L. Santana, G. B. Conde, L. P. Rego, C. A. Rocha, D. L. Cardoso, J. C. Costa, U. H. Bezerra, and C. R. Francês, "Predict–decision support system for load forecasting and inference: a new undertaking for brazilian power suppliers," *International Journal of Electrical Power & Energy Systems*, vol. 38, no. 1, pp. 33–45, 2012.

[239] L. Xiao, J. Wang, X. Yang, and L. Xiao, "A hybrid model based on data preprocessing for electrical power forecasting," *International Journal of Electrical Power & Energy Systems*, vol. 64, pp. 311–327, 2015.

[240] J. Sousa, L. Neves, and H. Jorge, "Assessing the relevance of load profiling information in electrical load forecasting based on neural network models," *International Journal of Electrical Power & Energy Systems*, vol. 40, no. 1, pp. 85–93, 2012.

[241] H. J. Sadaei, R. Enayatifar, A. H. Abdullah, and A. Gani, "Short-term load forecasting using a hybrid model with a refined exponentially weighted fuzzy time series and an improved harmony search," *International Journal of Electrical Power & Energy Systems*, vol. 62, pp. 118–129, 2014.

[242] Ö. F. Ertugrul, "Forecasting electricity load by a novel recurrent extreme learning machines approach," *International Journal of Electrical Power & Energy Systems*, vol. 78, pp. 429–435, 2016.

[243] R.-A. Hooshmand, H. Amooshahi, and M. Parastegari, "A hybrid intelligent algorithm based short-term load forecasting approach," *International Journal of Electrical Power & Energy Systems*, vol. 45, no. 1, pp. 313–324, 2013.

[244] G. Aneiros, J. Vilar, and P. Raña, "Short-term forecast of daily curves of electricity demand and price," *International Journal of Electrical Power & Energy Systems*, vol. 80, pp. 96–108, 2016.

[245] I. P. Panapakidis, "Clustering based day-ahead and hour-ahead bus load forecasting models," *International Journal of Electrical Power & Energy Systems*, vol. 80, pp. 171–178, 2016.

[246] M.-Y. Zhai, "A new method for short-term load forecasting based on fractal interpretation and wavelet analysis," *International Journal of Electrical Power & Energy Systems*, vol. 69, pp. 241–245, 2015.

[247] C. W. Lou and M. C. Dong, "A novel random fuzzy neural networks for tackling uncertainties of electric load forecasting," *International Journal of Electrical Power & Energy Systems*, vol. 73, pp. 34–44, 2015.

[248] S. Hassan, A. Khosravi, and J. Jaafar, "Examining performance of aggregation algorithms for neural network-based electricity demand forecasting," *International Journal of Electrical Power & Energy Systems*, vol. 64, pp. 1098–1105, 2015.

[249] D. Chaturvedi, A. Sinha, and O. Malik, "Short term load forecast using fuzzy logic and wavelet transform integrated generalized neural network," *International Journal of Electrical Power & Energy Systems*, vol. 67, pp. 230–237, 2015.

[250] A. Bakirtzis, J. Theocharis, S. Kiartzis, and K. Satsios, "Short term load forecasting using fuzzy neural networks," *IEEE Transactions on Power Systems*, vol. 10, no. 3, pp. 1518–1524, 1995.

[251] C. Holmes and B. Mallick, "Bayesian regression with multivariate linear splines," *Journal of the Royal Statistical Society: Series B (Statistical Methodology)*, vol. 63, no. 1, pp. 3–17, 2001.

[252] D. G. Denison, C. C. Mallick, B. K. Smith, *et al.*, *Bayesian methods for nonlinear classification and regression*. No. 519.536 B38, 2002.

[253] M. R. B. Khan, R. Jidin, and J. Pasupuleti, "Multi-agent based distributed control architecture for microgrid energy management and optimization," *Energy Conversion and Management*, vol. 112, pp. 288–307, 2016.

[254] A. H. Fathima and K. Palanisamy, "Optimization in microgrids with hybrid energy systems–a review," *Renewable and Sustainable Energy Reviews*, vol. 45, pp. 431–446, 2015.

[255] "Pv, wind data." `https://www.renewables.ninja`. Accessed: 2017-04-26.

[256] M. Lei, L. Shiyan, J. Chuanwen, L. Hongling, and Z. Yan, "A review on the forecasting of wind speed and generated power," *Renewable and Sustainable Energy Reviews*, vol. 13, no. 4, pp. 915–920, 2009.

[257] T.-L. Chen, C.-H. Cheng, and H.-J. Teoh, "High-order fuzzy time-series based on multi-period adaptation model for forecasting stock markets," *Physica A: Statistical Mechanics and its Applications*, vol. 387, no. 4, pp. 876–888, 2008.

[258] C. P. Rodriguez and G. J. Anders, "Energy price forecasting in the ontario competitive power system market," *IEEE Transactions on power systems*, vol. 19, no. 1, pp. 366–374, 2004.

[259] A. Kusagur, S. Kodad, and B. V. S. Ram, "Modeling, design & simulation of an adaptive neuro-fuzzy inference system (anfis) for speed control of induction motor," *International Journal of Computer Applications*, vol. 6, no. 12, pp. 29–44, 2010.

[260] M. Buragohain, *Adaptive network based fuzzy inference system (ANFIS) as a tool for system identification with special emphasis on training data minimization*. PhD thesis, 2009.

[261] T. Takagi and M. Sugeno, "Derivation of fuzzy control rules from human operator's control actions," *IFAC Proceedings Volumes*, vol. 16, no. 13, pp. 55–60, 1983.

[262] E. H. Mamdani and S. Assilian, "An experiment in linguistic synthesis with a fuzzy logic controller," *International journal of man-machine studies*, vol. 7, no. 1, pp. 1–13, 1975.

[263] J.-S. Jang, "Anfis: adaptive-network-based fuzzy inference system," *IEEE transactions on systems, man, and cybernetics*, vol. 23, no. 3, pp. 665–685, 1993.

[264] J.-S. R. Jang, C.-T. Sun, and E. Mizutani, "Neuro-fuzzy and soft computing: a computational approach to learning and machine intelligence," 1997.

[265] J.-S. Jang and C.-T. Sun, "Neuro-fuzzy modeling and control," *Proceedings of the IEEE*, vol. 83, no. 3, pp. 378–406, 1995.

[266] S. L. Chiu, "A cluster estimation method with extension to fuzzy model identification," in *Fuzzy Systems,Proceedings of the Third IEEE Conference on IEEE World Congress on Computational Intelligence*, pp. 1240–1245, IEEE, 1994.

[267] A. Shukla, K. Verma, and R. Kumar, "Consumer perspective based placement of electric vehicle charging stations by clustering techniques," in *National Power Systems Conference (NPSC)*, pp. 1–6, IEEE, 2016.

[268] S. L. Chiu, "Selecting input variables for fuzzy models," *Journal of Intelligent & Fuzzy Systems*, vol. 4, no. 4, pp. 243–256, 1996.

[269] J. C. Bezdek, R. Ehrlich, and W. Full, "Fcm: The fuzzy c-means clustering algorithm," *Computers & Geosciences*, vol. 10, no. 2-3, pp. 191–203, 1984.

[270] T. H. El-Fouly, E. F. El-Saadany, and M. M. Salama, "One day ahead prediction of wind speed and direction," *IEEE Transactions on Energy Conversion*, vol. 23, no. 1, pp. 191–201, 2008.

[271] E. E. Elattar, J. Goulermas, and Q. H. Wu, "Electric load forecasting based on locally weighted support vector regression," *IEEE Transactions on Systems, Man, and Cybernetics, Part C (Applications and Reviews)*, vol. 40, no. 4, pp. 438–447, 2010.

[272] M. R. B. Khan, R. Jidin, J. Pasupuleti, and S. A. Shaaya, "Optimal combination of solar, wind, micro-hydro and diesel systems based on actual seasonal load profiles for a resort island in the south china sea," *Energy*, vol. 82, pp. 80–97, 2015.

[273] W.-C. Hong, "Electric load forecasting by support vector model," *Applied Mathematical Modelling*, vol. 33, no. 5, pp. 2444–2454, 2009.

[274] Z. Hu, Y. Bao, and T. Xiong, "Electricity load forecasting using support vector regression with memetic algorithms," *The Scientific World Journal*, vol. 2013, 2013.

[275] J. Zeng and W. Qiao, "Support vector machine-based short-term wind power forecasting," in *Power Systems Conference and Exposition (PSCE), 2011 IEEE/PES*, pp. 1–8, IEEE, 2011.

[276] M. K. Okasha, "Using support vector machines in financial time series forecasting," *International Journal of Statistics and Applications*, vol. 4, no. 1, pp. 28–392, 2014.

[277] K.-j. Kim, "Financial time series forecasting using support vector machines," *Neurocomputing*, vol. 55, no. 1-2, pp. 307–319, 2003.

[278] W. R. Gilks, S. Richardson, and D. J. Spiegelhalter, "Introducing markov chain monte carlo," *Markov chain Monte Carlo in practice*, vol. 1, p. 19, 1996.

[279] P. J. Green, "Reversible jump markov chain monte carlo computation and bayesian model determination," *Biometrika*, vol. 82, no. 4, pp. 711–732, 1995.

[280] "Stateflow and Stateflow Coder, howpublished = http://fractale.gecif.net/si/logiciels/matlab/stateflow.pdf, note = Accessed: 2018-10-22."

[281] "Wright, david,"finite state machines." "http://www4.ncsu.edu/drwrigh3/docs/courses/csc216/fsm-notes.pdf,2005.

[282] S. Masina, K. Y. Lee, and R. Garduno-Ramirez, "An architecture of multi-agent system applied to fossil-fuel power unit," in *Power Engineering Society General Meeting, 2004. IEEE*, pp. 1982–1988, IEEE, 2004.

[283] A. Sujil and R. Kumar, "Smart micro grid test system for agent based energy management system," *2016 IEEE Seventh India International Conference on Power Electronics (IICPE-2016)*, 2016.